Validation of CLASSI and SASSI to Treat Seismic Wave Incoherence in SSI Analysis of Nuclear Power Plant Structures

XXXXXXXXXXX

DRAFT Final Report, July 7, 2007

EPRI Project Managers
R. Kassawara

ELECTRIC POWER RESEARCH INSTITUTE
3420 Hillview Avenue, Palo Alto, California 94304-1395 • PO Box 10412, Palo Alto, California 94303-0813 • USA
800.313.3774 • 650.855.2121 • askepri@epri.com • www.epri.com

CITATIONS

This report was prepared by

ARES Corporation, Inc.
5 Hutton Centre Drive
Suite 610
Santa Ana, CA 92707

Principal Investigators
S. Short
G. Hardy
K. Merz

James J. Johnson and Associates
7 Essex Court
Alamo, CA 94507

Principal Investigator
J. Johnson

This publication is a corporate document that should be cited in the literature in the following manner:

EPRI#_tbd_, Validation of CLASSI and SASSI to Treat Seismic Wave Incoherence in SSI Analysis of Nuclear Power Plant Structures, EPRI, Palo Alto, CA 2007.

ACKNOWLEDGEMENTS

EPRI wishes to acknowledge the members of the Technical Review and Advisory Group (TRAG) for their support of this research project:

Robert Kennedy (Chair)	RPK Structural Consulting
Orhan Gurbuz	Consultant
Don Moore	Southern Nuclear
John Richards	Duke Power
Carl Stepp	Earthquake Hazards Solutions

EPRI wishes to acknowledge Dan Ghiocel at GP Technologies, Inc. and Farhang Ostadan at Bechtel Engineering for their support of this project. Dan Ghiocel provided SASSI Simulation Mean results and Farhang Ostadan provided SASSI SRSS results for the Benchmark problem within Chapter 5 and Appendix A of this report.

CONTENTS

1 INTRODUCTION AND BACKGROUND 1-1

Background on Seismic Wave Incoherence 1-1

Summary - Effect of Seismic Wave Incoherence on Foundation and Building Response (EPRI and USDOE, 2006) 1-2

Scope of Current Research Effort 1-3

Contents of the Report 1-4

2 STUDY INPUT PARAMETERS 2-1

Coherency Function 2-1

Site Parameters and Input Ground Motion 2-3

Foundation Parameters 2-7

Structure Properties 2-8

3 CLASSI TECHNICAL APPROACH 3-1

General 3-1

Incorporation of the Coherency Function into CLASSI Procedures 3-1

General CLASSI Approach: Rigid Massless Foundation 3-2

CLASSI Random Vibration Approach: Rigid Massless Foundation 3-4

CLASSI Random Vibration Approach: Foundation and Structure Response 3-4

Procedure to Evaluate the Incoherency Transfer Function (ITF) 3-6

Procedure to Evaluate the Foundation and Structure Incoherent Response Spectra by CLASSI 3-7

Validation of Rigid, Massless Foundation Response 3-10

Objective and Scope 3-10

Ground Motion Coherence Function 3-10

Comparison of ITFs 3-12

Circular disk. 3-12

Square foundation. 3-17

Conclusions 3-20

4 SASSI TECHNICAL APPROACH 4-1
General 4-1
Coherency matrix 4-1
SASSI Approach 4-2
Approaches to Solve for SSI Response of Foundation and Structure 4-3
Randomization (SASSI – Simulation Mean) 4-3
Square Root of the Sum of the Squares (SASSI-SRSS) 4-5
SRSS Transfer Functions 4-6
SRSS – SSI Response 4-6
SRSS – Observations 4-7
Linear Algebraic Combination (SASSI – AS) 4-7

5 CLASSI AND SASSI IN-STRUCTURE RESPONSE SPECTRA COMPARISONS 5-1
General 5-1
CLASSI-SASSI Comparisons of In-Structure Response Spectra 5-4
Foundation Response 5-4
Auxiliary and Shield Building (ASB) 5-4
Containment Internal Structure (CIS) 5-5
Steel Containment Vessel (SCV) 5-5
Summary of CLASSI-SASSI Comparisons 5-6

6 GUIDELINES FOR APPLICATION OF CLASSI AND SASSI 6-1

7 CONCLUSIONS AND RECOMMENDATIONS 7-1

8 REFERENCES 8-1

A CLASSI-SASSI IN-STRUCTURE RESPONSE SPECTRA COMPARISONS FOR INDIVIDUAL INPUT DIRECTION COMPONENTS A-1
X-Direction Input Ground Motion A-3
Y-Direction Input Ground Motion A-17
Z-Direction Input Ground Motion A-31

1
INTRODUCTION AND BACKGROUND

Task S2.1 of the EPRI/DOE New Plant Seismic Issues Resolution Program is a multi-phase research project to assess the effects of seismic wave incoherence on the response of foundations and structures similar to those being considered for advanced reactor designs. The initial phases of this task focused on the objective of systematically studying seismic wave incoherence effects on structures/foundations. These phases were documented in *Program on Technology Innovation: Effect of Seismic Wave Incoherence on Foundation and Building Response* (EPRI and USDOE, 2006). Results of these initial phases are summarized later in this chapter.

The final phase of Task S2.1 is presented in Chapters 3-7 of this report. This phase entails the validation of analytical methods and their implementation in the soil-structure interaction (SSI) computer programs CLASSI and SASSI. The objective of this final phase is to complete the validation which demonstrates that CLASSI and SASSI adequately calculate the seismic response of foundations and structures when subjected to seismic wave fields including incoherence effects. In addition, guidelines on the appropriate application of both CLASSI and SASSI to accurately reflect the seismic response incorporating incoherency effects are developed and presented.

Background on Seismic Wave Incoherence

Seismic wave incoherence consists of spatial variation of both horizontal and vertical ground motion. Two sources of incoherence or horizontal spatial variation of ground motion are:

a. Local wave scattering: Spatial variation from scattering of waves due to the heterogeneous nature of the soil or rock along the propagation paths of the incident wave fields.

b. Wave passage effects: Systematic spatial variation due to difference in arrival times of seismic waves across a foundation due to inclined waves.

The focus of all phases of Task S2.1 is on local wave scattering.

The effect of seismic wave incoherence is that motions recorded on foundations of structures differ from those measured in the adjacent free-field. Generally, the motion measured on the foundation is less than the motion recorded in the free-field, especially at high-frequencies. Two aspects of soil-structure interaction contribute to the observations of foundation motion being less than the free-field: kinematic and inertial interaction. Kinematic interaction is due to the spatial variation of the free-field ground motion over the portion of the foundation/structure system abutting the soil or rock. For nuclear power plant structures, which have large and stiff foundation mats, the amplitudes of high-frequency seismic response of the foundation mat are

expected to be significantly less than those in the free-field due to horizontal spatial variation of ground motion including incoherence.

The phenomenon of seismic wave incoherence has been recognized for many years, but the lack of an adequately large set of recorded data prevented quantification of the phenomenon and the development of approaches for the incorporation of the effect into the dynamic analysis of NPP structures. Dr. Norm Abrahamson has developed state-of-the-art representations of the coherency functions based on the most applicable data available (Abrahamson, 2005, 2006, 2007). These coherency functions are based on a large number of densely spaced ground motion recordings. Coherency functions define the relationships between ground motion at separate locations as a function of the separation distance between the locations and the frequency of the ground motion. Coherency of motion decreases significantly with increasing frequency and increasing distance between points of interest. The coherency functions (Abrahamson, 2005, 2006, 2007) account for this effect of incoherence at all frequencies of interest and all discretized points on the foundation. For the purposes of this research study on the effects to foundations and structures to coherent/incoherent response, the original coherency function developed by Dr. Abrahamson (Abrahamson 2006) for soil sites has been utilized. This soil coherency model contains less coherency (more reduction from the coherent response) than the currently being developed rock site coherency model and was judged to be appropriate for benchmarking methods of calculating structural response to incoherent ground motion.

Summary - Effect of Seismic Wave Incoherence on Foundation and Building Response (EPRI and USDOE, 2006)

The initial phases of the Task S2.1 focused on evaluating seismic response for rigid, massless foundations and for example structural models on rigid foundation mats. CLASSI was the primary soil-structure interaction analysis program used for assessing seismic response including seismic wave incoherence. By the CLASSI methodology, the basic relationship between motion in the free-field and motion on the rigid massless foundation is developed based on random vibration theory. Basic inputs to incoherent SSI analyses are the coherency functions developed by Dr. Abrahamson (Abrahamson, 2005, 2006, 2007). As stated above, the coherency functions of Abrahamson (2005, 2006) were used in the initial phases and in this final phase of Task S2.1. Earlier vintage coherency functions by Luco and Wong (1986) are also employed in this final phase for comparisons of calculated response with that from published literature.

Seismic response of example structures considering seismic wave incoherence was calculated using the CLASSI family of SSI analysis programs. An important observation from these seismic analyses was that incoherence produced reduction in translational response but also induced rotational response. In general, each component of horizontal ground motion induces a horizontal translation and a companion torsional component. The vertical component of ground motion induces a vertical translation of the foundation and companion rocking components about the horizontal axes.

The CLASSI approach for seismic wave incoherence analysis was initially validated during the study by an independent comparison with different methodology and software. The random vibration approach used with CLASSI produced excellent agreement with an eigenfunction

decomposition approach used with SASSI for a limited subset of analysis conditions, i.e., locations with in the structures where the effect of induced rotations on the foundation are minimal. Expanding this validation to more complex situations is the subject of the current phase of Task S2.1.

The conclusions of the initial phases of Task S2.1, which are directly relevant to this phase, are:

- Soil-structure interaction (SSI) analysis is important to calculating seismic response to structures mounted on rock sites and subjected to high-frequency ground motion. SSI produces significant reductions in high-frequency response for these conditions.
- Consideration of incoherence is important for the proper evaluation of the response of large base mat structures to high-frequency ground motions (primarily greater than 10 Hz). Realistically accounting for ground motion incoherence on the seismic response of nuclear power plant structures is significant and should be properly incorporated into seismic design analyses.
- The effects of incoherence are three-dimensional. Induced torsion couples horizontal response in the two horizontal directions. Induced rocking couples horizontal and vertical response, i.e., incoherent vertical ground motion induces horizontal response in the structure. Incoherency-induced rocking and torsion are shown to be important to in-structure response depending on the structure and its dynamic characteristics.

Scope of Current Research Effort

The scope of the final phase of Task S2.1 is to further validate the analytical methods and their implementation in the SSI computer programs CLASSI and SASSI. The objective is to demonstrate that both CLASSI and SASSI adequately calculate the seismic response of foundations and structures when subjected to seismic wave fields including incoherence effects. Theoretical aspects of the approaches are expanded beyond those presented by EPRI and USDOE (2006). Validation of the individual methodologies includes theoretical (e.g. randomness in modes and phasing) and practical (e.g. number of spatial modes selected within SASSI for computational efficiency) aspects. Guidelines on their application are developed and presented as a part of this report.

Validation of CLASSI and SASSI to treat seismic wave incoherence in SSI analyses is accomplished by:

- Comparison of results computed using CLASSI and SASSI to those available from published literature.
- Comparison of CLASSI computed incoherent seismic response with SASSI computed incoherent seismic response for an example rock/structure model

As mentioned above, CLASSI and SASSI computed incoherent seismic response were compared and showed to be in good agreement in EPRI and USDOE (2006). However, the example soil/structure model considered in those benchmark analyses did not produce significant incoherency-induced torsion and rocking response. The example soil/structure model used for benchmark comparisons in this final phase has offsets of mass centers from the shear centers and significant "outriggers" (nodes extended from the mass center to simulate the

response at the perimeter of the building) to overemphasize seismic response from incoherency-induced rotations. It is judged that the example soil/structure model utilized in this phase provide an extreme (conservative) level of torsion and rocking response induced by seismic wave incoherence that validates the use of either CLASSI or SASSI for seismic analysis.

Incoherency induced rotations are a random phenomena resulting from the horizontal spatial variation of ground motion over the foundation area. For response quantities where several components of foundation motion contribute significantly, the phasing of those components must be adequately represented in order to produce reasonable seismic response. As a result, enhancements to the CLASSI and SASSI approaches as described in EPRI and USDOE (2006) were required to capture the random nature of multi-component seismic response. These enhancements have led to the review and recognition of two CLASSI methods and three SASSI methods for evaluating seismic response including seismic wave incoherence. These approaches include:

- CLASSIinco – deterministic phasing of foundation component response
- CLASSIinco-SRSS – SRSS combination of structural response computed from random phasing of foundation component response
- SASSI-SRSS – SRSS combination of modal transfer functions to represent random phasing of spatial modes
- SASSI Simulation Mean – Monte Carlo simulations to represent random phasing of spatial modes
- SASSI-AS – Algebraic summation of spatial modes with assumed deterministic phasing

Comparisons of seismic response by all of these methods are presented in this report for the example structure with mass offsets and outriggers that exaggerates incoherency induced rotations. The results from these comparison studies form the basis for the validation of CLASSI and SASSI to treat seismic wave incoherence in SSI analyses of nuclear power plant structures.

Contents of the Report

Chapter 2 defines the input parameters for this study: ground motion coherency functions, rock site conditions and the corresponding free-field ground motions, and structure/foundation parameters for the seismic analyses performed. Chapter 3 presents the derivation of the CLASSI/random vibration approach, including enhancements from the approach reported in EPRI and USDOE (2006). Chapter 4 presents the SASSI technical approach. This entails the decomposition of the ground motion coherency matrix into its eigen-system termed spatial modes and calculation of foundation/structure response. Three approaches to treating the spatial modes are highlighted: randomization, square-root-of-the-sum-of the squares (SRSS), and algebraic combination. Chapter 5 presents comparisons of foundation and in-structure responses calculated by the various methodologies described within Chapters 3 and 4. Chapter 6 summarizes guidelines for the application of CLASSI and SASSI as a function of physical and calculational characteristics. Chapter 7 presents a summary of the results, conclusions and recommendations from this research study. Chapter 8 documents the references and Appendix A contains CLASSI/SASSI response data for individual earthquake input directions.

2
STUDY INPUT PARAMETERS

Coherency Function

For this phase of Task S2.1, the Abrahamson plane wave (i.e., no wave passage effects) coherency functions (2005, 2006) were used. Coherency functions describe the relationship between ground motion at separate locations as a function of the separation distance and the frequency of the ground motion. The coherency functions take the following form:

$$\gamma_{PW} = \left[1+\left(\frac{f\,Tanh(a_3\xi)}{a_1 f_c}\right)^{n1}\right]^{-1/2}\left[1+\left(\frac{f\,Tanh(a_3\xi)}{a_2 f_c}\right)^{n2}\right]^{-1/2} \qquad \textbf{(Equation 2-1)}$$

Where γ_{PW} is the plane wave coherency representing random horizontal spatial variation of ground motion. The parameter f is ground motion frequency and ξ is the separation distance between locations in meters. Coefficients to be used in Equation 2-1 for horizontal and vertical ground motion are presented in Table 2-1.

Table 2-1
Coherency Function Coefficients

Coefficient	Horizontal Ground Motion	Vertical Ground Motion
a_1	1.647	3.15
a_2	1.01	1.0
a_3	0.4	0.4
n_1	7.02	4.95
n_2	5.1-0.51ln(ξ+10)	1.685
f_c	-1.886+2.221ln(4000/(ξ+1)+1.5)	Exp(2.43-0.025 ln(ξ+1)-0.048 (ln(ξ+1))^2)

The coherency function is plotted as a function of frequency for a number of separation distances in Figures 2-1 and 2-2 for horizontal and vertical ground motion, respectively. These figures show plane wave coherency (random spatial variation of ground motion) per Equation 2-1.

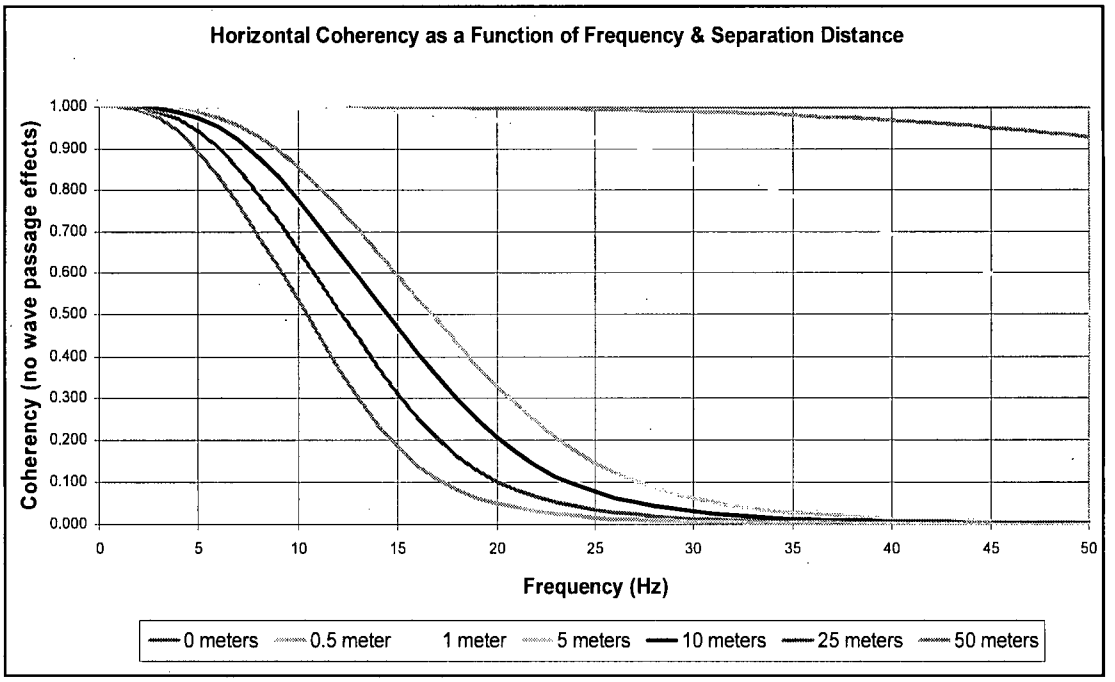

Figure 2-1
Coherency Function for Horizontal Ground Motion

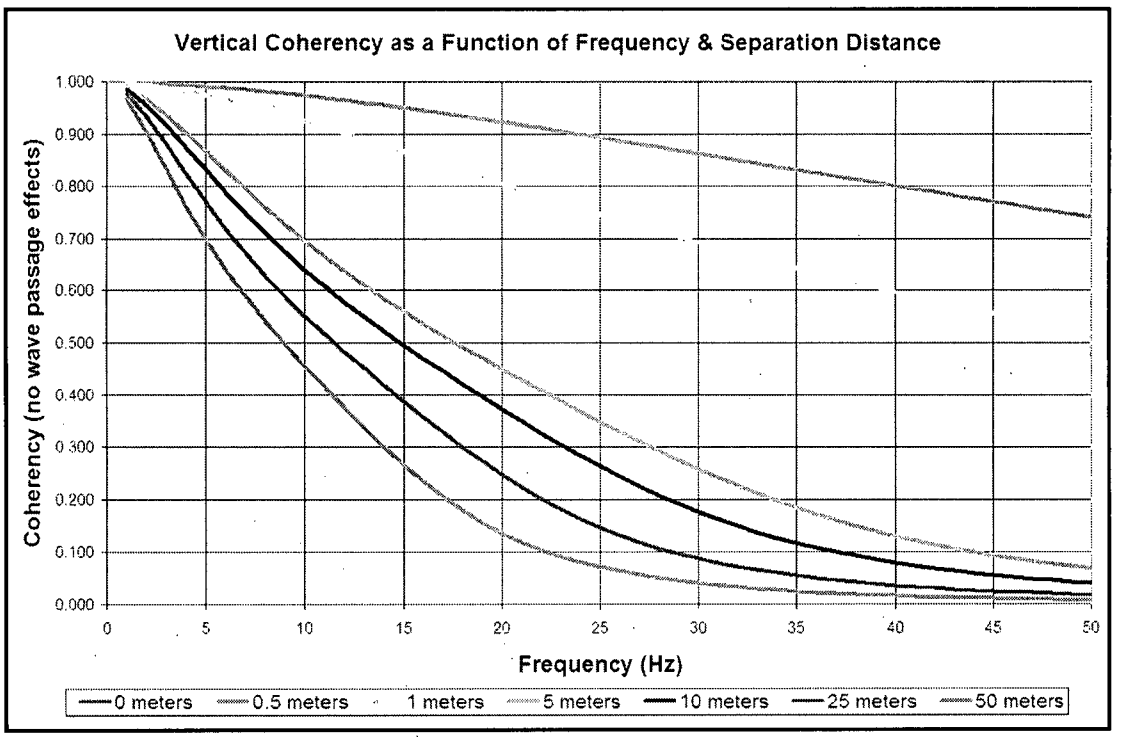

Figure 2-2
Coherency Function for Vertical Ground Motion

The coherency functions presented above have been developed from all available and applicable recorded ground motion from dense instrument arrays. Data are from a variety of site conditions and earthquake magnitudes. In the development of these functions, Dr. Abrahamson has reached the following conclusions (Abrahamson, 2005, 2006, 2007):

- Coherency functions are appropriate for all frequencies (including those above 20 Hz). Ground motion data analyzed to develop the coherency functions have frequency content of 20 Hz and less. It is logical that the trends observed should extrapolate to higher frequencies.
- Coherency is strongly affected by topography. Data with strong topographic effects were not included for development of the coherency function.
- Coherency does not vary as a function of earthquake magnitude. This is true for magnitudes of interest that are greater than magnitude 4.5 to 5.0.
- Each component of earthquake input can be treated as uncorrelated. The coherency of cross-components is near zero.
- Coherency varies as a function of site shear wave velocity, especially for "hard rock" sites, i.e., with shear wave velocities greater than about 1,000 m/sec (Abrahamson, 2007). For "hard rock" sites, ground motion coherency is greater than for soil sites for frequencies greater than 10 Hz. The ground motion coherency functions of equation 2-1 and Table 2-1 are most appropriate for soil sites and surface-founded structures. In spite of this recent development, these ground motion coherency functions are used in the current study to maintain consistency with all previous sensitivity studies and results. In addition, these ground motion coherency functions are likely to produce a more severe test of the validation of the approaches and their implementation since the effect on foundation/structure response will be greater than the impact of the "hard rock" coherency functions on foundation/structure response.

For the design of nuclear power plant structures, mean input ground motion is the goal. As a result, the goal is to use mean coherency. The functions of equation 2-1 and Table 2-1 model median coherency. Median coherency is slightly larger (only a few percent difference) than mean coherency.

Site Parameters and Input Ground Motion

The initial phases of the Task S2.1 (EPRI and USDOE, 2006) used two representative site profiles; one for soil and one for rock. These site profiles were selected to be representative of sites in the Central and Eastern United States. Site-specific response spectra compatible with each of the sites were developed and used in the initial study. The current phase only considers the rock site. For the rock site profile, shear wave velocities as a function of depth beneath the free-field ground surface are shown in Figure 2-3. The site profile shown in the figure extends down to the Central and Eastern United States (CEUS) generic rock that has shear wave velocity of about 9200 fps (McCann, 2004).

For the foundation areas considered for this incoherence study, it is sufficient to define the site profile to a depth of about 300 feet beneath the foundation. The soil layers and properties shown in Table 2-2 have been used for the evaluation of coherency effects in this study. These properties were taken from information provided within the advanced reactor submittals (North Anna contained on the NRC web site).

For CLASSI modeling purposes, the rock site is represented by nine layers extending to 130-ft below the surface, and underlain by a half-space of bedrock at a shear wave velocity of 9200 fps. Rock is assumed to have the low strain shear modulus (shear wave velocity) and no variation of damping at earthquake strain levels (i.e., linear elastic behavior). A damping ratio of 0.02 is assumed, which corresponds to about 0.001% shear strain.

For SASSI modeling purposes, the rock site is represented by thirteen layers extending to 130-ft below the surface, and underlain by a half-space of bedrock at a shear wave velocity of 9200 fps. In the SASSI model, layers 5, 6, 7, and 8 are all 10 feet thick as opposed to 20 feet thick in the CLASSI model as shown in Table 2-2. The same rock stiffness and damping properties are used for CLASSI and SASSI modeling.

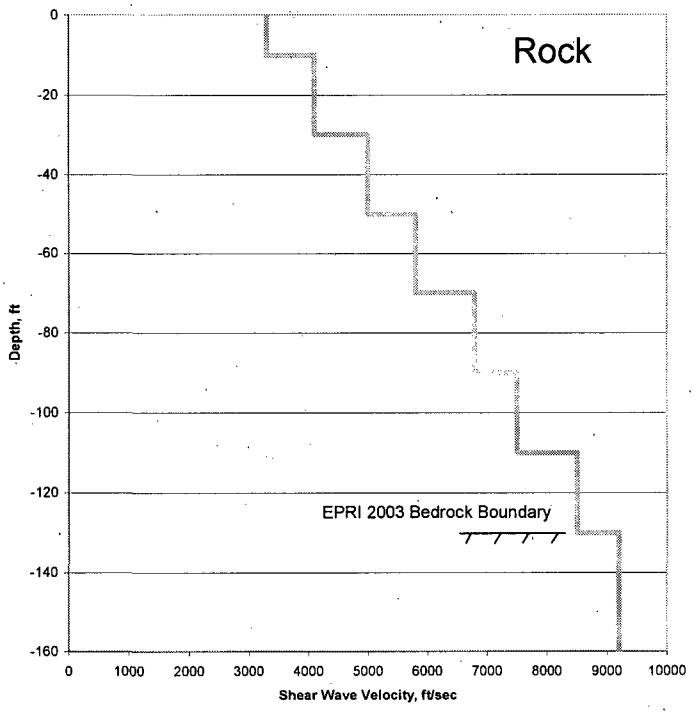

Figure 2-3
Rock Site Profile Shear Wave Velocities vs. Depth

Table 2-2
Layers and Properties for the Rock Site (EQ Strain)

Layer	Shear Wave Velocity (fps)	Weight Density (pcf)	Poisson's Ratio	Damping (fraction)	Thickness (ft)	Layer Top Depth (ft)
1	3300	160	0.33	0.02	5	0
2	3300	160	0.33	0.02	5	5
3	4100	160	0.33	0.02	10	10
4	4100	160	0.33	0.02	10	20
5	5000	160	0.33	0.02	20	30
6	5800	160	0.33	0.02	20	50
7	6800	160	0.33	0.02	20	70
8	7500	160	0.33	0.02	20	90
9	8500	160	0.33	0.02	20	110
10	9200	160	0.33	0.02	Half-space	130

Site-specific ground response spectra appropriate at the free ground surface at Elevation 0 for the rock site profile, as shown in Figure 2-3, were used for this coherency study. Five percent damped site-specific response spectra are illustrated in Figure 2-4 for the rock site. Also, plotted on the figure are the US NRC Regulatory Guide 1.60 design ground response spectra anchored to 0.3 g peak ground acceleration (PGA) for comparison purposes. The rock site-specific ground response spectra have peak amplification in the 20 to 30 Hz range.

For soil-structure interaction analyses and the evaluation of structure response including the effects of seismic wave incoherence, spectrum compatible time histories for the rock site were required. These were developed by Dr. Abrahamson. The computed spectra and the target spectra (Figure 2-4) are shown in Figure 2-5. Three uncorrelated components were generated for two horizontal directions and the vertical direction.

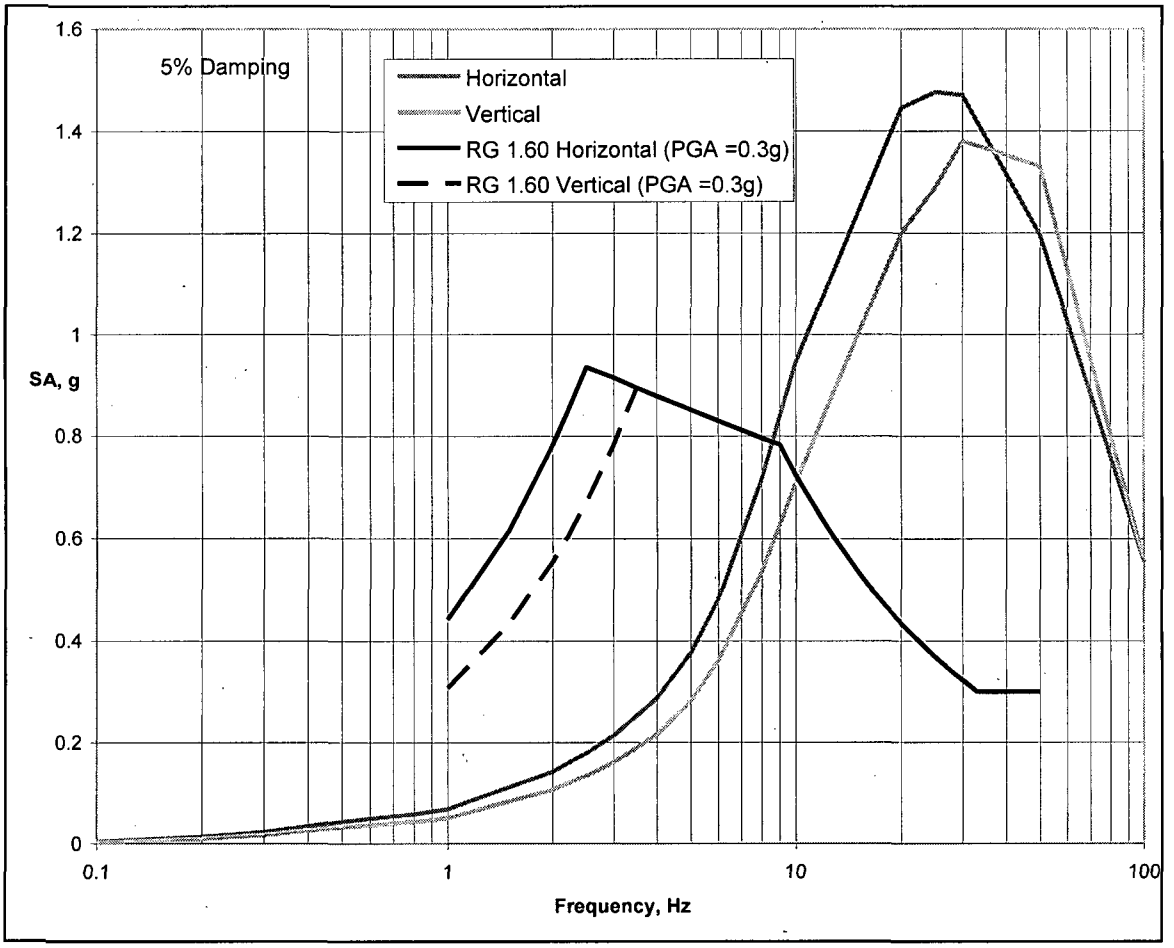

Figure 2-4
Site-Specific Response Spectra for Rock Site at Ground Surface (Depth 0-ft)

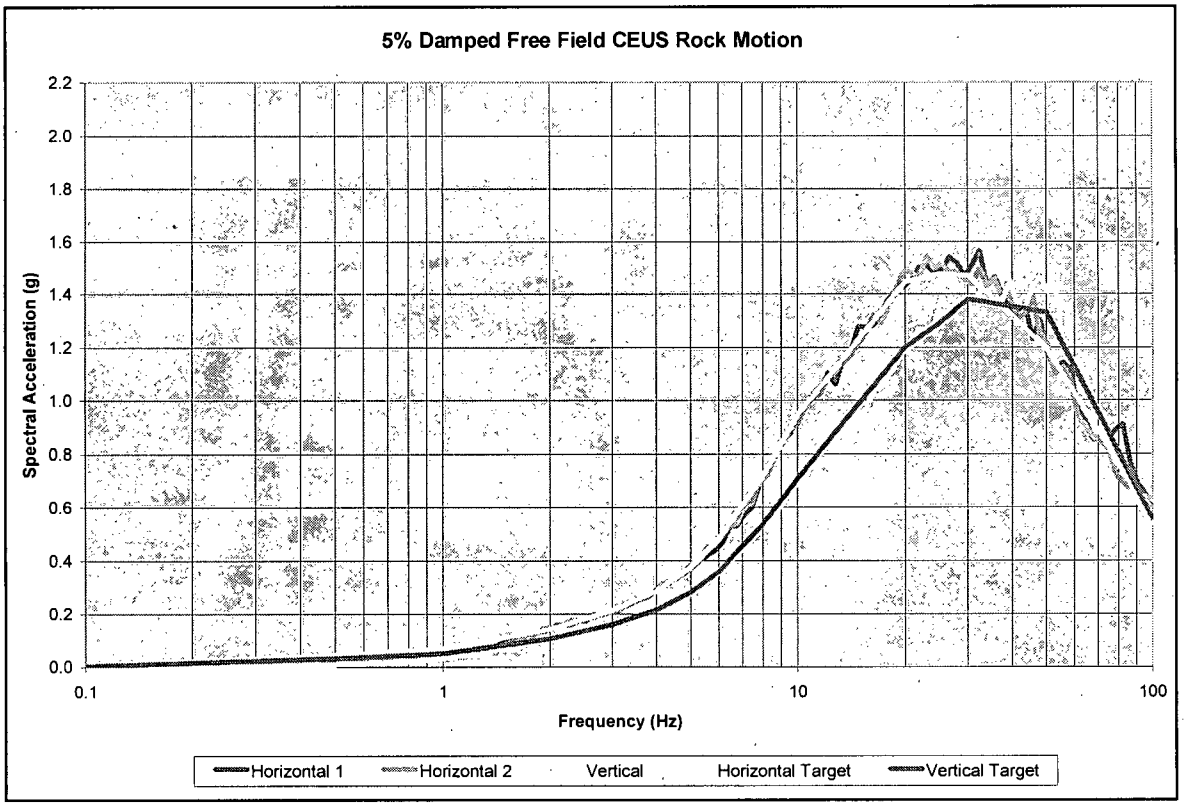

Figure 2-5
Computed and Target Response Spectra for Rock Site

Foundation Parameters

Initially, descriptions of two advanced reactor designs (AP1000 and ESBWR) were reviewed in order to understand the foundation and building configurations. Based on the foundation configurations presented for these two new plant designs, two foundations were studied - a rectangular foundation that is 225 x 100-ft in plan, and a square foundation that is 150 x 150-ft in plan. In addition, for validation purposes, a circular foundation footprint of the same area was considered. The foundation circle had a radius of 84.63 feet.

For the present phase of Task S2.1, the SSI seismic analyses, by CLASSI and SASSI, were performed for the 150-ft square foundation footprint. For these analyses, the foundation was assumed to be 15-ft thick. The resulting diagonal mass matrix terms are 1572 kip-sec^2/ft in the horizontal and vertical directions, 2.98 x 10^6 kip-ft-sec^2 about the horizontal axes, and 5.90 x 10^6 kip-ft-sec^2 about the vertical axes.

Structure Properties

Soil-structure interaction seismic analyses for the purpose of evaluating structure and foundation response including the effects of seismic wave incoherence have been performed using a stick model with three concentric sticks representing the Coupled Auxiliary and Shield Building (ASB), the Steel Containment Vessel (SCV), and the Containment Internal Structure (CIS). The original model (Orr, 2003) was modified to enable the appropriate effects of incoherence induced rotations. This model is illustrated in Figure 2-6 with model properties presented in Tables 2-3 and 2-4. Modifications to the original model include:

- At the top of the shield building, auxiliary building, steel containment vessel, and containment internal structure massless outrigger nodes have been added connected to the centerline by rigid links. The ASB and CIS outriggers extend 75 feet from the centerline in the X-direction. The SCV outrigger extends 65 feet from the centerline in the X-direction.

- Mass centers have been offset from the shear center at locations in the auxiliary building and the CIS to introduce natural torsion into the models. The shear centers of the three sticks are coincident along the Z-axis.

For CLASSI SSI seismic analyses, the structure properties input are described by the fixed-base dynamic modal properties including frequencies, mode shapes and participation factors. These dynamic properties were developed using the finite element program, SAP2000 (CSI, 2004). One hundred and sixty (160) modes were included with total mass participation in each direction of about 95 percent. The relative mass of the structures is approximately ASB – 86%, CIS – 11%, and SCV – about 3%.

The fixed-base modes of the three structure sticks provide some insight into their dynamic behavior. Fundamental fixed-base frequencies for each of the three structure concentric sticks are:

- Coupled Auxiliary and Shield Building (ASB)
  - X-Horizontal – 3.2 Hz
  - Y-Horizontal – 3.0 Hz
  - Z-Vertical – 9.9 Hz
- Steel Containment Vessel (SCV)
  - X-Horizontal – 5.5 Hz, 9.5 Hz, 9.9 Hz
  - Y-Horizontal – 6.10 Hz
  - Z-Vertical – 16.0 Hz
- Containment Internal Structure (CIS)
  - X-Horizontal – 13.3 Hz, 20.1 Hz, 28.9 Hz
  - Y-Horizontal – 12.0 Hz, 14.9 Hz, 17.5 Hz
  - Z-Vertical – 41.4 Hz

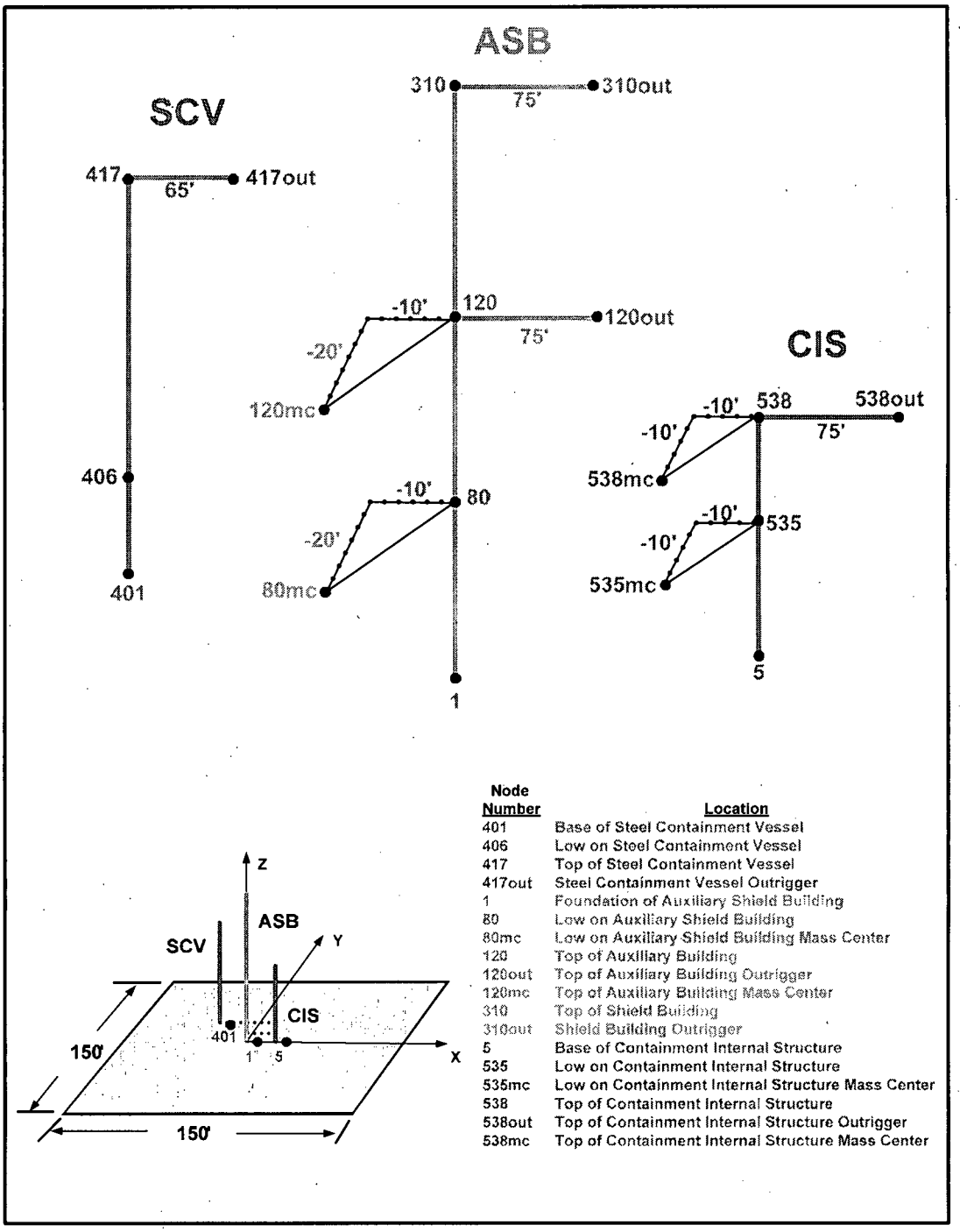

Node Number	Location
401	Base of Steel Containment Vessel
406	Low on Steel Containment Vessel
417	Top of Steel Containment Vessel
417out	Steel Containment Vessel Outrigger
1	Foundation of Auxiliary Shield Building
80	Low on Auxiliary Shield Building
80mc	Low on Auxiliary Shield Building Mass Center
120	Top of Auxiliary Building
120out	Top of Auxiliary Building Outrigger
120mc	Top of Auxiliary Building Mass Center
310	Top of Shield Building
310out	Shield Building Outrigger
5	Base of Containment Internal Structure
535	Low on Containment Internal Structure
535mc	Low on Containment Internal Structure Mass Center
538	Top of Containment Internal Structure
538out	Top of Containment Internal Structure Outrigger
538mc	Top of Containment Internal Structure Mass Center

Figure 2-6
Advanced Reactor Structure Stick Model with Outriggers and Offset Mass Centers

Table 2-3
Nodes and Mass Properties for Structural Model

				North-South Model			East-West Model		
NODE	**X**	**Y**	**Z**	**MX**	**MZ**	**Iy**	**MY**	**MZ**	**Ix**
ASB									
1	0	0	60.50						
11	0	0	66.50	236.400	236.400	1641500	236.400	236.400	466740
21	0	0	81.50	494.260	494.260	3612000	494.260	494.260	847820
31	0	0	91.50	307.080	439.280	1938300	307.080	439.280	456250
41	0	0	99.00	330.460	330.460	2619900	330.460	330.460	484190
51	0	0	106.17	210.100	210.100	1287500	210.100	210.100	390700
61	0	0	116.50	597.740	465.540	2526200	597.740	465.540	764330
80	0	0	134.87	0	441.849	3448492	0	441.849	710952
80mc	-10	-20	134.87	441.849	0	0	441.849	0	0
90	0	0	145.37	165.406	165.406	933560	165.406	165.406	293100
100	0	0	153.98	190.099	190.099	1022510	190.099	190.099	316650
110	0	0	164.51	164.371	164.371	422680	164.371	164.371	271344
120	0	0	179.56	0	200.431	323582	0	200.431	349825
120out	75	0	179.56	0	0	0	0	0	0
120mc	-10	-20	179.56	200.431	0.00	0.00	200.431	0.00	0.00
130	0	0	200.00	126.050	126.050	317710	126.050	126.050	317710
140	0	0	220.00	132.470	132.470	333900	132.470	132.470	333900
150	0	0	242.50	140.260	140.260	353540	140.260	140.260	353540
160	0	0	265.00	231.223	231.223	529020	231.223	231.223	529020
309	0	0	295.23	263.980	433.530	276470	263.980	433.530	276470
310	0	0	333.13	135.590	91.320	63050	135.590	91.320	63050
310out	75	0	333.13	0	0	0	0	0	0
320	0	0	296.77	0.000	0.000	0	0.000	0.000	0

				North-South Model			East-West Model		
NODE	**X**	**Y**	**Z**	**MX**	**MZ**	**Iy**	**MY**	**MZ**	**Ix**
CIS									
5	0	0	60.5						
500	0	0	66.5	595.3	593.4	568000	595.3	595.3	568000
531	0	0	82.5	927.6	927.6	1422000	927.6	927.6	137100
532	0	0	98	468.7	468.7	70800	468.7	468.7	680000
533	0	0	103	146.3	286.2	185000	146.3	286.2	177000
534	0	0	107.17	319.1	238.7	358900	319.1	238.7	319130
535	0	0	134.25	0	238.6	282150	0	238.6	255550
535mc	-10	-10	134.25	298.2	0	0	298.2	0	0

				North-South Model			East-West Model		
NODE	**X**	**Y**	**Z**	**MX**	**MZ**	**Iy**	**MY**	**MZ**	**Ix**
CIS									
536	0	0	153	14.6	14.6	2019	14.6	14.6	2504
537	0	0	153	30.8	30.8	6065	30.8	30.8	4321
538	0	0	169	0	9.4	748	0	9.4	696
538out	75	0	169	0	0	0	0	0	0
538mc	-10	-10	169	9.4	0	0	9.4	0	0

				North-South Model			East-West Model		
NODE	**X**	**Y**	**Z**	**MX**	**MZ**	**Iy**	**MY**	**MZ**	**Ix**
SCV									
401	0	0	100.000	1.739	1.739	3636	1.739	1.739	3636
402	0	0	104.125	5.541	5.541	11732	5.541	5.541	11732
403	0	0	110.500						
404	0	0	112.500	15.388	15.388	33362	15.388	15.388	33362
406	0	0	131.677	17.907	17.907	37914	17.907	17.907	37914
407	0	0	138.583						
408	0	0	141.500	17.904	17.904	38689	17.904	17.904	38689
409	0	0	162.000	18.349	18.349	38850	18.349	18.349	38850
410	0	0	169.927	28.994	28.994	61388	28.994	28.994	61388
411	0	0	200.000	28.340	28.340	60003	28.340	28.340	60003
412	0	0	224.000	40.251	51.739	81602	51.522	51.739	81602
413	0	0	224.208	15.746	15.746	33338	15.746	15.746	33338
414	0	0	255.021	11.271	11.271	21897	11.271	11.271	21897
415	0	0	265.833	10.288	10.288	14610	10.288	10.288	14610
416	0	0	273.833	10.070	10.070	8149	10.070	10.070	8149
417	0	0	281.901	5.618	5.618	0	5.618	5.618	0
417out	65	0	281.901	0	0	0	0	0	0
425	0	0	224.000	28.439	16.951		17.168	16.951	

Note: All values are in kip, seconds, feet units
Assume: **Iz = Ix + Iy**

Table 2-4
Element Properties for Structural Model

			North-South Model			East-West Model				
ELEM	**NODES**		**A**	**IYY**	**AshearY**	**A**	**IZZ**	**AshearZ**	**Material**	**Modal damping**
ASB										
1	1	11	15484.00	97176000	10322.67	15484.00	11236800	10322.67	Concrete	4 %
2	11	21	3462.50	6266240	1366.35	3462.50	4061440	1011.30	Concrete	4 %
3	21	31	3462.50	6266240	1366.35	3462.50	4061440	1011.30	Concrete	4 %
4	31	41	3462.50	6266240	1366.35	3462.50	4061440	1011.30	Concrete	4 %
5	41	51	3293.30	5744880	1214.35	3293.30	3562800	1008.14	Concrete	4 %
6	51	61	3293.30	5744880	1214.35	3293.30	3562800	1008.14	Concrete	4 %
7	61	80	3293.30	5744880	1214.35	3293.30	3562800	1008.14	Concrete	4 %
	80	80mc	Rigid Link							
31	80	90	3197.52	4196560	1185.61	3197.52	4412370	1360.04	Concrete	4 %
32	90	100	3197.52	4196560	1185.61	3197.52	4412370	1360.04	Concrete	4 %
33	100	110	2501.52	3676560	874.54	2501.52	3311570	1121.07	Concrete	4 %
34	110	120	1954.00	3083632	810.51	1954.00	3290960	746.70	Concrete	4 %
	120	120out	Rigid Link							
	120	120mc	Rigid Link							
35	120	130	1338.00	2700000	535.20	1338.00	2700000	535.20	Concrete	4 %
36	130	140	1338.00	2700000	535.20	1338.00	2700000	535.20	Concrete	4 %
37	140	150	1338.00	2700000	535.20	1338.00	2700000	535.20	Concrete	4 %
38	150	160	1338.00	2700000	535.20	1338.00	2700000	535.20	Concrete	4 %
301	160	309	50.45	1	0.000	50.45	1	0.000	Concrete	4 %
302	320	309	13.59	2680	10.872	13.59	2681.6	10.872	Concrete	4 %
303	309	310	704.50	431720	281.800	704.50	431720	281.800	Concrete	4 %
	310	310out	Rigid Link							
	160	320	Rigid	Rigid	Rigid	Rigid	Rigid	Rigid		

CIS										
500	5	500	15175	1.24E+07	9228.29	15175	1.11E+07	8311.88	Concrete	4 %
501	500	531	15175	1.24E+07	9228.29	15175	1.11E+07	8311.88	Concrete	4 %
502	531	532	6732	4.50E+06	2976.99	6732	3.33E+-6	2965.86	Concrete	4 %
503	532	533	7944	6.74E+06	4411.70	7944	5.95E+06	3948.04	Concrete	4 %
504	533	534	5160	4.60E+06	3026.91	5160	2.93E+06	2702.19	Concrete	4 %
505	534	535	1705	7.83E+05	613.65	1705	5.75E+05	405.33	Concrete	4 %
	535	535mc	Rigid Link							
506	535	536	326	3.15E+03	13.10	326	1.77E+04	67.36	Concrete	4 %
507	535	537	484	3.89E+04	93.98	484	1.58E+04	64.30	Concrete	4 %
508	537	538	164	2.11E+03	29.24	164	2.47E+03	17.16	Concrete	4 %
	538	538out	Rigid Link							

CIS										
	538	538mc	Rigid Link							
506	535	536	326	3.15E+03	13.10	326	1.77E+04	67.36	Concrete	4 %
507	535	537	484	3.89E+04	93.98	484	1.58E+04	64.30	Concrete	4 %
508	537	538	164	2.11E+03	29.24	164	2.47E+03	17.16	Concrete	4 %

			North-South Model			East-West Model				
ELEM	**NODES**		**A**	**IYY**	**AshearY**	**A**	**IZZ**	**AshearZ**	**Material**	**Modal damping**
SCV										
401	401	402	14.49	29,107	27.6	14.49	29,107	27.6	Steel	4 %
402	402	403	59.63	126,243	29.81	59.63	126,243	29.81	Steel	4 %
403	403	404	59.63	126,243	29.81	59.63	126,243	29.81	Steel	4 %
405	404	406	59.63	126,243	29.81	59.63	126,243	29.81	Steel	4 %
406	406	407	59.63	126,243	29.81	59.63	126,243	29.81	Steel	4 %
407	407	408	59.63	126,243	29.81	59.63	126,243	29.81	Steel	4 %
408	408	409	59.63	126,243	29.81	59.63	126,243	29.81	Steel	4 %
409	409	410	59.63	126,243	29.81	59.63	126,243	29.81	Steel	4 %
410	410	411	59.63	126,243	29.81	59.63	126,243	29.81	Steel	4 %
411	411	412	59.63	126,243	29.81	59.63	126,243	29.81	Steel	4 %
412	412	413	59.63	126,243	29.81	59.63	126,243	29.81	Steel	4 %
413	413	414	13.15	110,115	27.1	13.15	110,115	27.1	Steel	4 %
414	414	415	4.58	83,714	24.6	4.58	83,714	24.6	Steel	4 %
415	415	416	1.74	46,047	19.89	1.74	46,047	19.89	Steel	4 %
416	416	417	0.55	13,850	8.56	0.55	13,850	8.56	Steel	4 %
	417	417out	Rigid Link							
	Spring		Kz	Kx		Kz	Ky			
	412	425	27630	80439		27630	9467			4 %

Notes:

All values are in kip, seconds, feet units

Material properties:

Concrete:

Elastic modulus = 519,120 ksf

Poisson's ratio = 0.17

Steel:

Elastic modulus = 4,248,000 ksf

Poisson's ratio = 0.30

3
CLASSI TECHNICAL APPROACH

General

In order to incorporate seismic wave incoherence into seismic analyses, a stochastic approach has been employed as described in this chapter. This approach is described in detail in EPRI Report TR-102631 2225 (EPRI, 1997), authored by Tseng and Lilhanand, and briefly summarized in this chapter. By this approach, incoherency transfer functions have been developed for the rigid massless foundation and validated by comparison with published literature. As described in Chapter 2, coherency functions as a function of separation distance, frequency, apparent wave velocity, and direction of motion from Abrahamson (2005, 2006) are used as the basic input for all evaluations. The incoherency transfer functions have been generated for the rigid, massless foundation using the computer program, CLASSI. In addition, CLASSI has been used to evaluate seismic structural response of example rock/structure systems. The procedures used to evaluate incoherency transfer functions, to evaluate foundation response of rigid, massless foundations, and to evaluate structure and foundation response of example structural models accounting for soil-structure interaction and seismic wave incoherence are described in this Chapter. Following the description, validation of the approach in CLASSI is presented through benchmarking of the response of the rigid, massless foundation, i.e., the incoherency transfer functions (ITFs), for circular and square foundations by comparison with published literature.

Incorporation of the Coherency Function into CLASSI Procedures

To utilize CLASSI (Wong and Luco, 1980), one must first define the foundation footprint plan dimensions, underlying soil layers with properties of density, shear wave velocity, Poisson's ratio, material damping, and layer thickness, and frequencies for analysis. The foundation footprint is divided into n sub-regions for input to CLASSI. The coherency function is evaluated at the mid-point of each of these sub-regions with the separation distance being the distance between all of the combinations of sub-region mid-points.

Based on the assumption that ground motions can be represented by a stationary random process, the coherency function between ground motions $x_i(t)$ and $x_j(t)$, denoted by $\gamma(f)$, is a complex function of frequency, f, defined by:

$$\gamma(f) = \frac{S_{ij}(f)}{\sqrt{S_{ii}(f) S_{jj}(f)}} \qquad \textbf{(Equation 3-1)}$$

in which S_{ij} is the cross power spectral density function between motions $x_i(t)$ and $x_j(t)$ and S_{ii} and S_{jj} are the power spectral density functions for motions $x_i(t)$ and $x_j(t)$ in the same orthogonal direction, respectively.

The matrix [γ] is evaluated as a 3n by 3n matrix of the Abrahamson coherency function based on the separation distances between sub-regions for each selected frequency and for input apparent wave velocity or slowness. It should be noted that the motions in each orthogonal direction are not correlated with each other, thus the cross terms involving xy (yx), xz (zx), or yz (zy) motions of the coherency matrix [γ] are taken as zero.

Since the coherency function is defined in terms of power spectral density functions it is necessary to consider the CLASSI procedures reformulated into a random vibration analysis approach.

General CLASSI Approach: Rigid Massless Foundation

Let the modification of the field-field surface motion due to the presence of the rigid surface inclusion be represented by six component vector $\{U_0\}$. The average free-field surface motion of each of n sub-regions that represents the interface of the rigid foundation area with the half-space surface is represented by the 3n component vector $\{U_n\}$. The motion of a reference point of the rigid inclusion $\{U_0\}$ in terms of the set of sub-region motions $\{U_n\}$ is related by the 6 x 3n scattering transfer function [F]:

$$\{U_0\} = [F]\{U_n\} \qquad \textbf{(Equation 3-2)}$$

It may be noted that the 3n x6 rigid body transformation array $[\alpha_b]$ is defined by:

$$\{U_n\} = [\alpha_b]\{U_0\} \qquad \textbf{(Equation 3-3)}$$

The matrix $[\alpha_b]$ is only a function of the foundation footprint geometry and the location of the n sub-regions and not of the properties of soil layers. As a result, comparison of Equations 3-2 and 3-3 shows that [F] must be independent of the soil conditions.

Using the CLASSI methodology, [F] is determined by:

$$[F] = [C]\,[T]^T \qquad \textbf{(Equation 3-4)}$$

where [C] is the 6 by 6 compliance matrix (equal to the inverse of the impedance matrix $[K]^{-1}$); and [T] is a 3n by 6 traction matrix representing contact tractions on all n sub-regions subjected to unit rigid body motions.

$$[T] = [G]^{-1}\,[\alpha_b] \qquad \textbf{(Equation 3-5)}$$

[G] is the 3n by 3n Green's function matrix containing displacement responses to unit harmonic loads on the surface of the soil/rock supporting the foundation and at each of the sub-regions and

$[\alpha_b]$ is a 3n by 6 rigid body transformation matrix. One of the program modules to CLASSI uses soil profile properties to determine the Green's function.

The 6 x 6 impedance matrix [K] relates the driving forces applied to the rigid inclusion, $\{P_0\}$ to the displacements of the rigid inclusion, $\{U_0\}$ by:

$$\{P_0\} \approx [K]\{U_0\} \qquad \textbf{(Equation 3-6)}$$

The impedance matrix may also be expressed in terms of the 3n x 3n array [G] of Green's functions integrated over each sub-region, and the 3n x6 rigid body transformation array $[\alpha_b]$ by:

$$[K] = [\alpha_b]^T[G]^{-1}[\alpha_b] \qquad \textbf{(Equation 3-7)}$$

Combining Equations 3-3, 3-6, and 3-7, it may be noted that $\{P_0\} = [\alpha_b]^T[G]^{-1}[\alpha_b]]\{U_0\} = [\alpha_b]^T[G]^{-1}\{U_n\}$. The array $[G]^{-1}[\alpha_b]$ may be identified as the 3n x 6 traction array [T] from Equation 3-5. Transposing Equation 3-5 gives $[T]^T = [\alpha_b]^T[G]^{-1}$. As a result:

$$\{P_0\} \approx [T]^T\{U_n\} \qquad \textbf{(Equation 3-8)}$$

Equating Equations 3-6 and 3-8 so that $\{P_0\} = [K]\{U_0\} = [T]^T\{U_n\}$, we may write express $\{U_0\}$ in terms of $\{U_n\}$ as:

$$\{U_0\} \approx [K]^{-1}[T]^T\{U_n\} = [C][T]^T\{U_n\} = [F]\{U_n\} \qquad \textbf{(Equation 3-9)}$$

where $[C] = [K]^{-1}$ is the 6 x6 compliance array of the rigid, massless foundation reference point. The scattering transfer function, [F] may be identified as $[C][T]^T$ which was stated in Equation 3-4.

From Equation 3-3, $\{U_n\} = [\alpha_b]\{U_0\}$. Multiplying both sides to this equation gives $[\alpha_b]^T\{U_n\} = [\alpha_b]^T[\alpha_b]\{U_0\}$. $\{U_0\}$can then be related to $\{U_n\}$ by $\{U_0\} = ([\alpha_b]^T[\alpha_b])^{-1}[\alpha_b]^T\{U_n\}$ which may be identified as the least squares solution for the average motion of the rigid surface foundation given the over-determined free-field motion of the n sub-regions $\{U_n\}$. Hence, from Equation 3-2, it may be seen that the scattering transfer function [F] is given by:

$$[F] = ([\alpha_b]^T[\alpha_b])^{-1}[\alpha_b]^T \qquad \textbf{(Equation 3-10)}$$

Equation 3-10 shows that the scattering transfer function is independent of any soil properties, being determined only by the rigid body kinematics of the rigid foundation motion. The use of the identity $[F] = [C][T]^T$ is actually equivalent to the least squares solution, and is a convenient means of computation for the scattering transfer function given the CLASSI computation of [K] and [T] for solution of the SSI problem.

CLASSI Random Vibration Approach: Rigid Massless Foundation

The PSD of the rigid massless foundation considering incoherent input motion is determined using $[S_{UG}]$, a 3n by 3n covariance matrix of actual incoherent ground motions as determined by Equation 3-11.

$$[S_{UG}] = [S_o^{1/2}] [\gamma] [S_o^{1/2}] \quad \textbf{(Equation 3-11)}$$

where $[S_o^{1/2}]$ is a 3n by 3n on-diagonal PSD matrix on the input ground motion and $S_o(f)$ is the power spectral density of the input free-field ground motion.

$[S_{Uo}]$, the 6 by 6 cross PSD of rigid massless foundation motion is determined from:

$$[S_{Uo}] = [F] [S_{UG}] [FC]^T \quad \textbf{(Equation 3-12)}$$

where [F] is taken as the 6 by 3n scattering transfer function matrix relating sub-region displacements to rigid body displacements, along with its complex conjugate [FC], which is determined in the manner described above.

CLASSI is used to evaluate the impedance matrix [K] and the traction matrix [T] at each selected frequency. Normal outputs are impedance and scattering matrices. Also, [T], a Green's function matrix [G], and $[\alpha_b]$ are generated internally by the program. Input is the foundation footprint and the definition of sub-regions along with soil properties. For this study, the foundation footprint was divided into 10-ft square sub-regions. Around the periphery of the foundation, the outside 10-ft was further divided into 5-ft square sub-regions. A sensitivity study was performed on the number of sub-regions and concluded that this discretization was adequate.

CLASSI Random Vibration Approach: Foundation and Structure Response

The 6 by 6 cross PSD of foundation response motion, $[S_{UF}]$ may be determined by pre-multiplying $[S_{Uo}]$, the 6 by 6 cross PSD of rigid massless foundation motion by $[H_F]$ a 6 by 6 transfer function matrix between foundation response and the scattered foundation input motions and post-multiplying by $[H_FC]$, the complex conjugate of $[H_F]$:

$$[S_{UF}] = [H_F] [S_{Uo}] [H_FC]^T \quad \textbf{(Equation 3-13)}$$

The foundation transfer function matrix is given by:

$$[H_F] = ([I]-\omega^2 [C] ([M_b] + [M_s(f)]))^{-1} \quad \textbf{(Equation 3-14)}$$

In the above equation, [I] is an identity matrix, ω is the frequency of interest in radians per second, [C] is the compliance matrix previously defined, $[M_b]$ is the 6 by 6 diagonal mass matrix containing the foundation mass and mass moment of inertia, and $[M_s(f)]$ is the 6 by 6 equivalent mass matrix of the structure about its base computed by:

$$[M_s] = [\alpha_s]^T [M] [\alpha_s] + [\Gamma_s]^T [D(f)] [\Gamma_s] \quad \textbf{(Equation 3-15)}$$

where [D(f)] is the k by k diagonal modal amplification matrix (k is the number of fixed-base structure modes) given by:

$$[D] = \left[\frac{(\omega/\omega_r)^2}{\left(1 - \frac{\omega^2}{\omega_r^2}\right) + 2i\beta_r(\omega/\omega_r)} \right] \quad \text{where r goes from 1 to k} \quad \textbf{(Equation 3-16)}$$

$[\alpha_s]$ is a q by 6 rigid body transformation matrix of the structure about its base where q is the number of structure dynamic degrees of freedom above its base. $[\alpha_s]$ is given by:

$$[\alpha_s] = \begin{bmatrix} \cdots\cdots & & & & & \\ \cdots\cdots & & & & & \\ 1 & 0 & 0 & 0 & z^j & -y^j \\ 0 & 1 & 0 & -z^j & 0 & x^j \\ 0 & 0 & 1 & y^j & -x^j & 0 \\ 0 & 0 & 0 & 1 & 0 & 0 \\ 0 & 0 & 0 & 0 & 1 & 0 \\ 0 & 0 & 0 & 0 & 0 & 1 \end{bmatrix} \quad \textbf{(Equation 3-17)}$$

where j goes from 1 to q, the number of structure nodes with coordinates x, y, and z. $[\Gamma s]$ is a k by 6 matrix of modal participation factors given by:

$$[\Gamma_s] = [\phi_s]^T [M] [\alpha_s] \quad \textbf{(Equation 3-18)}$$

in which $[\phi_s]$ is the q by k fixed-base mode shape matrix of the structure and [M] is the q by q structure mass matrix.

The q by q cross PSD of structural response motion, $[S_{US}]$ is determined by pre-multiplying $[S_{Uo}]$, the 6 by 6 cross PSD of rigid massless foundation motion by $[H_T]$ (a q by 6 transfer function matrix between structural response and the scattered foundation input motions) and post-multiplying by $[H_TC]$, the complex conjugate of $[H_T]$:

$$[S_{Us}] = [H_T] [S_{Uo}] [H_TC]^T \quad \textbf{(Equation 3-19)}$$

The structure transfer function matrix is given by:

$$[H_T] = ([\alpha_s] + [\phi_s] [D] [\Gamma_s]) [H_F] \quad \textbf{(Equation 3-20)}$$

where all matrices and terms have been previously defined.

Procedure to Evaluate the Incoherency Transfer Function (ITF)

The diagonal terms of $[S_{Uo}]$, the 6 by 6 cross PSD of rigid massless foundation motion, given by Equation 3-12, provide the spectral density functions for the constrained rigid body motion of the reference point of the rigid massless foundation. If these terms are normalized by the respective free-field functions (two horizontal and torsion terms normalized by the horizontal free-field PSD; vertical and two rocking terms normalized by the vertical free-field PSD), then the square root of these normalized terms may be interpreted as transfer functions (Luco and Wong, 1986). Symbolically, the normalization can be accomplished by consideration of the evaluation of Equation 3-12 using a unit PSD input function.

The incoherency transfer function, ITF(f) is then defined as the amplitude of the square root of the diagonal terms of $[S_{UoI}]$ where $[S_{UoI}]$ is the 6 by 6 cross PSD matrix of rigid massless foundation motion subjected to unit PSD input.

$$[S_{UoI}] = [F]\,[S_{UGI}]\,[FC]^T \qquad \textbf{(Equation 3-21)}$$

where [F] is a 6 by 3n scattering transfer function matrix relating sub-region displacements to rigid body displacements and [FC] is the complex conjugate of [F] and $[S_{UGI}]$ is a 3n by 3n covariance matrix of incoherent ground motions for unit PSD input given by [I] [γ] [I] where [I] is an identity matrix.

The difference between $[S_{UGI}]$ and $[S_{UG}]$, used in Equation 3-12, is that the identity matrix, [I] is used instead of $[S_o^{1/2}]$. The procedure used is shown in Table 3-1.

Based on CLASSI determined [K], [T], [G], and $[\alpha_b]$ the 6 by 6 cross PSD, $[S_{UoI}]$ of the rigid massless foundation to unit PSD input due to incoherent input motion is generated. For this purpose, the coherency matrix, [γ], the covariance matrix for unit PSD input, $[S_{UGI}]$ and the scattering transfer function, [F] are evaluated. Also, incoherency transfer function, ITF, which is equal to the amplitude of the square root of the diagonal terms of $[S_{UoI}]$ is calculated.

Table 3-1
Procedure to Evaluate Incoherency Transfer Function

• Define soil profile and specify properties by soil layers Define foundation footprint and specify as n sub-regions
• Input coherency function, $\gamma(f,s)$ as a function of frequency, f and separation distance, s
• Run CLASSI modules to evaluate the impedance matrix and Green's function matrix
• From Green's function matrix and rigid foundation assumption, evaluate the traction matrix, [T]. Invert the impedance matrix to evaluate the compliance matrix, [C]
• Evaluate $[S_{UoI}]$, the cross PSD matrix of rigid massless foundation motion subjected to unit PSD input $[S_{UoI}] = [F]\,[S_{UGI}]\,[FC]^T$ where $[F] = [C]\,[T]^T$ and $[S_{UGI}] = [I]\,[\gamma]\,[I]$
• Evaluate the incoherency transfer function, ITF(f) as the amplitude of the complex square root of the diagonal terms of $[S_{UoI}]$

Procedure to Evaluate the Foundation and Structure Incoherent Response Spectra by CLASSI

The complete random vibration approach could be employed to generate foundation and structure response including the conversion of ground motion response spectra into power spectral density functions (PSDFs)and reversing the process at the foundation and structure response locations. However, the formulation of CLASSI and its ease of use permitted implementation of a more direct approach to the SSI analysis of structure/foundation.

In general, the CLASSI program modules generate the complex impedance and scattering matrices at each frequency considered. The impedance matrix represents the stiffness and energy dissipation of the underlying soil medium. The foundation input motion is related to the free-field ground motion by means of a transformation defined by a scattering matrix. The term "foundation input motion" refers to the result of kinematic interaction of the foundation with the free-field ground motion. In general, the foundation input motion differs from the free-field ground motion in all cases, except for surface foundations subjected to vertically incident coherent waves. The soil-foundation interface scatters waves because points on the foundation are constrained to move according to its geometry and stiffness. Modeling of incoherent ground motions is one aspect of this phenomena and the focus of this study.

In essence, the incoherency transfer function may be interpreted as a scattering matrix accounting for the effects of seismic wave incoherency over the dimensions of the foundation. For this application, a 6 by 6 complex incoherency transfer function matrix [ITF] is evaluated by taking the square root of the diagonal terms of $[S_{UoI}]$, the 6 by 6 complex cross PSD matrix of rigid massless foundation motion to unit PSD input for each direction of translational input. Since the free-field motions are uncorrelated in each orthogonal direction, we may consider the evaluation of Equation 3-21 using each free-field input direction separately. Three sets of ITF vectors are obtained by taking the square root of each PSD evaluation. The CLASSI scattering

matrix (6 x 3) is comprised of 3 vectors each of which determines the foundation input motion for the three components of free-field ground motion. Each vector of the scattering matrix is replaced by the incoherency transfer function vectors that correspond to each component of free-field ground motion. Each frequency is treated independently. CLASSI SSI analyses are then performed in a conventional manner to evaluate the structure and foundation in-structure response spectra. CLASSI solves the SSI problem in the frequency domain. Ground motion time histories are transformed into the frequency domain, SSI parameters (impedances and scattering matrices) are complex-valued, frequency-dependent, and the structure is modeled using its fixed-base eigen-systems.

Two variations of the CLASSI approach have been implemented and applied to the example structure. The difference in the two approaches is the treatment of the phase of the foundation scattering terms or ITFs. The following describes the two approaches:

- CLASSIinco – Retain the deterministic phasing of the foundation scattering functions as determined from the complex square root of the diagonal terms of the matrix [S_{UoI}]. This is most appropriate for the case of phenomena, such as wave passage. However, the benchmarking of EPRI and USDOE (2006) and those presented herein demonstrate its validity in producing engineering acceptable solutions in many situations for seismic wave incoherence effects. Table 3-2 summarizes this approach.
- CLASSIinco-SRSS – SRSS combination of the structure response induced by the individual foundation scattering terms (ITFs) applied independently, i.e., assuming the relationship between the phases of the scattering terms behaves randomly. This results in performing six SSI analyses for each direction of ground motion and SRSSing the end quantity of interest. In this report, the end items of interest are in-structure response spectra. Table 3-3 summarizes this approach.

In CLASSI, the dynamic characteristics of the structures to be analyzed are described by their fixed-based eigen-system and modal damping factors. Modal damping factors are the viscous damping factors for the fixed-base structure expressed as a fraction of critical damping. The structures' dynamic characteristics are then projected to a point on the foundation at which the total motion of the foundation, including SSI effects, is determined.

The final step in the CLASSI substructure approach is the actual SSI analysis. The results of the previous steps – foundation input motion (scattering matrix defined by the incoherency transfer function), foundation impedances, and structure model – are combined to solve the equations of motion for the coupled soil-structure system. For a single rigid foundation, the SSI response computation requires solution of, at most, six simultaneous equations – the response of the foundation. The derivation of the solution is obtained by first representing the response in the structure in terms of the foundation motions and then applying that representation to the equation defining the balance of forces at the soil/foundation interface. The formulation is in the frequency domain. Once the foundation motion is calculated (including all aspects of SSI), in-structure responses are determined for locations of interest in the structure, i.e., by solving the dynamic equations of motion in modal coordinates for the base excited system. The resulting in-structure response spectra at structure and foundation locations of interest include the effects of soil-structure interaction and seismic wave incoherence.

Table 3-2
Procedure to Evaluate the Foundation and Structure Incoherent Response Spectra by CLASSIinco

• Define free-field ground motion time histories compatible with response spectra, [Rs_o]
• Define soil profile and specify properties by soil layers Define foundation footprint and specify as n sub-regions Define foundation thickness and mass properties Define a fixed-base structural model
• Input coherency function, $\gamma(F,S)$ as a function of frequency, F and separation distance, S
• Run CLASSI modules to evaluate the impedance matrix
• Evaluate the scattering matrix as the incoherency transfer function. Each column of the scattering matrix corresponds to a direction of input excitation and is given by the diagonal terms from the incoherency transfer function at each frequency of interest.
• Evaluate fixed-base modal properties of the structure
• Run CLASSI modules that combine the structure properties, impedance matrix, scattering matrix, and input time histories, and evaluates output time histories
• Run standard response spectrum evaluation program to determine in-structure response spectra for the foundation and structure locations

Table 3-3
Procedure to Evaluate the Foundation and Structure Incoherent Response Spectra by CLASSIinco-SRSS

• Define free-field ground motion time histories compatible with response spectra, [Rs_o]
• Define soil profile and specify properties by soil layers Define foundation footprint and specify as n sub-regions Define foundation thickness and mass properties Define a fixed-base structural model
• Input coherency function, $\gamma(F,S)$ as a function of frequency, F and separation distance, S
• Run CLASSI modules to evaluate the impedance matrix
• Evaluate the scattering matrix as the incoherency transfer function. Each column of the scattering matrix corresponds to a direction of input excitation and is given by the diagonal terms from the incoherency transfer function at each frequency of interest.
• Evaluate fixed-base modal properties of the structure
• Run CLASSI modules that combine the structure properties, impedance matrix, scattering matrix, and input time histories, and evaluates output time histories. Perform analyses with CLASSI for each component of the scattering matrix independently (for three components of free-field motion and a 3D structure, eighteen CLASSI analyses are performed.
• Run standard response spectrum evaluation program to determine in-structure response spectra for the foundation and structure locations for each of the eighteen analysis results.. Perform SRSS of the ISRS.

Validation of Rigid, Massless Foundation Response

Objective and Scope

The objective of this validation effort is to benchmark the procedure and results generated with CLASSI versus published literature. This version of CLASSI is denoted CLASSIinco for the purpose of identification. The theory and development of CLASSIinco is described in detail in the preceding sections.

The quantities of interest for benchmarking are the Incoherent Transfer Functions (ITFs), scattering functions in CLASSI nomenclature. Incoherent Transfer Functions relate the free-field ground motion to the response of a rigid massless foundation taking into account the spatial incoherence of the ground motion. One aspect of the benchmark problems is simplified, specifically the supporting media is a uniform visco-elastic half-space with the following properties:

Shear Wave Velocity, Vs = 6300 ft/sec = 1920.24 m/sec

Mass Density, ρ = .004969 k-sec2/ft4

Poisson's Ratio, ν = 0.33

Damping, ξ = 0.01

Two foundation shapes are considered – a circular rigid disk of radius of 84.63 ft. and a square foundation 150 ft. on a side. These foundations have equal areas – 22,500 ft.*ft. The foundations are founded on the surface of the half-space. The ITFs of interest are the horizontal, vertical, rocking, and torsion components. Torsion is induced by the spatial incoherence of the horizontal ground motion. Rocking is induced by the spatial incoherence of the vertical ground motion. The bases of comparison are: Luco and Mita (1987) and Veletsos and Prasad (1989) for the circular disk; and Luco and Wong (1986) for the square foundation.

Ground Motion Coherence Function

The form of the ground motion coherency functions (horizontal and vertical directions) is exponential decay as a function of frequency and distance between observation points:

$$\Gamma(|r1 - r2|,\omega) = \exp[-(\gamma\omega|r1 - r2|/Vs)^2] \qquad \text{(Equation 3-22)}$$

where $|r1 - r2|$ is the distance between points on the foundation (subregion centroids)

γ is a dimensionless incoherence parameter,

ω is the angular frequency (radians/sec),

Vs is the representative shear wave velocity of the soil profile.

For benchmark purposes, calculations were made for values of $\gamma = 0.1, 0.2, 0.3, 0.4$ and 0.5.

Luco and Wong (1986) state that a reasonable value for γ might be

$$Vs * 2 \times 10^{-4} \text{ sec-m}^{-1} \leq \gamma \leq Vs * 3 \times 10^{-4} \text{ sec-m}^{-1}$$

For the uniform halfspace under consideration (Vs = 6300 ft/sec = 1920 m/sec), this yields a value of γ between about 0.4 and 0.6. Therefore, a value of $\gamma = 0.5$ is selected for comparison with the Abrahamson ground motion coherency function. However, comparison of ITFs are presented for the five values of γ.

The Abrahamson ground motion coherency functions, Equations 2-1 and 2-2, and Table 2-1, are compared with those of Equation 3-22 ($\gamma = 0.5$). The comparison of the Abrahamson ground motion coherency function for horizontal motion is plotted in Figure 3-1 for comparison with Equation 3-22 ($\gamma = 0.5$) for varying values of distance between observation points and frequency. One observes that for distances less than 50 m. and constant frequency, the Abrahamson coherency functions are significantly lower than Equation 3-1. For a distance of 50 m., the two functions are approximately the same. For distances greater than 50 m., the Abrahamson coherency functions are greater.

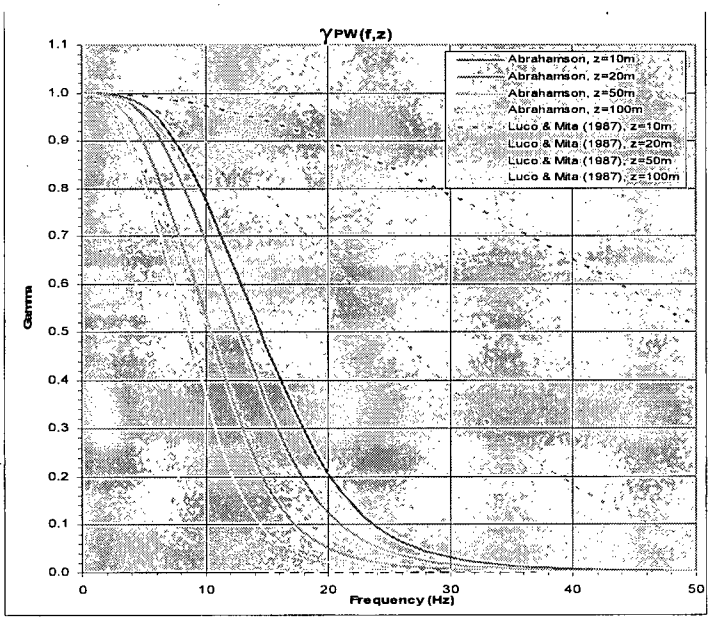

Figure 3-1
Comparison of coherency ground motion functions, horizontal direction – Abrahamson (2005, 2006) and Luco and Mita (1987) for $\gamma = 0.5$.

Comparison of ITFs

CLASSIinco, modified to implement the ground motion coherency function of Equation.3-22, is used to calculate the ITFs or scattering functions. In the ensuing paragraphs, comparisons are made for rigid, massless foundation response: horizontal motion due to horizontal input (S11), induced torsion due to horizontal input motion (S61), vertical motion due to vertical input motion (S33), and induced rocking due to vertical input motion (S43).

The frequency axis in Figures 3-24 through 6 and 10 through 13 is in terms of dimensionless frequency:

$a0 = \omega$ (rad/sec) * Cl / Vs

where

Cl = characteristic length = 84.63 ft.

Vs = 6300 ft/sec

The following table converts values of a0 to frequencies in Hz. for these cases.

Frequency (Hz)	a0
10	0.84404123
20	1.68808245
25	2.11010307
30	2.53212368
50	4.22020613

The legend in Figures 3-3 through 3-6 and 3-10 through 3-13 uses "g" to represent γ.

Circular disk.

The circular foundation model for the CLASSIinco analysis was discretized into 112 subregions as shown in Figure 3-2. This discretization was used in numerous previous studies, including as a foundation model of the Zion reactor building for the NRC Seismic Safety Margins Research Program.

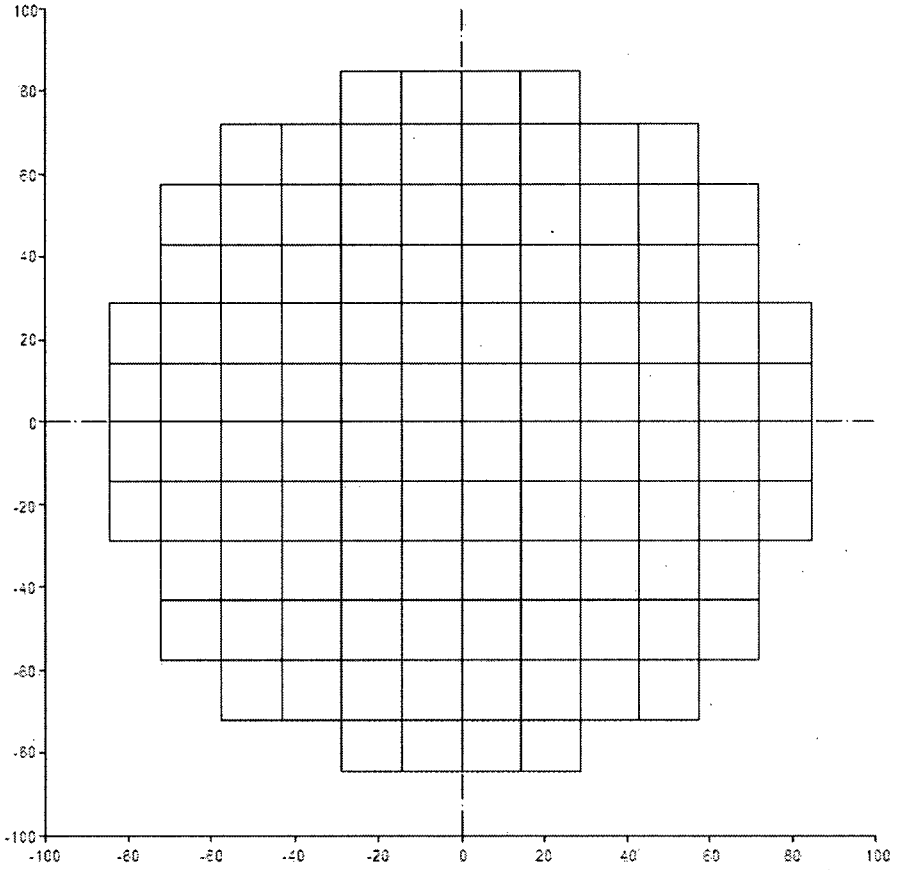

Figure 3-2
Foundation Model, Circular Disk, CLASSIinco.

For the circular disk, Figures 3-3 through 3-6 show the comparisons of the scattering functions calculated with CLASSIinco and those tabulated in Luco and Mita (1987) Table 1. Further, a comparison was made with the approach of Veletsos and Prasad (1989) shown in Figures 3-7 and 3-8.

The comparisons with Luco and Mita demonstrate excellent agreement for all four scattering terms.

Figures 3-7 and 3-8 show comparisons of the CLASSIinco scattering functions for rigid, massless foundation response – horizontal and induced torsion – due to horizontal input motion with those of Veletsos and Prasad (1989), Equations 9a and 9b. These comparisons are plotted as functions of the dimensionless frequency $\tilde{a}0 = a0*\gamma$ for $\gamma = 0.5$. In this case, the CLASSIinco responses for horizontal foundation response are very close. For induced torsion, the CLASSIinco results are slightly lower than the results of the approach of Veletsos and Prasad (a maximum of about 15%).

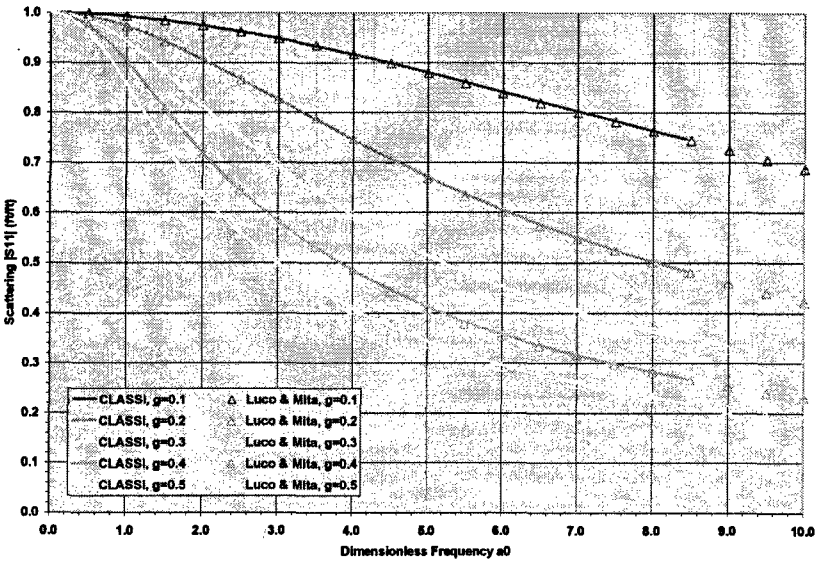

Figure 3-3
Circular Foundation, Comparison of CLASSIinco Results with Luco and Mita (1987), Horizontal Transfer Function S11.

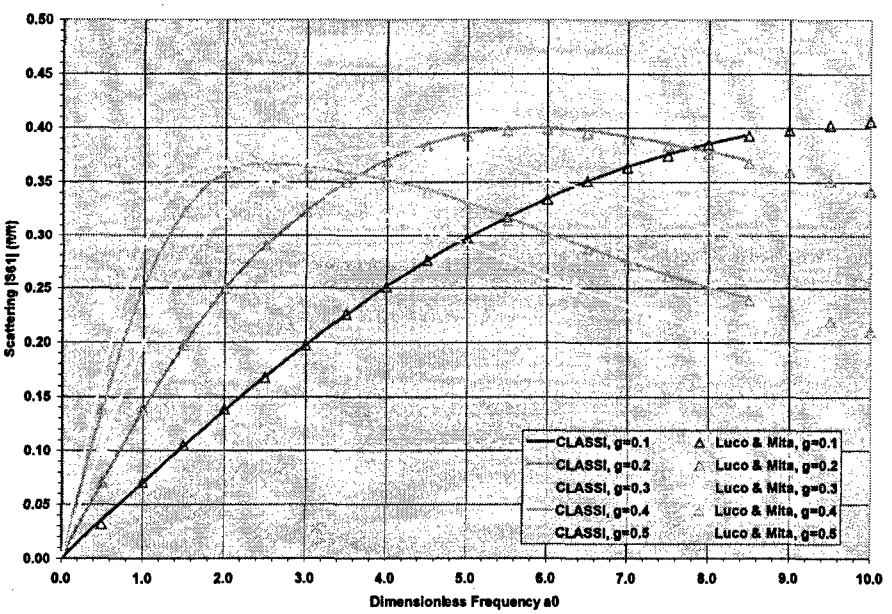

Figure 3-4
Circular Foundation, Comparison of CLASSIinco Results with Luco and Mita (1987), Torsional Transfer Function S61.

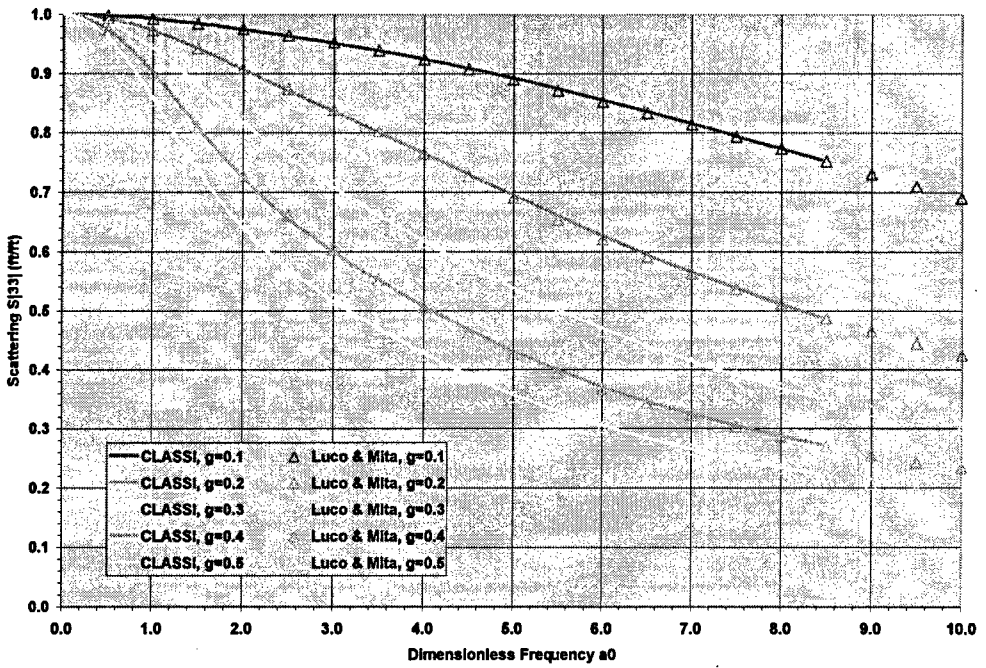

Figure 3-5
Circular Foundation, Comparison of CLASSIinco Results with Luco and Mita (1987), Vertical Transfer Function S33.

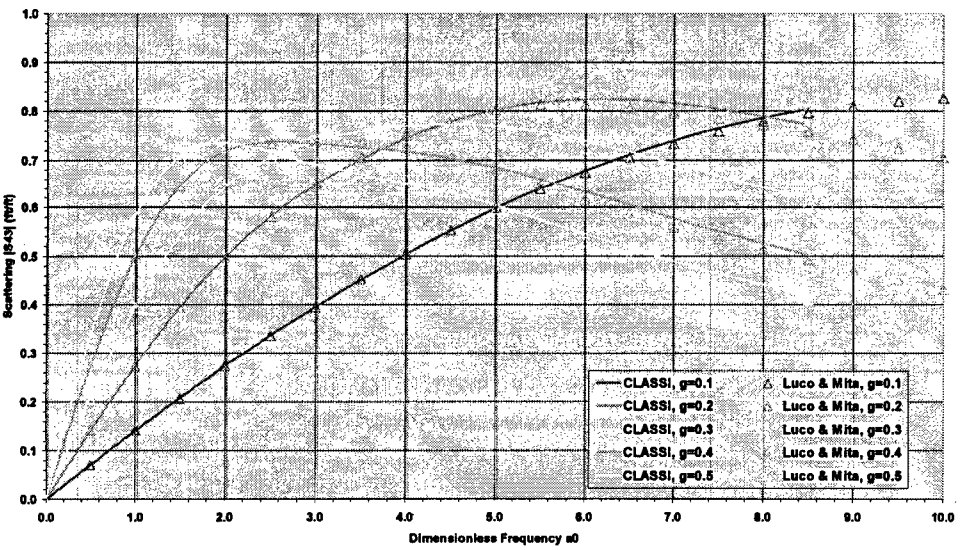

Figure 3-6
Circular Foundation, Comparison of CLASSIinco Results with Luco and Mita (1987), Rocking Transfer Function S43.

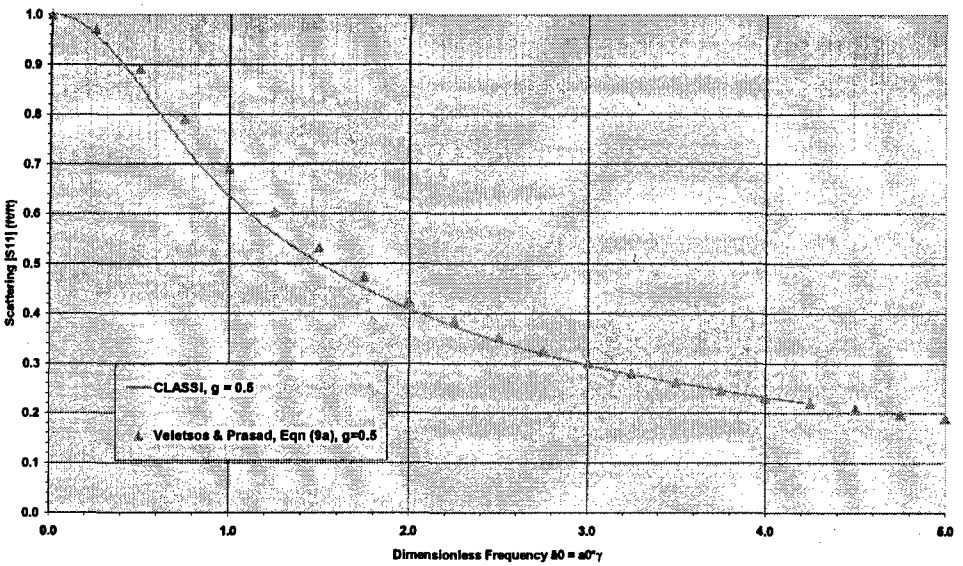

Figure 3-7
Circular Foundation, Comparison of CLASSIinco Results with Veletsos and Prasad (1989), Horizontal Transfer Function S11.

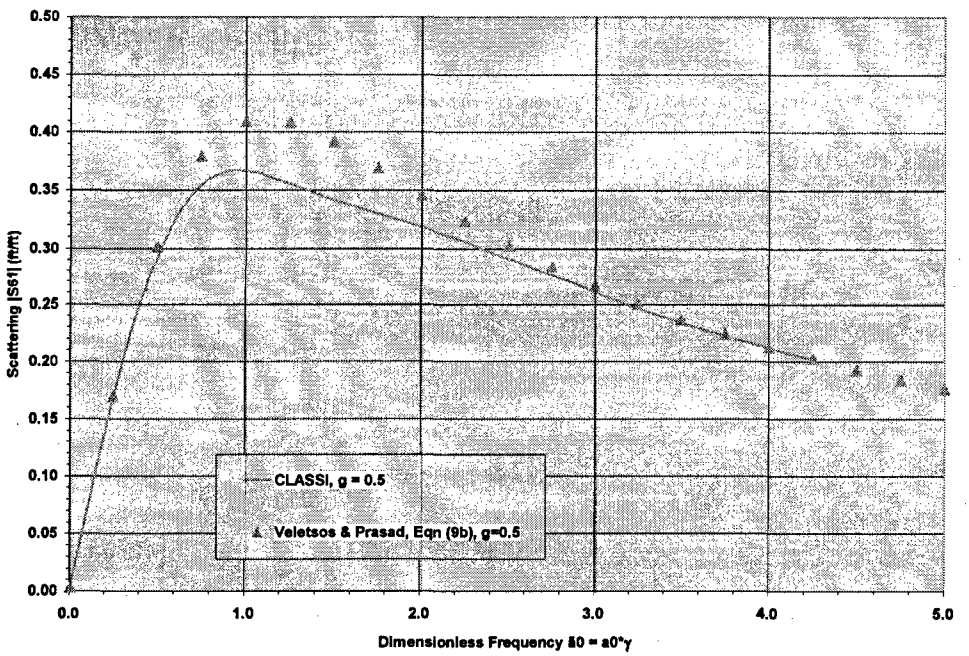

Figure 3-8
Circular Foundation, Comparison of CLASSIinco Results with Veletsos and Prasad (1989), Torsional Transfer Function S61

Square foundation.

The square foundation is the same as that used in the numerous sensitivity studies of EPRI and USDOE (2006) and in the current phase of the Program, i.e., 150 ft. on a side and discretized into 393 subregions as shown in Figure 3-9. The discretization consists of 169 (13 X 13) 10-ft square subregions surrounded by two rows of 5-ft square subregions. A sensitivity study confirmed the adequacy of this discretization during the execution of the effort reported in EPRI and USDOE (2006).

For the square foundation, the published data was taken from Luco & Wong (1986), Figures 2 and 3.

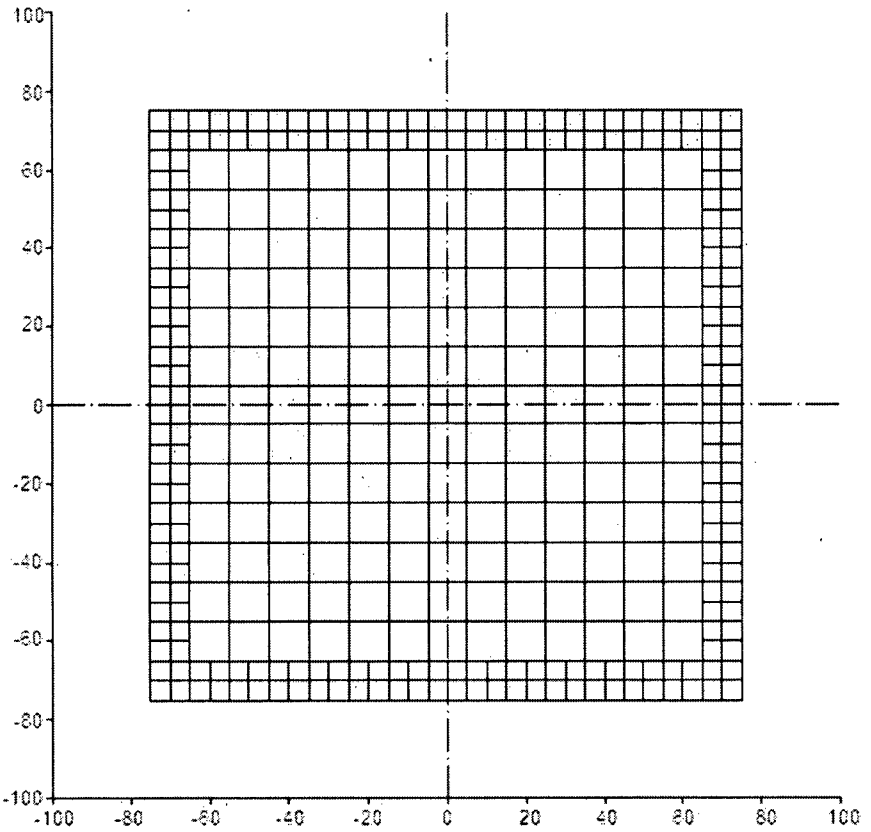

Figure 3-9
Square Foundation Model, CLASSIinco.

For the square foundation, Figures 3-10 through 3-13 show the comparisons of the scattering functions calculated with CLASSIinco and those reported in Luco and Wong (1986), Figures 2 and 3. Note, the values reported in Luco and Wong were only in graphical form. Hence, the values plotted herein were read from the curves in Figures 2 and 3.

In general, the comparisons with Luco and Wong show the CLASSIinco results for translational scattering functions to be slightly less and the corresponding induced rotations are somewhat more than the values reported by Luco and Wong. The fact that the CLASSIinco approach and the approach of Luco and Wong apply differing simplifications and discretizations of the foundation lead to the conclusion that the benchmark comparison is very good.

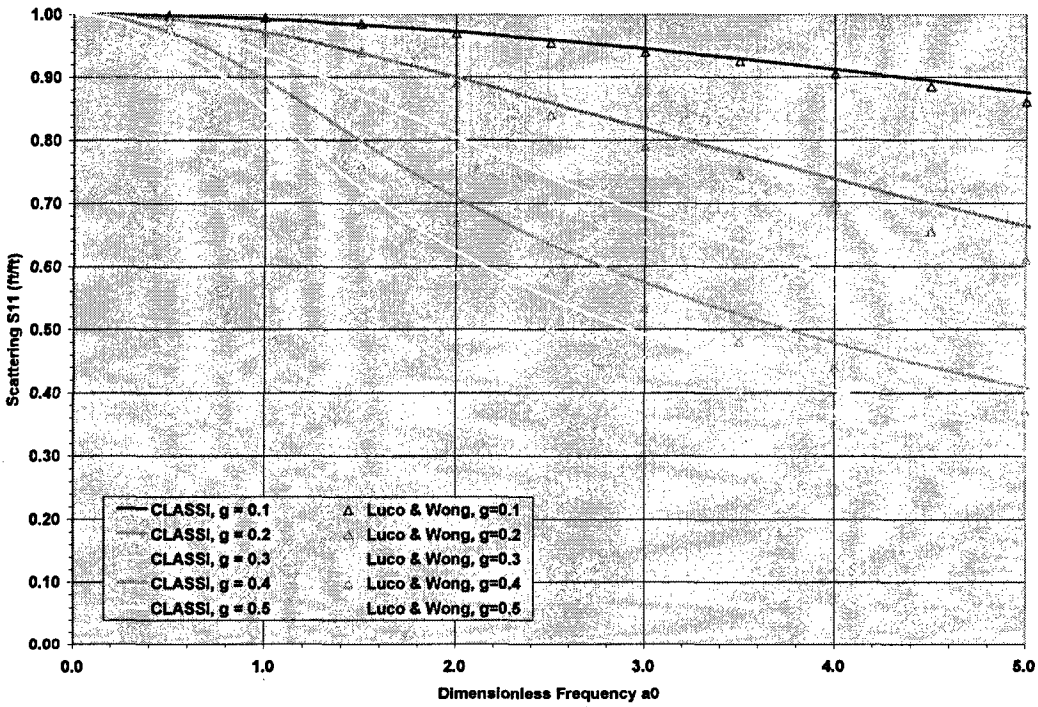

Figure 3-10
Square Foundation, Comparison of CLASSIinco Results with Luco and Wong (1986), Horizontal Transfer Function S11.

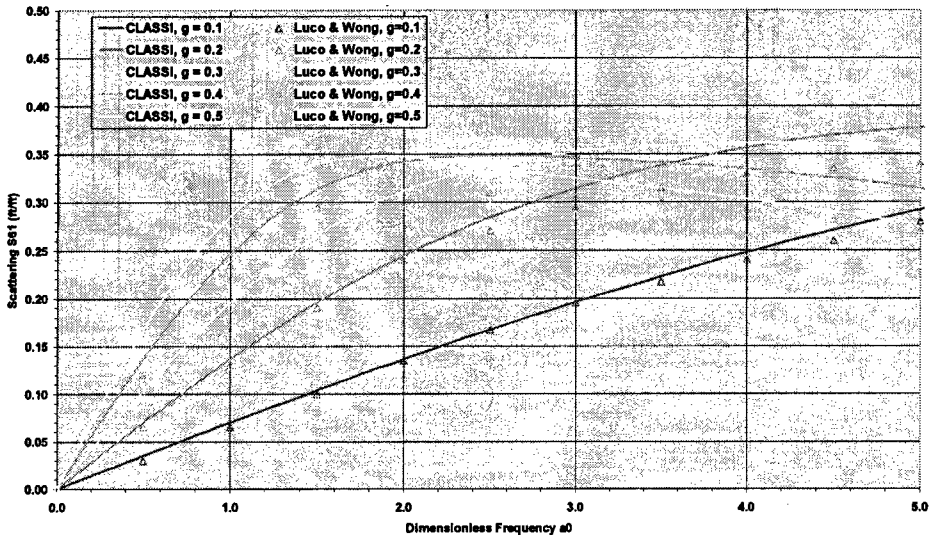

Figure 3-11
Square Foundation, Comparison of CLASSIinco Results with Luco and Wong (1986), Torsional Transfer Function S61.

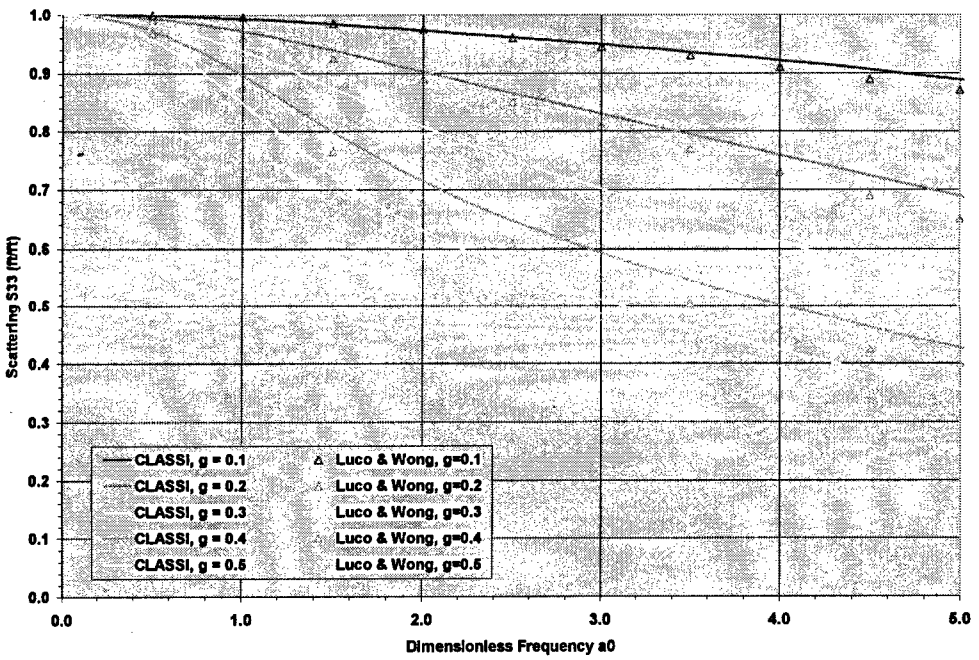

Figure 3-12
Square Foundation, Comparison of CLASSIinco Results with Luco and Wong (1986), Vertical Transfer Function S33.

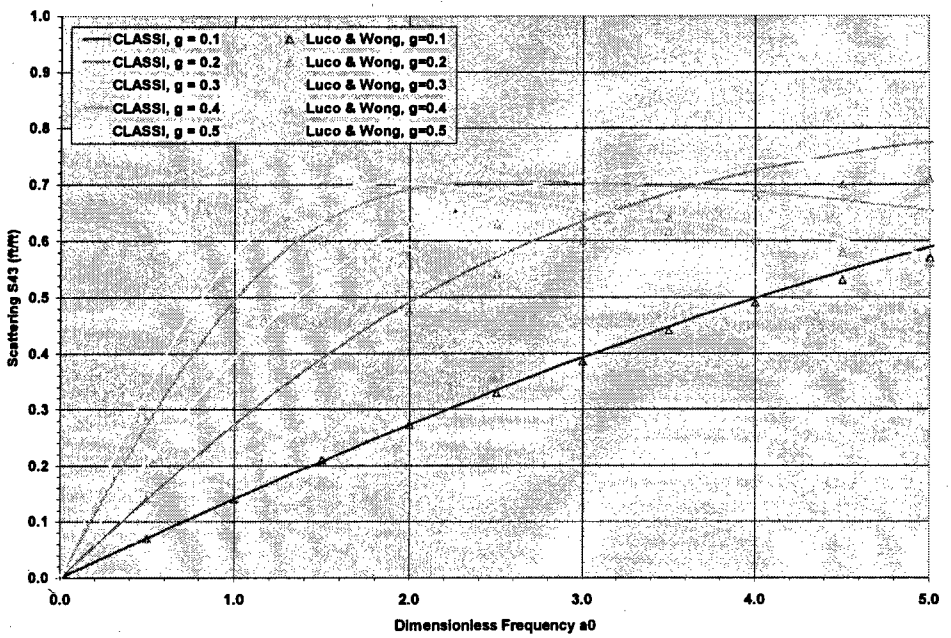

Figure 3-13
Square Foundation, Comparison of CLASSIinco Results with Luco and Wong (1986), Rocking Transfer Function S43.

Conclusions

The benchmark performed of the amplitudes of the Incoherency Transfer Functions calculated with CLASSIinco when compared with published literature validates the procedure and implementation in CLASSIinco.

4
SASSI TECHNICAL APPROACH

General

A parallel effort to the stochastic approach described in Chapter 3 is denoted "Deterministic Method" by Tseng and Lilhanand (EPRI, 1997) from which the derivation implemented in several versions of SASSI is based. The key elements of the approach are summarized here and follow directly the Tseng and Lilhanand derivation. Ghiocel (2004) presents theoretical aspects of the approach itemized in EPRI (1997) and provides the basis for the ACS SASSI treatment of the phenomena (Ghiocel, 2006). EPRI and USDOE (2006), Appendix C provides additional background on the SASSI analysis approaches. Tubino et al. (2003) present an approach to modeling multi-support systems accounting for spatial variation of input motion and lists several additional references on the subject.

The approaches described in Chapters 3 and 4 are general in the sense of treating local wave scattering and wave passage effects. However, as defined in Chapter 1, local wave scattering is the focus and ensuing discussion is limited to this case.

Coherency matrix

The starting point is the matrix $[\gamma]$, a $3N$ by $3N$ matrix of the Abrahamson coherency function based on the separation distances between the "N" SASSI interaction node point DOFs. The factor 3 is for the three directions of free-field ground motion. As in the case of the stochastic approach, the effects of incoherence of ground motion are uncoupled for the three directions of free-field ground motion. This parallels the analysis procedure typically used in SASSI, i.e., treating each of the three directions independently and combining the response results appropriately. At each discrete frequency, the matrix $[\gamma]$ of Chapters 3 and 4 is identical when the centroids of the sub-regions of the CLASSI analysis coincide with the locations of the SASSI interaction node points.

The CLASSI approach applies the constraint of the rigid foundation behavior to determine the amplitude of the tractions on each of the sub-regions which produce the rigid body motion and the CPSD of the motion of the rigid massless foundation. The SASSI approach utilizes the characteristics of the matrix $[\gamma(\omega)]$, specifically the assurance that it can be decomposed into its eigensystem (termed spatial modes), to provide computational efficiency in the SSI analysis. Whereas the CLASSI approach requires determination of the scale factors for the sub-region tractions, the SASSI approach proceeds along a parallel path where a number of analysis decisions are required, as described next.

Before proceeding, some important observations concerning the coherency matrix, $[\gamma(\omega)]$ and its decomposition into its eigensystem are stated:

1. For a given frequency ω the coherency matrix is independent of all other frequencies.

2. The matrix $[\gamma(\omega)]$ is Hermitian and positive-definite and therefore, can be decomposed into its complex eigenvalues and associated eigenvectors (Eqn. 3-19, EPRI, 1997):

   $([\gamma(\omega)] - \lambda_i^2[I])\ \{\phi(\omega)\}_i) = \{0\},\ i = 1,2,...N$ (Equation 4-1)

   Where $[\gamma(\omega)]$ is the (N x N) coherency matrix for N SASSI interaction node points and considering a single component of input motion, $\lambda_i(\omega)$ is the ith eigenvalue, and $\{\phi(\omega)\}_i$ is the (N x 1) corresponding eigenvector to $\lambda_i(\omega)$.

   If wave passage is not considered in the derivation of $[\gamma(\omega)]$, the eigensystem $[\phi(\omega)]$ and $[\lambda^2(\omega)]$ is real-valued.

3. Equation 3-22 of EPRI (1997) yields the reconstruction of the matrix $[\gamma(\omega)]$:

   $[\gamma(\omega)] = [\phi(\omega)]\ [\lambda^2(\omega)][\phi_c(\omega)]^T$ (Equation 4-2)

   Where$[\phi_c(\omega)]$ is the complex conjugate of $[\phi(\omega)]$ and "T" denotes transpose.

   This equation defines a check that may be performed on the calculated eigensystem to determine the accuracy of the calculated eigensystem to represent the coherency matrix $[\gamma(\omega)]$. This equation may also provide guidance on the number of spatial modes required to represent the matrix $[\gamma(\omega)]$, i.e., a check on the adequacy of a subset of spatial modes to represent $[\gamma(\omega)]$.

SASSI Approach

Derivation of the approach to address the effects of incoherency of ground motion on SSI analysis of foundations and structures as implemented in SASSI (EPRI version INCOH, Bechtel SASSI, and ACS SASSI) follows the approach of Tseng and Lilhanand (EPRI, 1997), Chap. 3 "Deterministic Method."

As noted above, the coherency matrix $[\gamma(\omega)]$ possesses special characteristics and thereby produces the following solution to the incoherent response at each SASSI interaction node, which follows the generalized solution denoted Karhunen-Loeve (KL) (Ghiocel, 2004). Further, given the eigensystem decomposition, the resulting expression for the incoherent motion at SASSI interaction node points is:

$\{U_g^I\} = [\phi(\omega)]\ [\lambda(\omega)]\ \{\eta_\theta(\omega)\}\ U_0(\omega)$ (Equation 2-3)

Where $\{\eta_\theta(\omega)\}$ is a (N x 1) random phase vector of the form $e^{i\theta(\omega)}$ for each spatial mode and θ is uniformly distributed from $-\pi$ to π - therefore a median value of η is unity, and $U_0(\omega)$ is the single ground motion component of interest. This expression includes all modes, but a subset could be assumed. This is Eqn. 3-29 of EPRI (1997).

In very general terms, this expression defines the transfer function of the input free-field ground motion to the interaction node points' degrees of freedom due to incoherence without effects of soil-structure interaction (SSI).

Approaches to Solve for SSI Response of Foundation and Structure

Recall that each frequency is treated independently and eigensystems or spatial modes are calculated independently for each frequency of solution. Therefore, in general, for N interaction degrees of freedom, there will be N spatial modes calculated at each solution frequency.

Three approaches have been identified as possible solution techniques.

Randomization (SASSI – Simulation Mean).

The randomization approach entails the following steps:

(i) For each SASSI frequency (rad/sec) to be solved explicitly - randomize the phase term in Equation 4-3 assuming a uniform distribution of the phase angle θ, sample the phase from this uniform distribution for each spatial mode of interest (N modes, if all are included), calculate the interaction node point transfer functions (input) from Equation 4-3 at this SASSI frequency (Equation 4-3 shows all spatial modes included, whereas, a subset may be considered, i.e., reduced to a limited number of spatial modes – it seems likely that a small number of spatial modes may be adequate at low frequencies, whereas, a larger number of modes may be necessary at higher frequencies). For this approach, the number of spatial modes included in the response calculation at each frequency does not dominate the computational effort – the number of simulations is the dominant factor.

(ii) Repeat this process for all SASSI frequencies.

(iii) An intermediate output of this process is one simulation of the transfer functions of interest, e.g., foundation quantities (translational or rotational displacements, velocities, accelerations) and in-structure quantities, e.g., displacements, velocities, accelerations. These transfer functions include all SSI effects.

(iv) Calculate SSI time history response of foundation and structure and derived quantities such as in-structure response spectra; this represents one realization or simulation of the process – one random sample.

(v) Repeat the process for an appropriate number of simulations to calculate the end responses of interest, e.g., peak values of displacements, accelerations, forces, or in-structure response spectra. Calculate statistics of these end items for use in the seismic design or qualification process. For this effort, we seek mean response conditional on the free-field ground motion. The input coherency ground motion functions are assumed to be mean. Hence, mean values of the responses of interest for seismic design should be calculated.

This approach appears to be straight-forward to implement, but computationally intensive. The results of 20 simulations of random phasing for vertical input to a rigid massless foundation are shown in Figures 4-1 and 4-2.

Results presented in Chapter 5 and Appendix A calculated by this approach are denoted SASSI – Simulation mean.

Figure 4-1
SASSI Calculated Foundation Transfer Function for Vertical Translation – Randomization (20 Simulations) (to be added)

Figure 4-2
SASSI Calculated Foundation Transfer Function for Induced Rocking due to Vertical Translation – Randomization (20 Simulations) (to be added)

The randomization approach can be considerably enhanced through advanced sampling techniques, interpolation schemes, etc.

Square Root of the Sum of the Squares (SASSI-SRSS)

Conceptually, the SRSS approach can be implemented at the transfer function or at the SSI dynamic response stage. Equation 4-4 (Equation 3-33, EPRI, 1997) is of interest:

$$\{Us(\omega)\}_i = [Hs(\omega)]\,[\phi(\omega)]_i\,[H^c(\omega)]\,\lambda_i(\omega)\,U_0(\omega);\ i = 1, 2, \ldots, m \qquad \text{(Equation 4-4)}$$

Where $\{Us(\omega)\}_i$ is the Fourier transform of the response at a given foundation/structure degree of freedom due to spatial mode i, $[Hs(\omega)]$ is the transfer function relating structure response to the input motion at the SASSI interaction nodes, $[H^c(\omega)]$ is the transfer function that relates the coherent ground motion vector at the SASSI interaction nodes to the control motion at the

reference station $U_0(\omega)$ accounting for wave passage effects (for no wave passage effects, this is unity), $[\phi(\omega)]_i$ and $\lambda_i(\omega)$ represent the spatial mode(s) i, and $\eta_\theta(\omega) = 1$, for all values of i.

SRSS Transfer Functions

For each SASSI frequency (rad/sec) to be solved explicitly:

(i) The transfer functions for foundation and structure response are calculated for each of the spatial modes independently assuming phase angle $\theta = 0$ and consequently $\eta_\theta(\omega) = 1$. The transfer function (complex-valued) calculated for each of the spatial modes assuming zero phase are combined by SRSS.

$$TFj(\omega) = \sqrt{\sum (\sum <Hsj(\omega)> \; [\{\phi_1(\omega)\,\lambda_1(\omega)\} \ldots \{\phi_i(\omega)\,\lambda_i(\omega)\} \ldots \{\phi_q(\omega)\,\lambda_q(\omega)\}])^2}$$

Where j denotes the foundation/structure degree of freedom of interest; Hsj is the transfer function between SASSI interaction nodes and response degree of freedom j (total of N SASSI interaction nodes) – Hsj is (1 x N); the inside summation is over the interaction node points 1 to N; the result is the transfer function for degree of freedom j due to each spatial mode i for a given ω; the outside summation represents the summation of these q values squared, q being the number of modes considered; and the square root of the result is taken.

(ii) Repeat this process for all SASSI frequencies.

(iii) The end result of steps (i) and (ii) are SRSS transfer functions for response quantities of interest of the foundation and structure.

(iv) Using these transfer functions, calculate SSI time history response of foundation and structure and derived quantities such as in-structure response spectra; this represents the SRSS response.

All results presented in Chapter 5 and Appendix A denoted SASSI – SRSS are for this approach.

SRSS – SSI Response

The SRSS – SSI response approach is the application of Equation 4-4, including the applying the condition of no wave passage, i.e., $U_0(\omega) = 1$, and $\eta_\theta(\omega) = 1$, for all values of i, to the stage of determining the Fourier transform of the response quantity of interest, performing the Inverse Fourier transform to calculate the time history of response, and then from this time history determining the specific item of interest, such as peak value, in-structure response spectrum, etc.

If all spatial modes were included at all SASSI frequencies, this would lead to q values of the response. These q values could then be SRSSed as the end product.

Tseng and Lilhanand (EPRI, 1997) applied this approach.

SRSS – Observations

For both SRSS approaches, the number of spatial modes to be considered in the response calculations is dictated by the number of modes required for accuracy at high frequencies. Even though a small number of spatial modes may be adequate for low frequencies the number of response simulations to be SRSSed is dictated by the higher frequencies.

Linear Algebraic Combination (SASSI – AS).

For each SASSI frequency to be solved explicitly, the Linear Algebraic Combination (algebraic sum) approach takes the phase angle associated with each spatial mode as zero ($\theta = 0$ and $\eta_\theta(\omega) = 1$). Consequently, the motion at each interaction node point degree of freedom is calculated by Equation 4-3 assuming a linear algebraic combination is applicable.

Advanced numerical techniques are applied to account for the appropriate phase relationship between spatial modes.

5
CLASSI AND SASSI IN-STRUCTURE RESPONSE SPECTRA COMPARISONS

General

CLASSI and SASSI computed incoherent seismic response were compared and shown to be in good agreement in EPRI and USDOE (2006). However, the example rock/structure model considered in those benchmark analyses did not produce significant incoherency-induced torsion and rocking response. The example rock/structure model used for benchmark comparisons in this study has offsets of mass centers from the shear centers and significant outriggers to overemphasize seismic response from incoherency-induced rotations as described in Chapter 2. It is judged that this example rock/structure model provides an extreme (conservative) level of torsion and rocking response induced by seismic wave incoherence for validation of either CLASSI or SASSI for seismic analysis.

Incoherency induced rotations are a random phenomena resulting from the horizontal spatial variation of ground motion over the foundation area. In addition, there are response quantities where several components of foundation motion contribute significantly such that the phasing of those components must be adequately represented in order to produce reasonable seismic response. Based on these considerations, two CLASSI methods as described in Chapter 3 and three SASSI methods as described in Chapter 4 are used herein for evaluating seismic response including seismic wave incoherence. These approaches include:

- CLASSIinco – deterministic phasing of foundation component response
- CLASSIinco-SRSS – SRSS combination of structural response computed from random phasing of foundation component response
- SASSI-SRSS – SRSS combination of modal transfer functions to represent random phasing of spatial modes
- SASSI Simulation Mean – Monte Carlo simulations to represent random phasing of spatial modes
- SASSI-AS – Algebraic summation of spatial modes with assumed deterministic phasing

Comparisons of seismic response by all of these methods are presented in Chapter 5 for the example nuclear power plant structure model as illustrated in Figure 5-1. Note that node numbers as used in CLASSI and SASSI analyses have been superimposed on this figure as compared to the similar figure in Chapter 2. These node numbers are referred to in the response spectra comparison figures of this chapter.

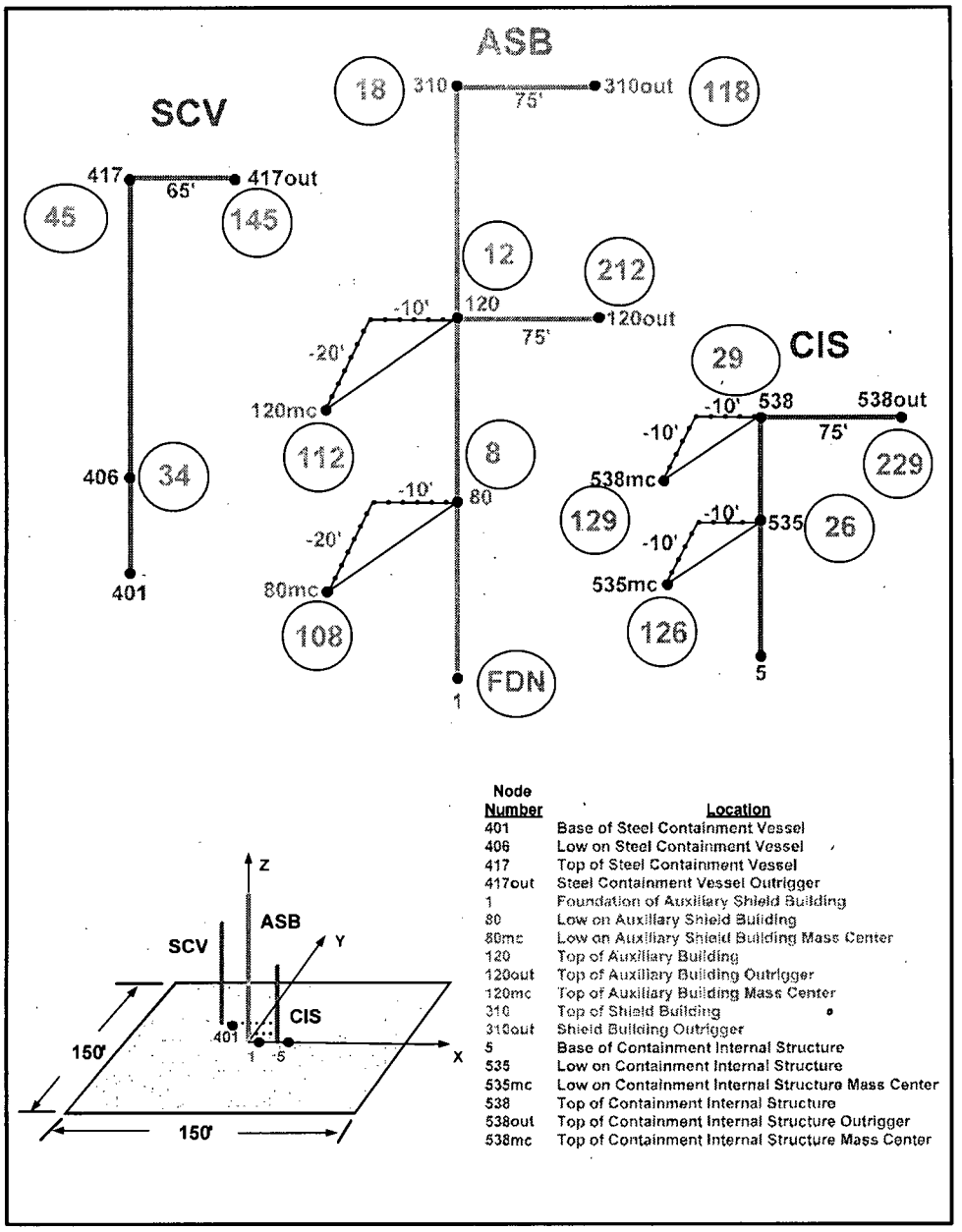

Figure 5-1
Locations on the AP1000-Based Stick Model with Offsets and Outriggers Where In-Structure Response Spectra are Computed

Chapter 5 provides a summary of the results of the investigation into the effects of incoherence of ground motion on the response of a nuclear power plant structure. The structure being analyzed is a simplified model based on some of the AP1000 properties (described in Chapter 2). Note the structure model is comprised of three sticks with limited inter-connectivity at upper elevations. This model includes mass offsets and outriggers that exaggerate incoherency induced rotations. The structure is anchored to a 15-ft thick, 150-ft square foundation. This structure is founded on the surface of the rock site profile described in Chapter 2. The high frequency content free-field ground motion compatible with the rock site profile also described in Chapter 2 was used. For all analyses, spectrum compatible time histories defined the free-field ground motion. All analyses reported in this chapter considered three directions of simultaneous earthquake input motion. Analyses were performed for three individual input motions (X, Y, and Z) and the resulting response spectra were combined by the square root of the sum of the squares (SRSS) to obtain response to the combined simultaneous input motion.

Note that the same coherency functions from Dr. Norm Abrahamson as were used in EPRI and USDOE (2006) are also used in this study (i.e., the soil site coherency functions). Recently, updated coherency functions have been developed by Dr. Abrahamson. However, the previous soil site coherency functions correspond to less coherent ground motion that will likely induce greater rotations that must be captured by the CLASSI and SASSI methods considered. Hence, the original coherency is judged to be a more stringent test for CLASSI-SASSI validation.

Six sets of analyses have been performed for the example structural model:

1. SSI analysis with coherent input motion determined by CLASSI (light blue curves in all Chapter 5 response spectra figures)
2. CLASSIinco with incoherent input motion (dark blue curves in all Chapter 5 response spectra figures)
3. CLASSIinco-SRSS with incoherent input motion (green curves in all Chapter 5 response spectra figures)
4. SASSI-SRSS with incoherent input motion (yellow curves in all Chapter 5 response spectra figures)
5. SASSI Simulations with incoherent input motion (black curves in all Chapter 5 response spectra figures). The mean of 15 simulations of randomly phased spatial modes is used for the analyses of this chapter.
6. SASSI-AS with incoherent input motion (red curves in all Chapter 5 response spectra figures)

To evaluate the effects of incoherency on in-structure response, response spectra were calculated and compared for the various analyses at the foundation, at the tops of the structure sticks, and on outriggers extending 65 or 75-ft. from the top of each stick in the X direction. To evaluate the effects of induced rocking, the representative responses on the edge of the foundation, at the structure mass center and on the outrigger were examined. To evaluate the effects of induced

torsion, the representative responses on the edge of the foundation and on the outriggers were examined.

CLASSI-SASSI Comparisons of In-Structure Response Spectra

Results presented are in-structure response spectra (5% damping) at the foundation and at representative points on each of the three models (ASB, SCV, CIS) as shown in Figure 5-1. Responses at the top of each model and on the foundation are calculated and compared for the six analysis methods listed above. Foundation response considered included X, Y, and Z foundation translation and XX, YY, and ZZ foundation rotation. The foundation rotation response is scaled by 75 feet to correspond to translation at the edge of the 150 foot square foundation. Two ASB, three CIS, and two SCV responses are considered. These correspond to the top of the structure shear center and an outrigger extending from the top of the structure. At the top of the ASB and SCV the shear and mass centers are assumed to be coincident. At the top of the CIS, the mass center is assumed to be offset from the shear center. In-structure response spectra at these eight locations for response in two horizontal directions, X and Y, and the vertical direction, Z, are presented in Figures 5-2 through 5-28. Again, all analyses considered three directions of simultaneous earthquake input motion. Results from the three individual input motion cases are presented in Appendix A.

Foundation Response

Foundation response is presented in Figures 5-2 through 5-7. Comparing the foundation translation response spectra including incoherency effects with results for coherent ground motion in Figures 5-2, 5-3, and 5-4, generally shows significant reductions over those due to coherent SSI effects at frequencies greater than 10 Hz. Comparing the foundation rotation response spectra including incoherency effects with results for coherent ground motion in Figures 5-5, 5-6, and 5-7, shows little or no reduction due to incoherency and, in some cases, increased response due to incoherency. The horizontal spatial variation of ground motion comprising incoherency produces reduced translation response but also induces additional rotational response.

There is very close agreement in the incoherent results by all five methods considered for translational foundation response. Agreement is also quite good for the foundation rotational response. There is somewhat more deviation in rotational response between the various CLASSI and SASSI methods but it is judged to be acceptable for engineering purposes.

Auxiliary and Shield Building (ASB)

- **Top of Shield Building.** Responses at the top of the coupled auxiliary and shield building (ASB) are presented in Figures 5-8, 5-9, and 5-10. Comparing the response spectra due to incoherency effects with the coherent results, generally, shows significant reductions due to incoherency for frequencies greater than 12 Hz for the horizontal directions and at frequencies greater than 10 Hz for the vertical direction. For horizontal directions, the

reductions are, generally, greater than 30% up to 30 Hz and less as one approaches the ZPA frequency. For the vertical direction, substantial reductions are observed in the frequency range above 10 Hz, including at the ZPA frequency. At frequencies of peak amplification less than 10 Hz (X-direction 3.2 and 6.5 Hz; Y-direction 3 Hz and 6 Hz), slight increases in spectral accelerations of the incoherent case above the coherent case are observed. As was the case in earlier phases of this study, it was concluded that this effect is due to incoherency-induced rotations.

There is very close agreement among all five approaches for considering incoherency effects for the horizontal response. For vertical response, the agreement is good (acceptable for engineering purposes) but with somewhat greater deviations than for horizontal response.

The responses of the outrigger, extending 75-ft. in the X-direction, are presented in Figures 5-11, 5-12, and 5-13. The reductions in response spectral accelerations generally follow the trend of the values on the centerline, but the reductions are observed to be less.

There is very close agreement among all five approaches for considering incoherency effects for both horizontal and vertical response. The various CLASSI and SASSI methods agree within 10 percent at all frequencies, generally with differences much less than 10 percent.

Containment Internal Structure (CIS)

- **Top of CIS.** Responses at the top of the containment internal structure (CIS) are presented in Figures 5-14 through 5-19. Responses of the outrigger extending 75-ft in the X direction from the top of the containment internal structure (CIS) are presented in Figures 5-20, 5-21, and 5-22.Comparing the response spectra due to incoherency effects with coherent seismic response, generally, shows significant reductions over those due to coherent SSI effects at frequencies greater than about 12 Hz. As expected for a high frequency structure like the CIS, these reductions are 50% or greater compared to the SSI coherent ground motion case.

  For this high frequency structure, there is very close agreement in incoherent seismic response at all frequencies for the CIS. The two CLASSI approaches and the three SASSI approaches agree well within engineering expectations.

Steel Containment Vessel (SCV)

- **Top of SCV.** Response at the top of the steel containment vessel (SCV) at the centerline is presented in Figures 5-23, 5-24, and 5-25. The responses of the outrigger extending 75-ft in the X direction from the top of the steel containment vessel (SCV) are presented in Figures 5-26, 5-27, and 5-28. Comparing the response spectra due to incoherency effects with those for coherent ground motion, generally, show significant reductions in response for frequencies greater than about 12 Hz with less reductions at the ZPA. In the vertical direction, significant reductions are observed for all frequencies greater than 10 Hz.

For the SCV, there is again very close agreement in incoherent seismic response at all frequencies. The two CLASSI approaches and the three SASSI approaches again agree well within engineering expectations.

Summary of CLASSI-SASSI Comparisons

Figures 5-2 through 5-28 demonstrate significant reductions in high-frequency response as a result of seismic wave incoherence. In the horizontal response directions, these translational reductions in response spectra are tempered somewhat due to incoherency induced rocking and torsion. Even with this phenomena of incoherency induced rocking and torsion, the fundamental conclusion remains that there are significant reductions in high-frequency response due to seismic wave incoherence.

Figures 5-2 through 5-28 also demonstrate close agreement between the five methods of computing incoherent seismic response (i.e., CLASSIinco, CLASSIinco-SRSS, SASSI-SRSS, SASSI Simulations, and SASSI-AS). It is demonstrated by this study that any of these five methods is suitable for accurately determining seismic response to incoherent input ground motion. In Appendix A, response spectra for individual directions of input motion are presented. In the appendix, all methods agree well but there are some deviations by the CLASSIinco method and by the SASSI-AS method. The other methods (CLASSIinco-SRSS, SASSI-SRSS, SASSI Simulations) explicitly consider the random nature of incoherence and are preferable from a theoretical standpoint and produce slightly more accurate results. However, SASSI-SRSS and SASSI Simulations require significantly greater computation time than the CLASSIinco, CLASSIinco-SRSS, and SASSI-AS methods.

Based on the results presented in this chapter, CLASSI and SASSI are judged to be validated to treat seismic wave incoherence in SSI analyses of nuclear power plant structures. CLASSIinco, CLASSIinco-SRSS, SASSI-SRSS, SASSI Simulations, and SASSI-AS are all recommended for this use.

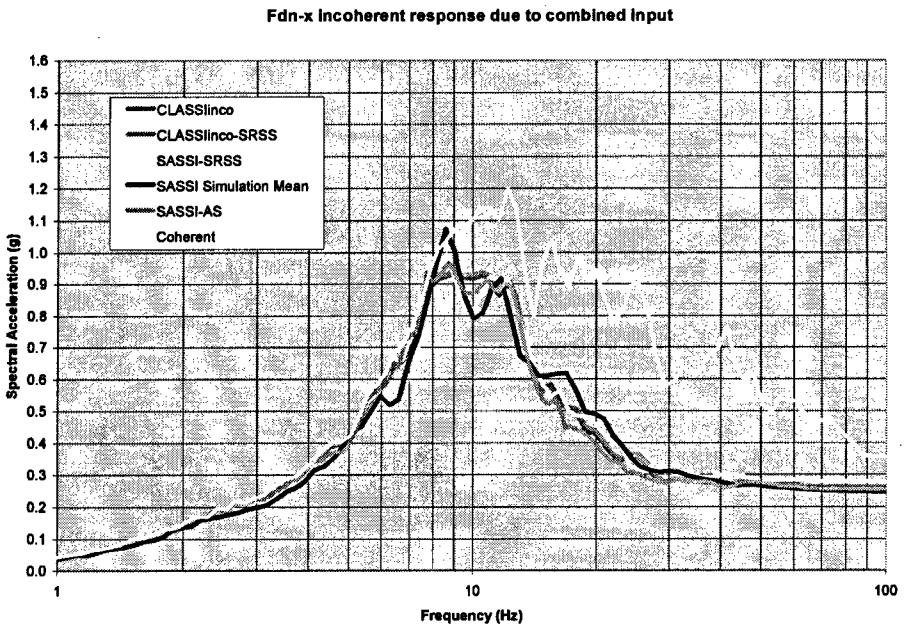

Figure 5-2
Center of Foundation Response Spectra – X Direction – CLASSIinco, CLASSIinco-SRSS, SASSI-SRSS, SASSI Simulation Mean, SASSI-AS (Node 1)

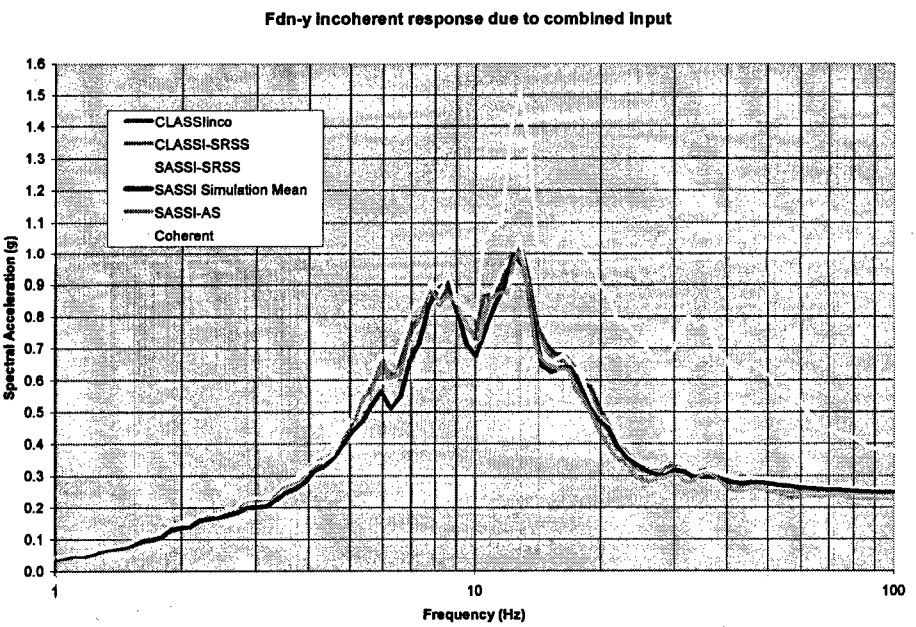

Figure 5-3
Center of Foundation Response Spectra – Y Direction – CLASSIinco, CLASSIinco-SRSS, SASSI-SRSS, SASSI Simulation Mean, SASSI-AS (Node 1)

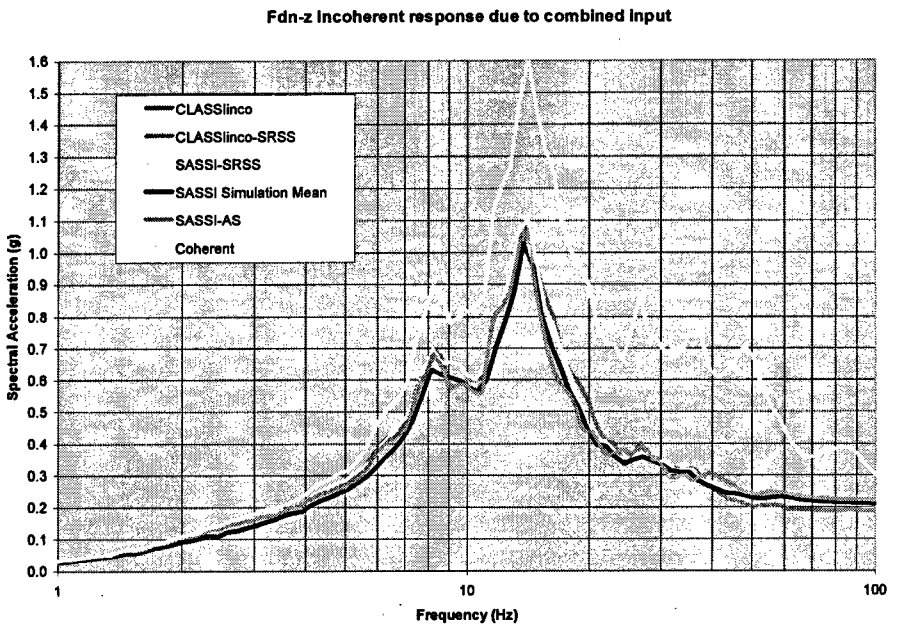

Figure 5-4
Center of Foundation Response Spectra – Z Direction – CLASSIinco, CLASSIinco-SRSS, SASSI-SRSS, SASSI Simulation Mean, SASSI-AS (Node 1)

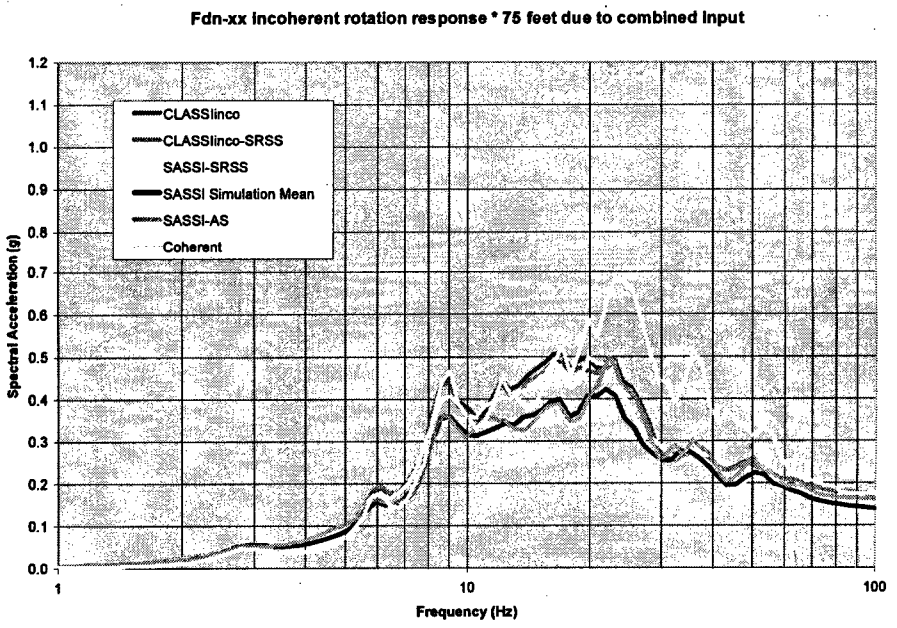

Figure 5-5
Edge of Foundation Response Spectra –XX Rotation – CLASSIinco, CLASSIinco-SRSS, SASSI-SRSS, SASSI Simulation Mean, SASSI-AS (Node 1)

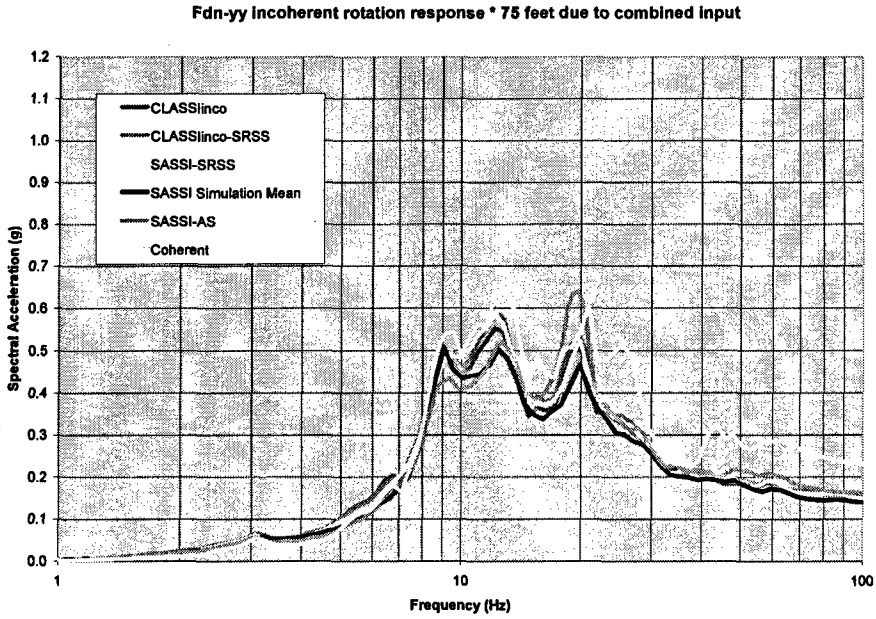

Figure 5-6
Edge of Foundation Response Spectra –YY Rotation – CLASSIinco, CLASSIinco-SRSS, SASSI-SRSS, SASSI Simulation Mean, SASSI-AS (Node 1)

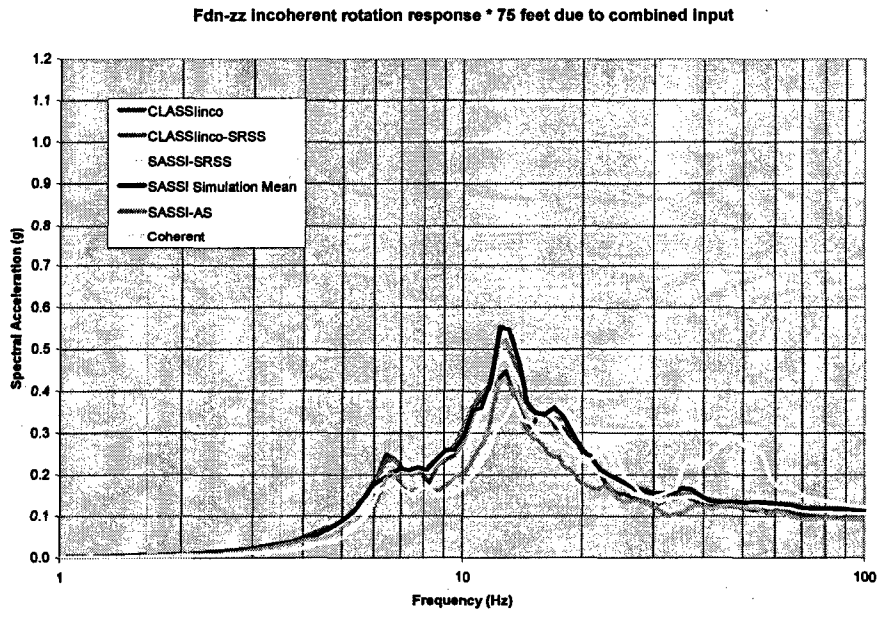

Figure 5-7
Edge of Foundation Response Spectra –ZZ Rotation – CLASSIinco, CLASSIinco-SRSS, SASSI-SRSS, SASSI Simulation Mean, SASSI-AS (Node 1)

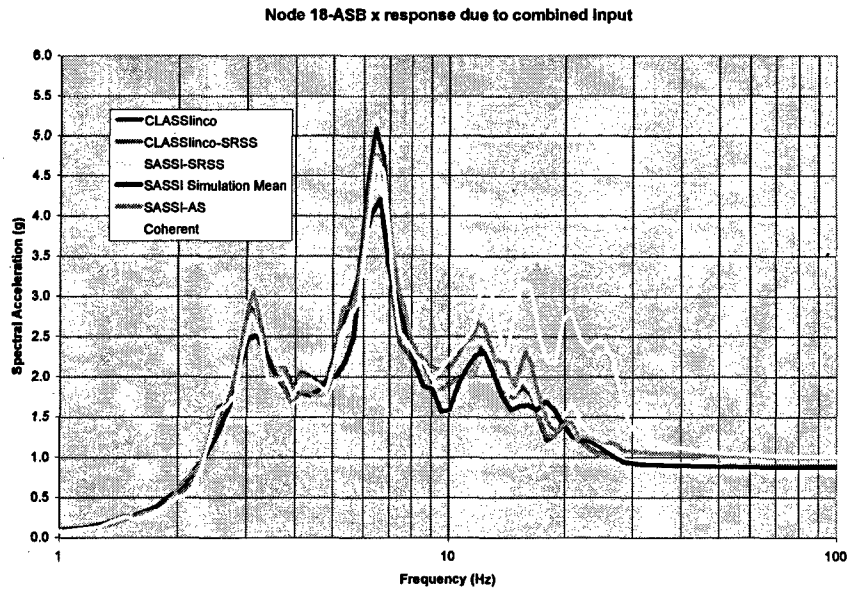

Figure 5-8
Top of ASB Response Spectra – X Direction – CLASSIinco, CLASSIinco-SRSS, SASSI-SRSS, SASSI Simulation Mean, SASSI-AS (Node 18)

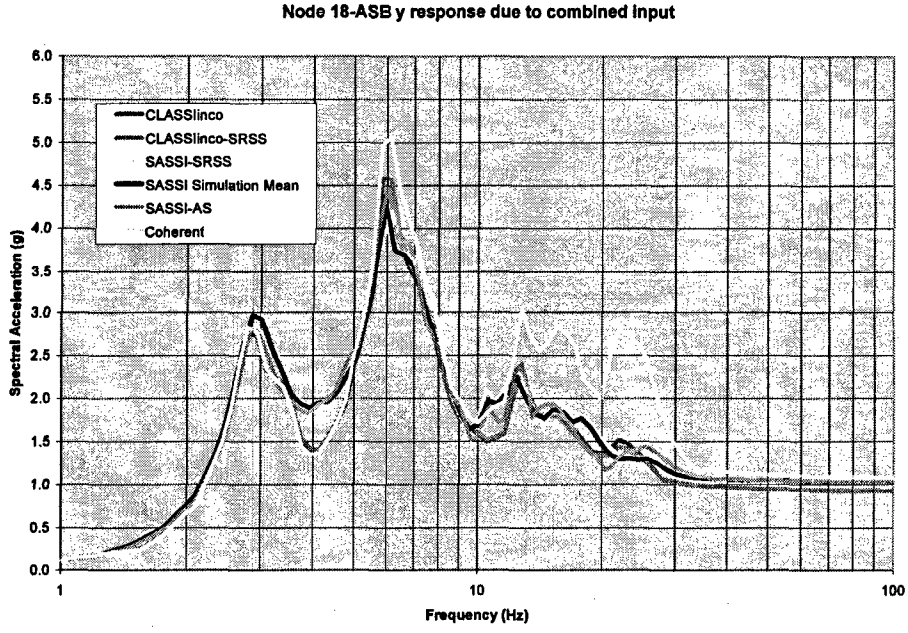

Figure 5-9
Top of ASB Response Spectra – Y Direction - CLASSIinco, CLASSIinco-SRSS, SASSI-SRSS, SASSI Simulation Mean, SASSI-AS (Node 18)

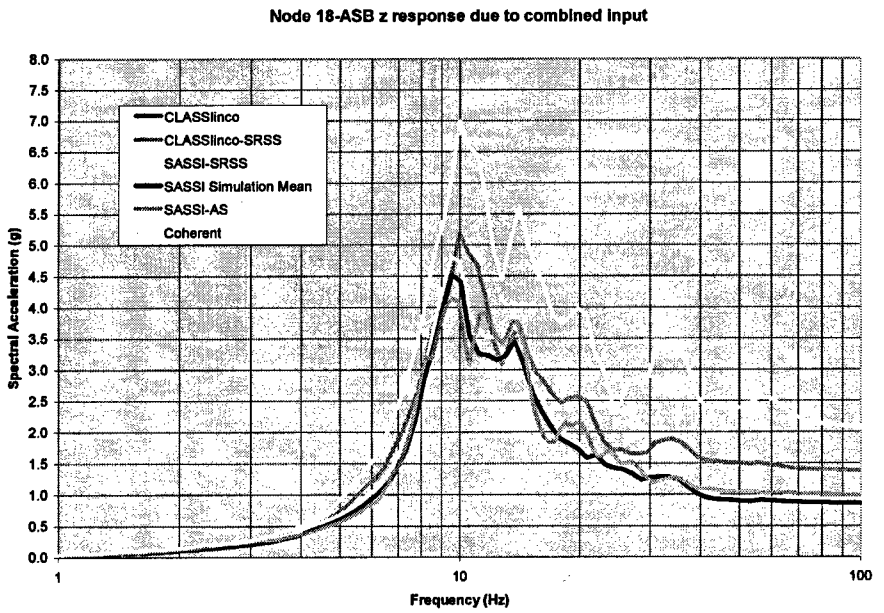

Figure 5-10
Top of ASB Response Spectra – Z Direction – CLASSIinco, CLASSIinco-SRSS, SASSI-SRSS, SASSI Simulation Mean, SASSI-AS (Node 18)

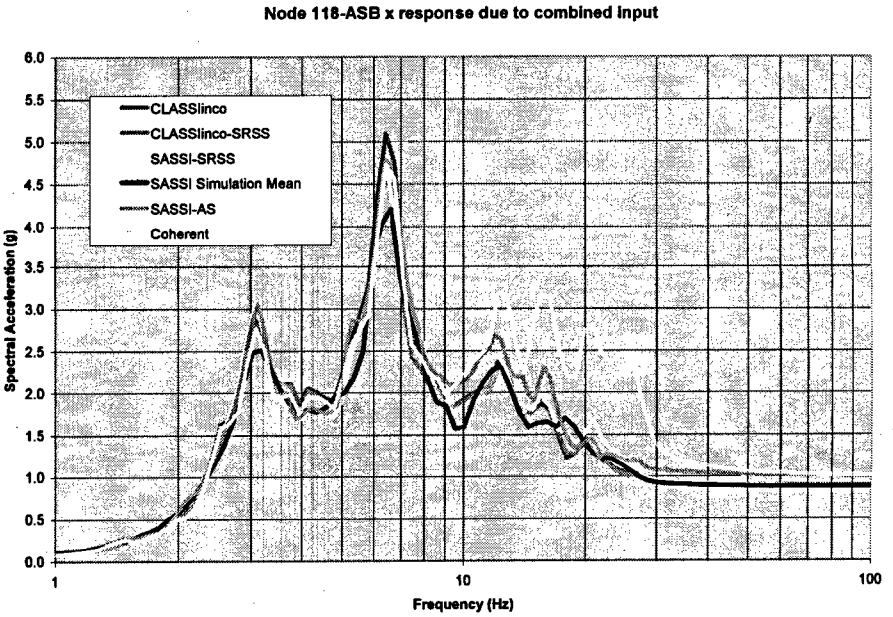

Figure 5-11
ASB Outrigger Response Spectra – X Direction – CLASSIinco, CLASSIinco-SRSS, SASSI-SRSS, SASSI Simulation Mean, SASSI-AS (Node 118)

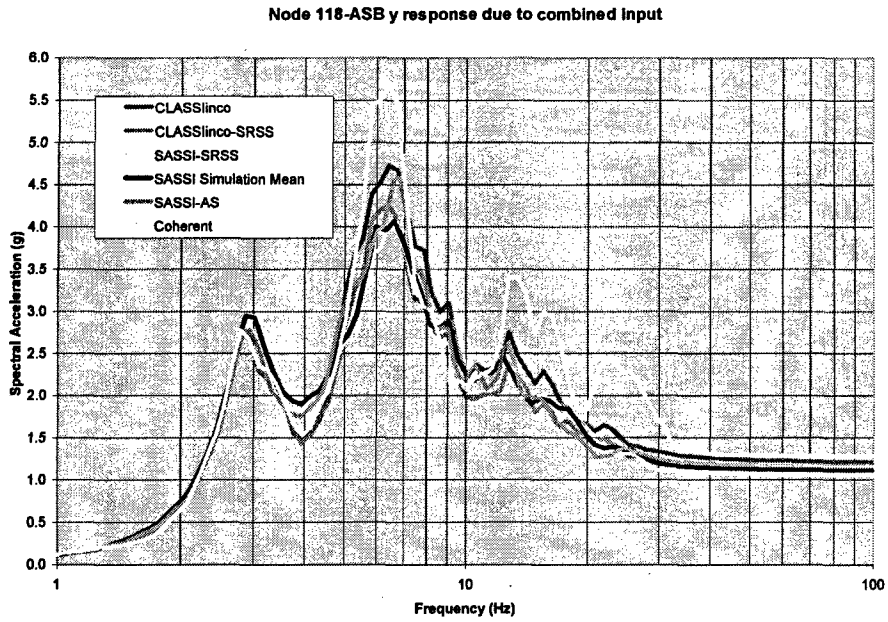

Figure 5-12
ASB Outrigger Response Spectra – Y Direction due – CLASSIinco, CLASSIinco-SRSS, SASSI-SRSS, SASSI Simulation Mean, SASSI-AS (Node 118)

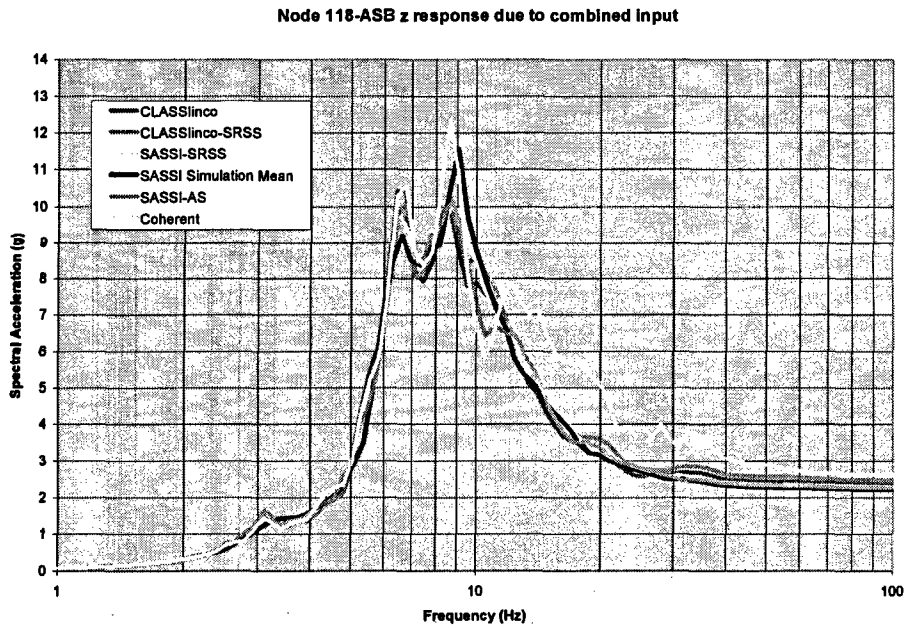

Figure 5-13
ASB Outrigger Response Spectra – Z Direction – CLASSIinco, CLASSIinco-SRSS, SASSI-SRSS, SASSI Simulation Mean, SASSI-AS (Node 118)

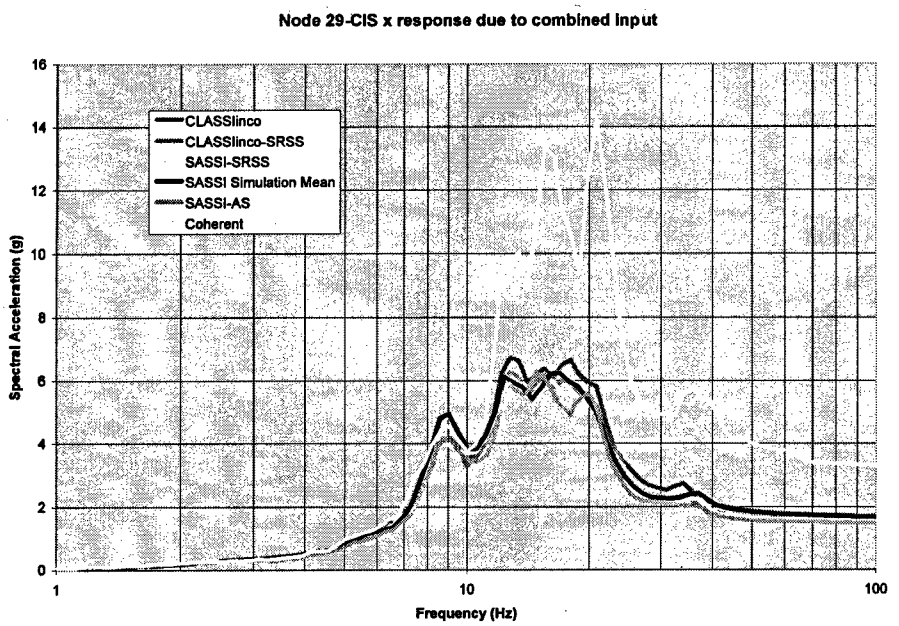

Figure 5-14
Top of CIS Shear Center Response Spectra – X Direction – CLASSIinco, CLASSIinco-SRSS, SASSI-SRSS, SASSI Simulation Mean, SASSI-AS (Node 29)

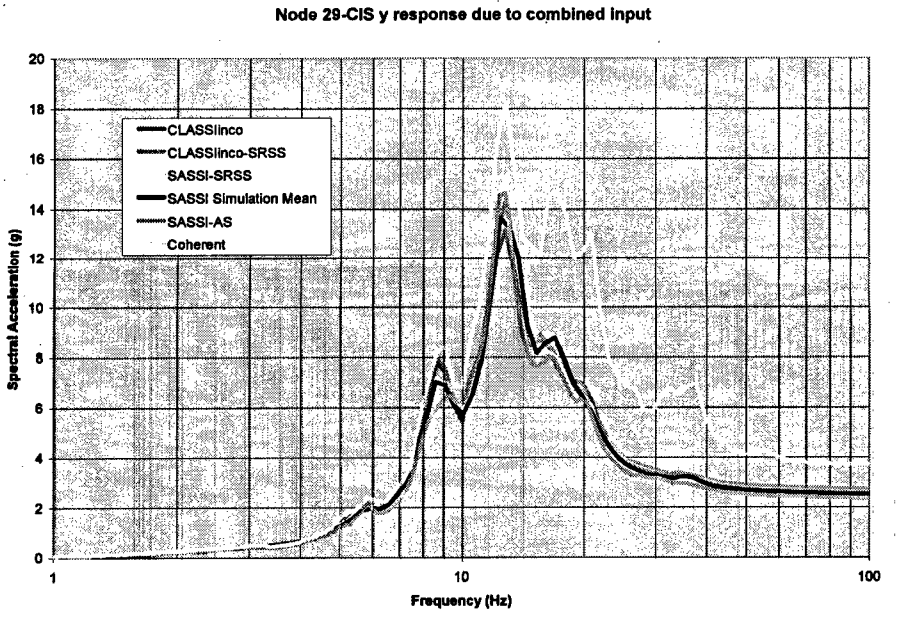

Figure 5-15
Top of CIS Shear Center Response Spectra – Y Direction – CLASSIinco, CLASSIinco-SRSS, SASSI-SRSS, SASSI Simulation Mean, SASSI-AS (Node 29)

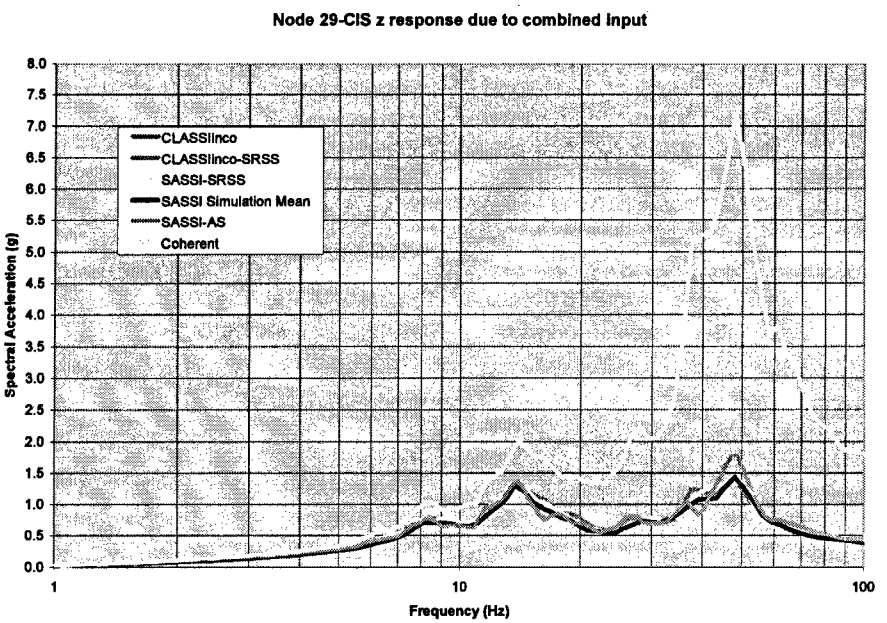

Figure 5-16
Top of CIS Shear Center Response Spectra – Z Direction – CLASSIinco, CLASSIinco-SRSS, SASSI-SRSS, SASSI Simulation Mean, SASSI-AS (Node 29)

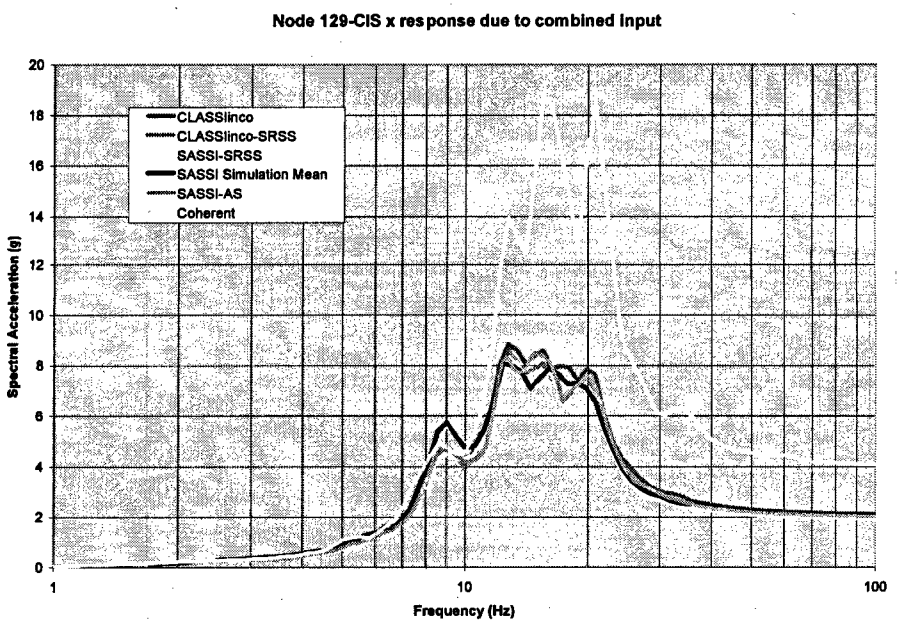

Figure 5-17
Top of CIS Horizontal Mass Center Response Spectra – X Direction – CLASSIinco, CLASSIinco-SRSS, SASSI-SRSS, SASSI Simulation Mean, SASSI-AS (Node 129)

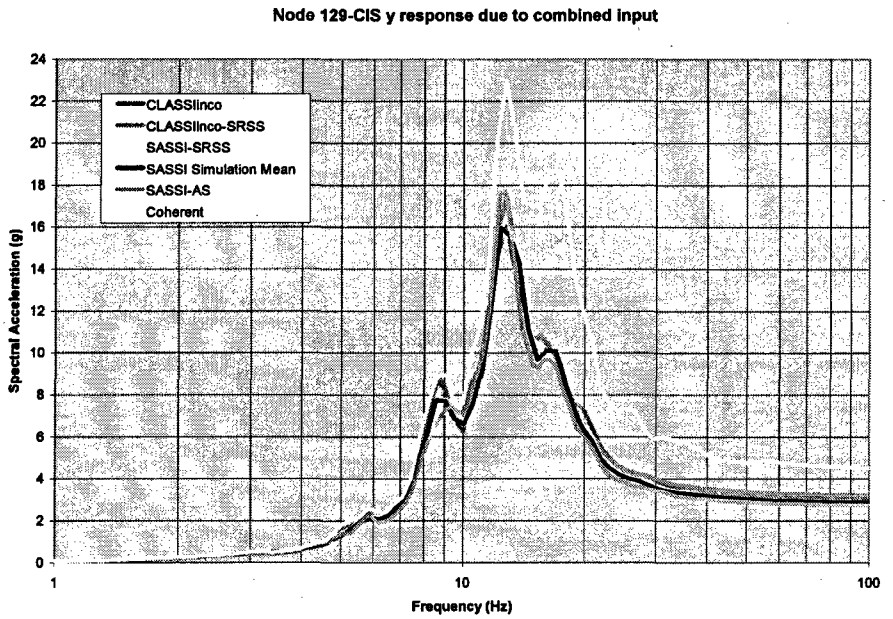

Figure 5-18
Top of CIS Horizontal Mass Center Response Spectra – Y Direction – CLASSIinco, CLASSIinco-SRSS, SASSI-SRSS, SASSI Simulation Mean, SASSI-AS (Node 129)

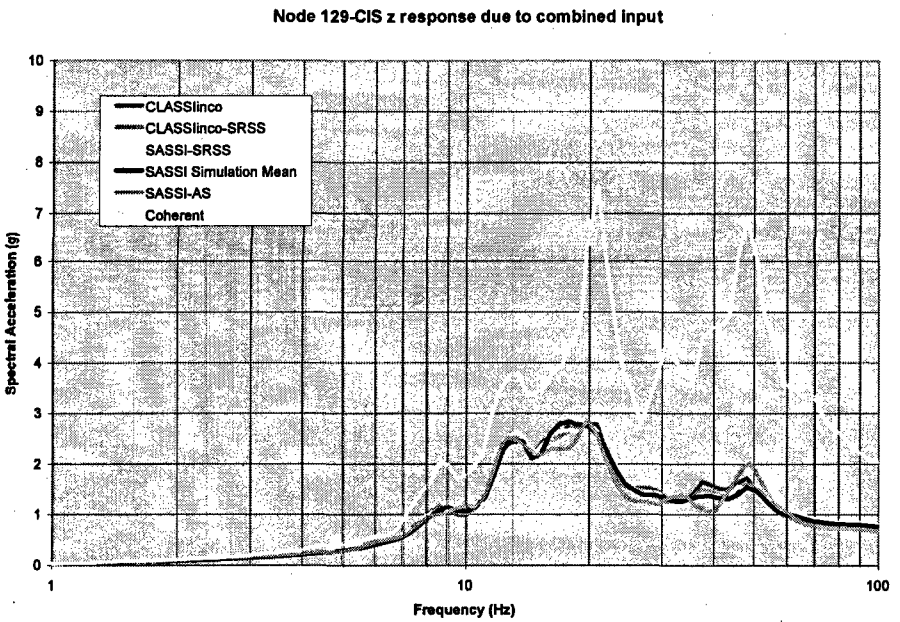

Figure 5-19
Top of CIS Horizontal Mass Center Response Spectra – Z Direction – CLASSIinco, CLASSIinco-SRSS, SASSI-SRSS, SASSI Simulation Mean, SASSI-AS (Node 129)

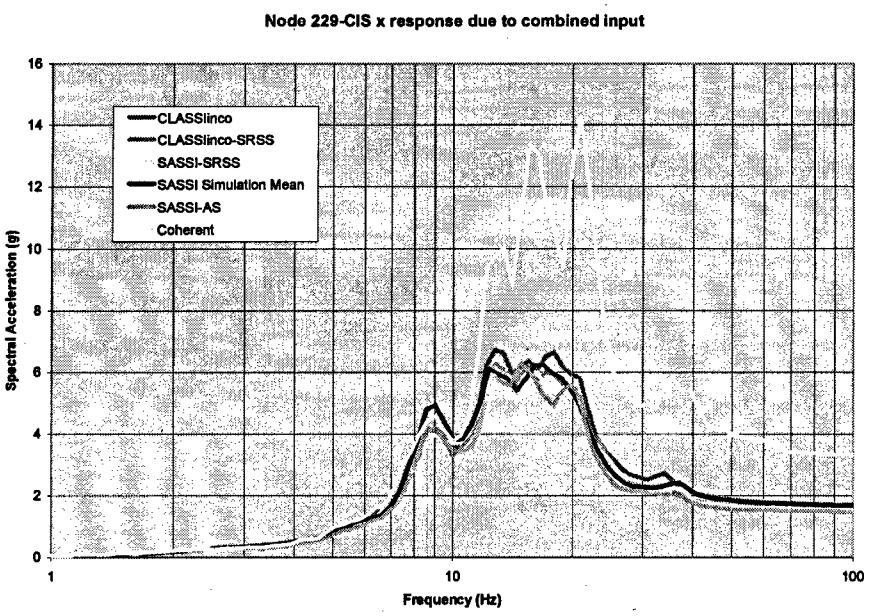

Figure 5-20
CIS Outrigger Response Spectra – X Direction – CLASSIinco, CLASSIinco-SRSS, SASSI-SRSS, SASSI Simulation Mean, SASSI-AS (Node 229)

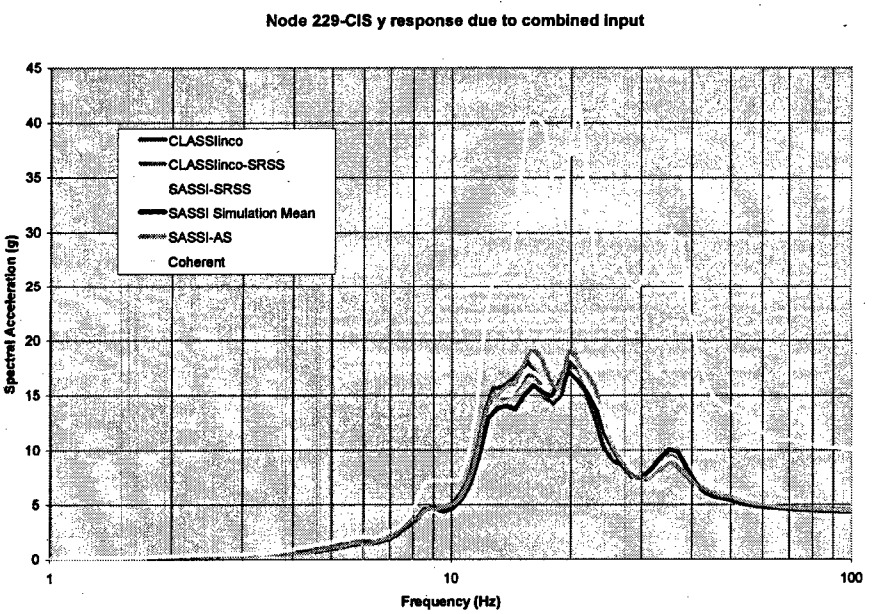

Figure 5-21
CIS Outrigger Response Spectra – Y Direction – CLASSIinco, CLASSIinco-SRSS, SASSI-SRSS, SASSI Simulation Mean, SASSI-AS (Node 229)

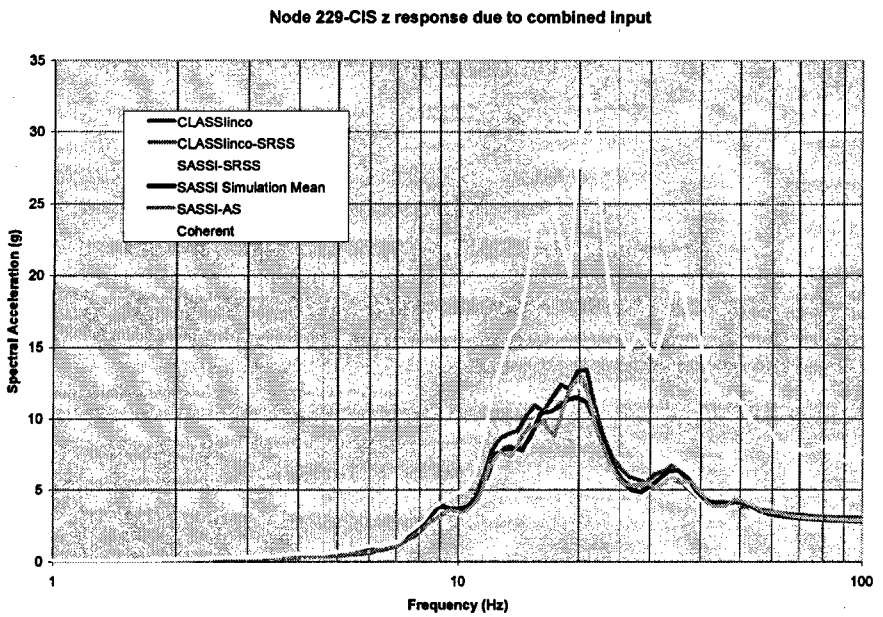

Figure 5-22
CIS Outrigger Response Spectra – Z Direction – CLASSIinco, CLASSIinco-SRSS, SASSI-SRSS, SASSI Simulation Mean, SASSI-AS (Node 229)

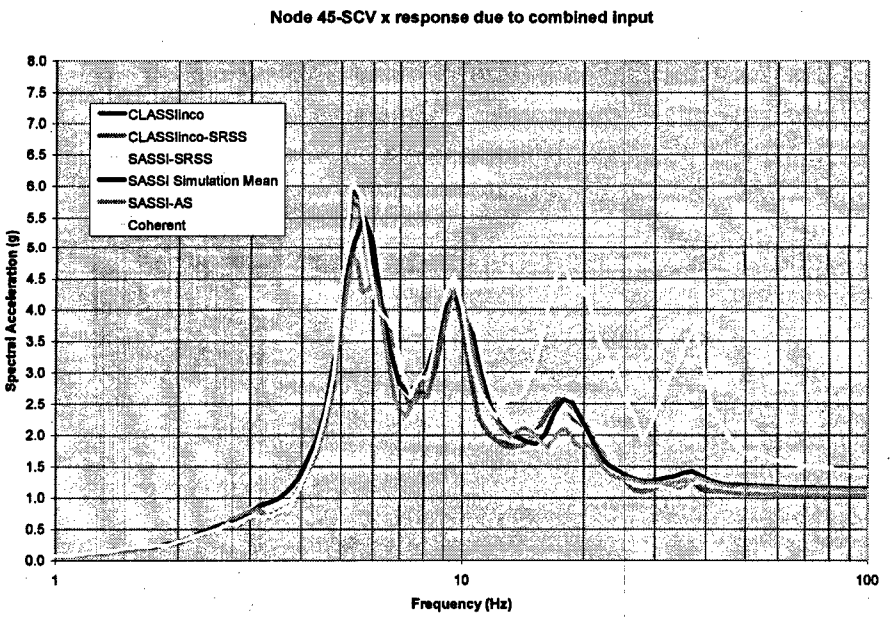

Figure 5-23
Top of SCV Response Spectra – X Direction – CLASSIinco, CLASSIinco-SRSS, SASSI-SRSS, SASSI Simulation Mean, SASSI-AS (Node 45)

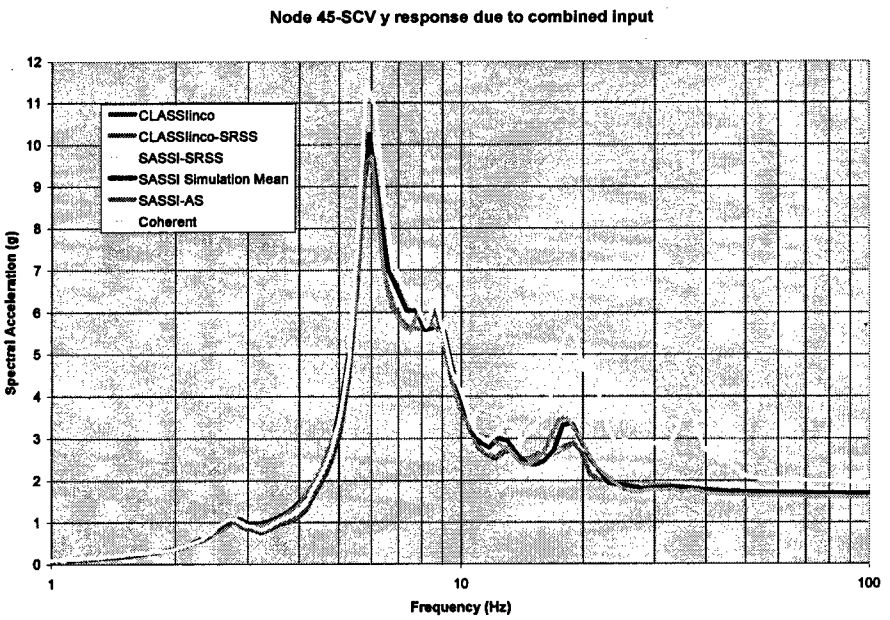

Figure 5-24
Top of SCV Response Spectra – Y Direction – CLASSIinco, CLASSIinco-SRSS, SASSI-SRSS, SASSI Simulation Mean, SASSI-AS (Node 45)

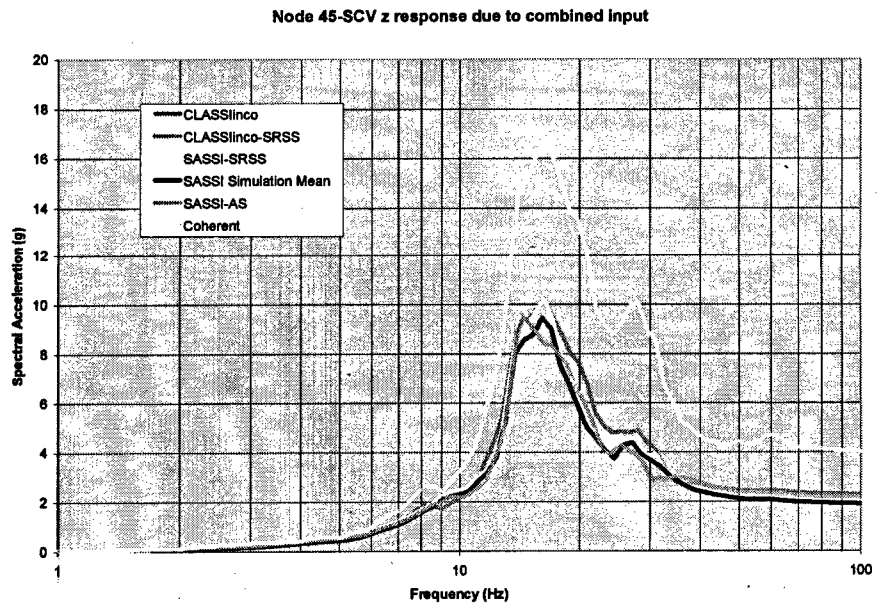

Figure 5-25
Top of SCV Response Spectra – Z Direction – CLASSIinco, CLASSIinco-SRSS, SASSI-SRSS, SASSI Simulation Mean, SASSI-AS (Node 45)

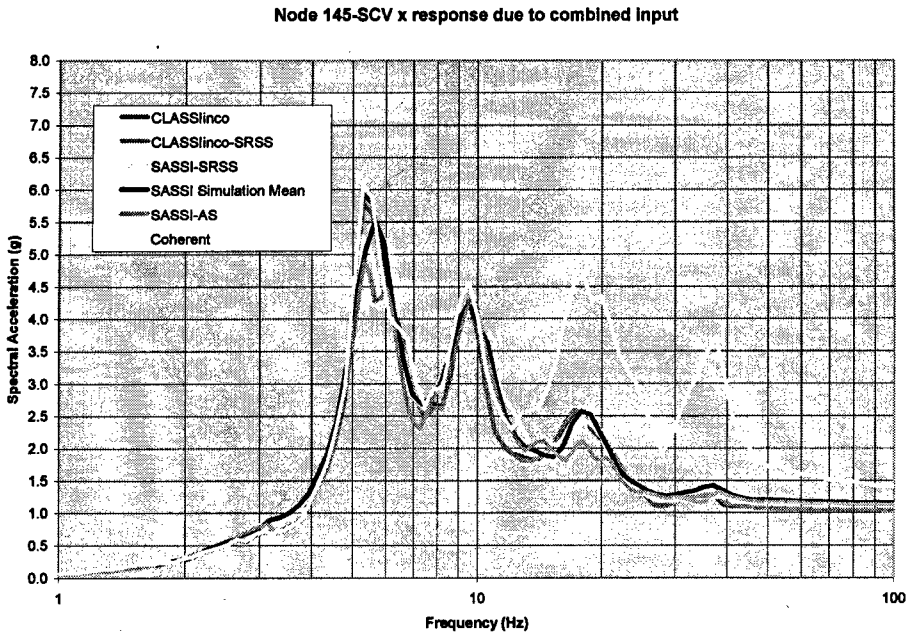

Figure 5-26
SCV Outrigger Response Spectra – X Direction – CLASSIinco, CLASSIinco-SRSS, SASSI-SRSS, SASSI Simulation Mean, SASSI-AS (Node 145)

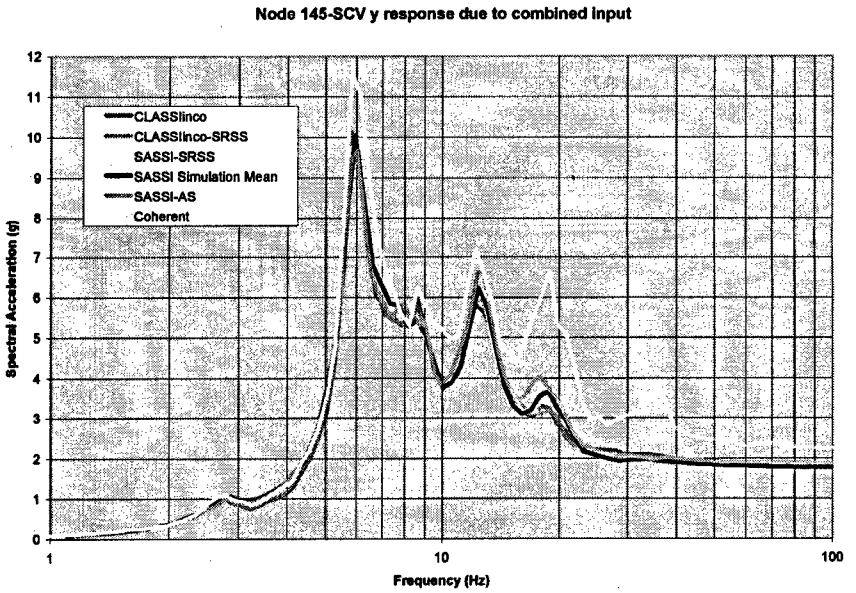

Figure 5-27
SCV Outrigger Response Spectra – Y Direction – CLASSIinco, CLASSIinco-SRSS, SASSI-SRSS, SASSI Simulation Mean, SASSI-AS (Node 145)

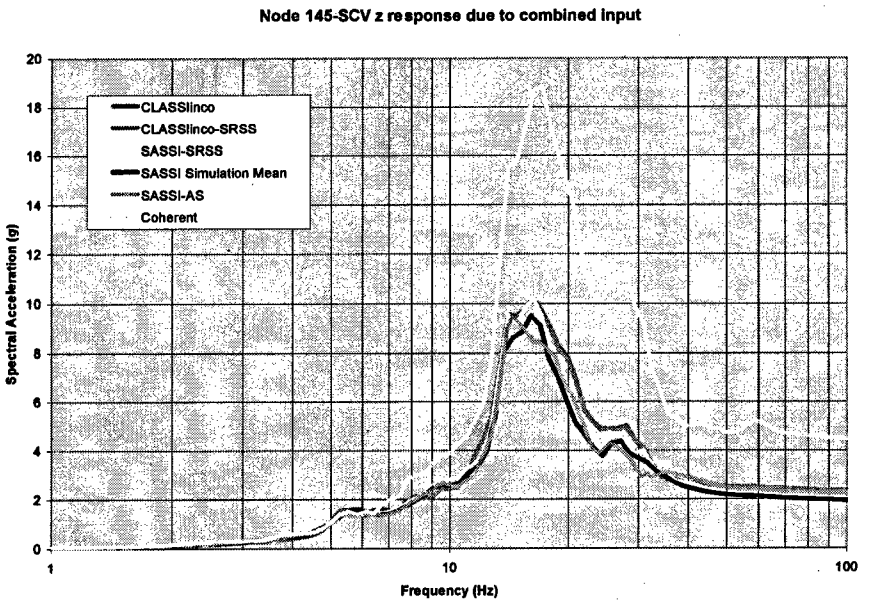

Figure 5-28
SCV Outrigger Response Spectra – Z Direction – CLASSIinco, CLASSIinco-SRSS, SASSI-SRSS, SASSI Simulation Mean, SASSI-AS (Node 145)

6
GUIDELINES FOR APPLICATION OF CLASSI AND SASSI

Will be incorporated in the July 27 draft of this report.

7
CONCLUSIONS AND RECOMMENDATIONS

1. Soil-structure interaction (SSI) analysis is important to calculating seismic response to structures mounted on rock sites and subjected to high-frequency ground motion. SSI produces significant reductions in high-frequency response for these conditions.

2. CLASSIinco and CLASSIinco-SRSS are computationally efficient methods for conducting SSI analyses including incoherency, but are limited to rigid surface foundations. For structures with foundations for which the combined behavior of foundation/structure is deemed flexible and for embedded foundations/partial structure, a version of SASSI is required to accurately capture seismic response.

3. Utilization of SASSI-AS to compute the response for incoherent input requires computational effort comparable to standard SASSI analysis for coherent input. SASSI-SRSS and SASSI Simulation require significantly greater computational effort to analyze the incoherent response for complex structural models.

4. The SSI analysis programs CLASSIinco, CLASSIinco-SRSS, SASSI-SRSS, SASSI-Simulation, and SASSI-AS have been validated to treat the phenomena of incoherency for nuclear power plant structures when applied in the seismic design/qualification process. The bases of the validation are:

    - Agreement of results computed using CLASSI and SASSI to those available from published literature (Chapter 3).

    - Comparison of CLASSI computed incoherent seismic response with SASSI computed incoherent seismic response for an example rock/structure model with agreement within engineering accuracy (Chapter 5).

5. CLASSIinco-SRSS, SASSI-SRSS, and SASSI-Simulation are the most theoretically correct techniques since they recognize and treat the random nature of the phase of the incoherent SSI response. The results of the analyses where the three input directions are treated independently (Appendix A) demonstrates that the agreement between these three is excellent even for this case.

6. The more simplified approaches of CLASSIinco and SASSI-AS may be shown to capture all important aspects of SSI response and, therefore, may be used for final design/qualification purposes. Examples include:

    - The rock/structure model analyzed herein, with results reported in Chapter 5.

- The relatively simple model used in the validation effort of EPRI and USDOE (2006) Appendix C.

- Other examples likely include structure configurations where it can be demonstrated that induced rotation effects are adequately treated with these methodologies, e.g., large plan dimension/low height structures.

Sensitivity studies may be performed to demonstrate this applicability.

8
REFERENCES

Abrahamson, N. (2007). *Hard Rock Coherency Functions Based on the Pinyon Flat Data*, April 2.

Abrahamson, N. (2006). *Spatial Coherency for Soil-Structure Interaction*, Electric Power Research Institute, Final Report 1014101, Palo Alto, CA. August (Draft).

Abrahamson, N. (2005). *Spatial Coherency for Soil-Structure Interaction*, Electric Power Research Institute, Technical Update Report 1012968, Palo Alto, CA. December.

ASCE (2000). *Seismic Analysis of Safety-Related Nuclear Structures and Commentary*, American Society Civil Engineers, Report. ASCE 4-98.

Chang, C.-Y., M.S. Power, I.M. Idriss, P. Sommerville, W. Silva, and P.C. Chen. (1986). *Engineering Characterization of Ground Motion, Task I1: Observational Data on Spatial Variations of Earthquake Ground Motion*, NUREG/CR-3805, Vol. 3.

CSI (2004). *Computers and Structures Incorporated, SAP2000, Integrated Software for Structural Analysis and Design*, Version 9.

Der Kiureghian, A. (1980). *Structural Response to Stationary Excitation*, Journal of the Engineering Mechanics Division, American Society Civil Engineers, December.

EPRI (1997). *Soil-Structure Interaction Analysis Incorporating Spatial Incoherence of Ground Motions*, Electric Power Research Institute, Report TR-102631 2225, Palo Alto, CA. November.

EPRI (1993). *Guidelines for Determining Design Basis Ground Motions, Volume 1: Method and Guidelines for Estimating Earthquake Ground Motion in Eastern North America*, Electric Power Research Institute, Report TR-102293, Palo Alto, CA. November.

EPRI (1991). *A Methodology for Assessment of Nuclear Power Plant Seismic Margin (Rev 1)*, Electric Power Research Institute, Report NP-6041-SL, Palo Alto, CA. August.

EPRI and USDOE (2006). *Program on Technology Innovation: Effect of Seismic Wave Incoherence on Foundation and Building Response*, Electric Power Research Institute, Palo Alto, CA and USDOE, Germantown, MD. Report No. TR-1013504. November.

Ghiocel, D (2004). *Stochastic Simulation Methods for Engineering Predictions*, CRC Engineering Design Reliability Handbook, Chapter 20, CRC Press, New York, NY.

Ghiocel Predictive Technologies, Inc. (2006). *ACS-SASSI, An Advanced Computational Software for 3D Dynamic Analysis Including Soil-Structure Interaction*, Version 2.1, Pittsford, New York.

Johnson, J.J. (2003). *Soil-Structure Interaction*, Earthquake Engineering Handbook, Chapter 10, W-F Chen, C. Scawthorn, eds., CRC Press, New York, NY.

Kim, S. and J.P. Stewart (2003). *Kinematic Soil-Structure Interaction from Strong Motion Recordings*, Journal of Geotechnical and Geoenvironmental Engineering, ASCE, April.

Luco, J.E. and A. Mita (1987). *Response of Circular Foundation to Spatially Random Ground Motion*, Journal of Engineering Mechanics, American Society of Civil Engineers, Vol. 113, No. 1, January. 1987, pp. 1-15.

Luco, J.E. and H.L. Wong (1986). *Response of a Rigid Foundation Subjected to a Spatially Random Ground Motion*, Earthquake Engineering and Structural Dynamics, Vol. 14, pp. 891-908.

McCann, M., J. Marrone, and R. Youngs (2004). *CEUS Ground Motion Project Final Report*, TR-1009684, Electric Power Research Institute, Palo Alto, CA, December.

Orr, R. (2003). *AP1000 Inputs for 2D SASSI Analyses*, Calculation No. APP-1000-S2C-052, Rev. 0, Westinghouse.

Orr, R., Westinghouse Corporation (2006). Personal email communication on AP1000 Model Properties to Greg Hardy, ARES Corporation, August.

Ostadan, F., Bechtel Corporation (2006). Personal email communication on SASSI SSI Analysis Results to Steve Short, ARES Corporation, August.

Tubino, F., L. Carassale, and G. Solari (2003). Seismic Response of Multi-Supported Structures by Proper Orthogonal Decomposition, Earthquake Engineering and Structural Dynamics, Vol. 32, pp. 1639-1654.

U.S. Department of Energy (2002). *Natural Phenomena Hazards Design and Evaluation Criteria for Department of Energy Facilities*, DOE-STD-1020-2002, January.

Veletsos, A.S. and A.M. Prasad (1989). *Seismic Interaction of Structures and Soils: Stochastic Approach*, ASCE Journal of Structural Engineering, Vol. 115, pp. 935-956, April.

Veletsos, A.S. and Y. Tang (1990). *Deterministic Assessment of Effects of Ground-Motion Incoherence*, ASCE Journal of Engineering Mechanics, Vol. 116, pp. 1109-1124, May.

Wong, H.L. and J.E. Luco (1980). *Soil-Structure Interaction: A Linear Continuum Mechanics Approach (CLASSI)*, Report CE, Department of Civil Engineering, University of Southern California, Los Angeles, California.

A
CLASSI-SASSI IN-STRUCTURE RESPONSE SPECTRA COMPARISONS FOR INDIVIDUAL INPUT DIRECTION COMPONENTS

In Chapter 5, in-structure response spectra computed by two CLASSI methods and three SASSI methods for evaluating seismic response including seismic wave incoherence were presented. Again, these approaches include:

- CLASSIinco – deterministic phasing of foundation component response
- CLASSIinco-SRSS – SRSS combination of structural response computed from random phasing of foundation component response
- SASSI-SRSS – SRSS combination of modal transfer functions to represent random phasing of spatial modes
- SASSI Simulation Mean – Monte Carlo simulations to represent random phasing of spatial modes
- SASSI-AS – Algebraic summation of spatial modes with assumed deterministic phasing

The comparisons of response spectra in Chapter 5 were for response in the x, y, and z directions for simultaneous application of input motion in the x, y, and z directions. These spectra were determined from the square root of the sum of the squares combination of spectra due to individual x, y, and z input motion. The response spectra for the individual x, y, and z input motion are presented in this appendix for the 5 computational methods listed above. Response locations are identified by the node numbers of the CLASSI and SASSI models as shown in Figure A-1. Response spectra for x input motion are presented in Figures A-2 through A-28. Response spectra for y input motion are presented in Figures A-29 through A-55. Response spectra for z input motion are presented in Figures A-56 through A-82.

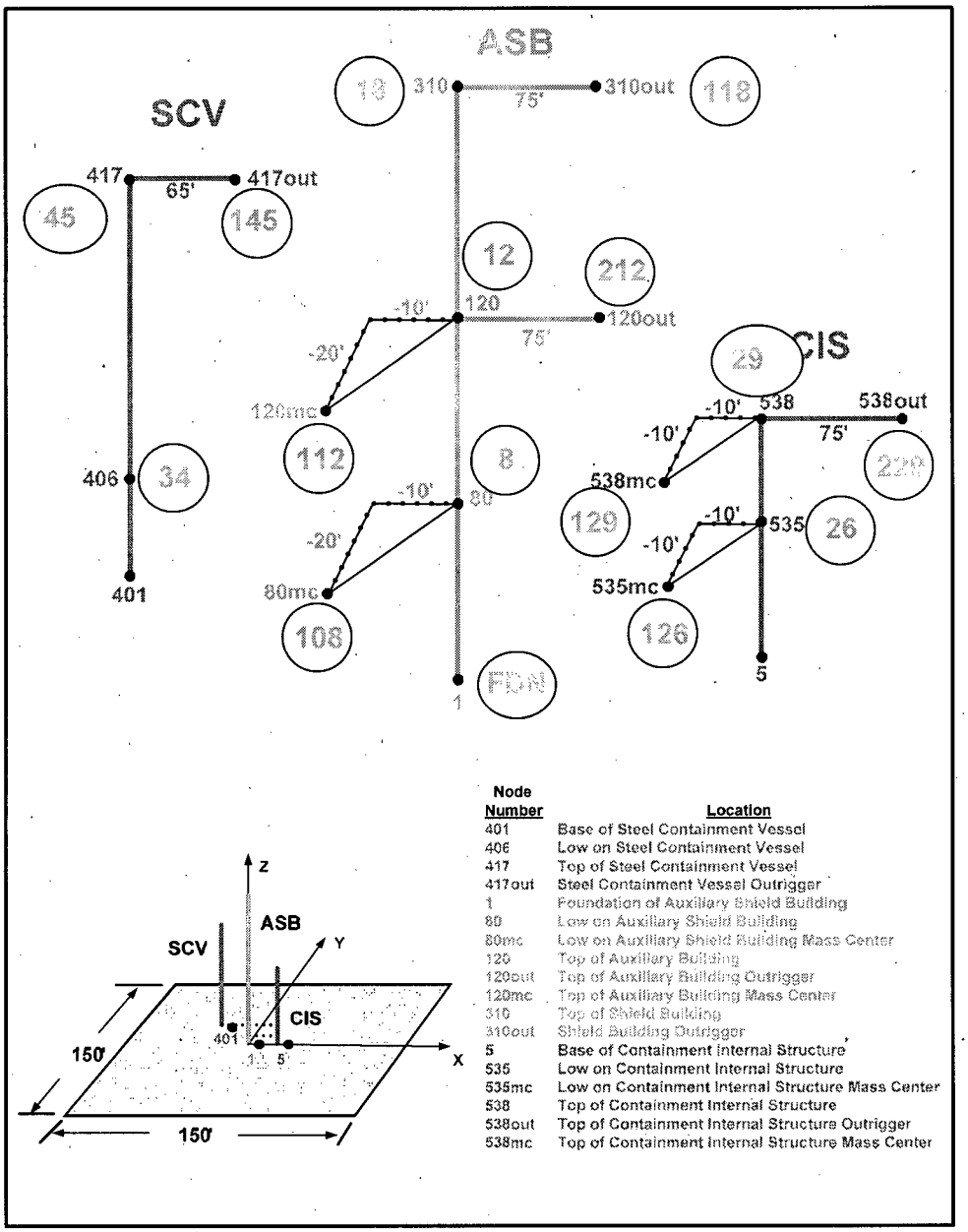

Figure A-1
Locations on the AP1000-Based Stick Model Where In-Structure Response Spectra are Computed

X-Direction Input Ground Motion

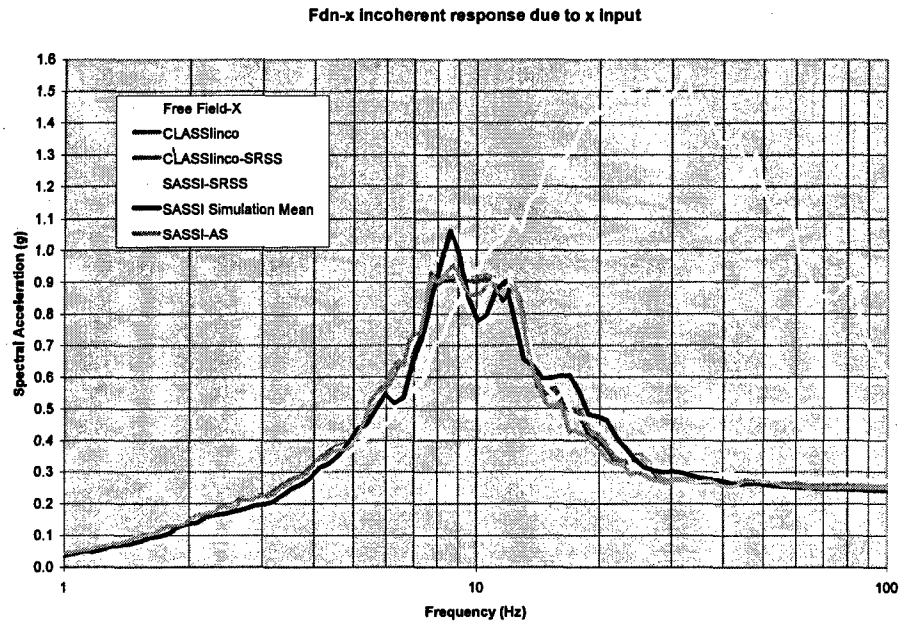

Figure A-2
Center of Foundation Response Spectra – X Direction due to X Input –CLASSIinco, CLASSIinco-SRSS, SASSI-SRSS, SASSI Simulation Mean, SASSI-AS (Node 1)

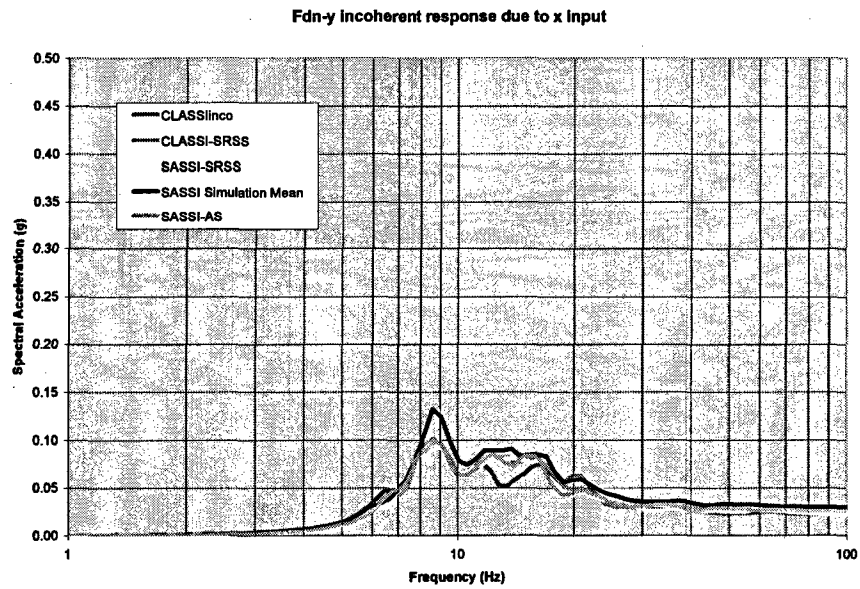

Figure A-3
Center of Foundation Response Spectra – Y Direction due to X Input –CLASSIinco, CLASSIinco-SRSS, SASSI-SRSS, SASSI Simulation Mean, SASSI-AS (Node 1)

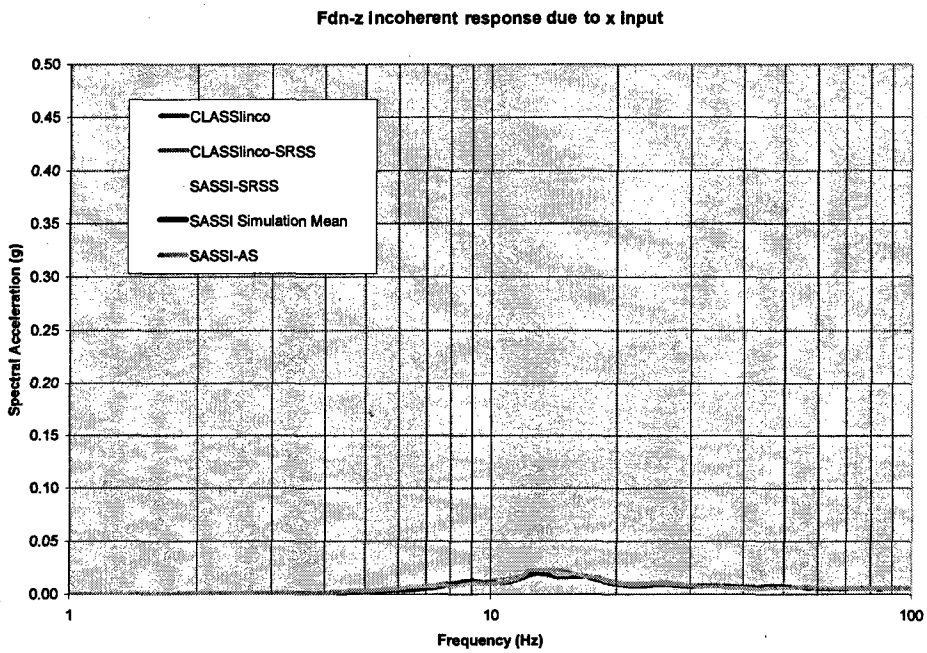

Figure A-4
Center of Foundation Response Spectra – Z Direction due to X Input –CLASSIinco, CLASSIinco-SRSS, SASSI-SRSS, SASSI Simulation Mean, SASSI-AS (Node 1)

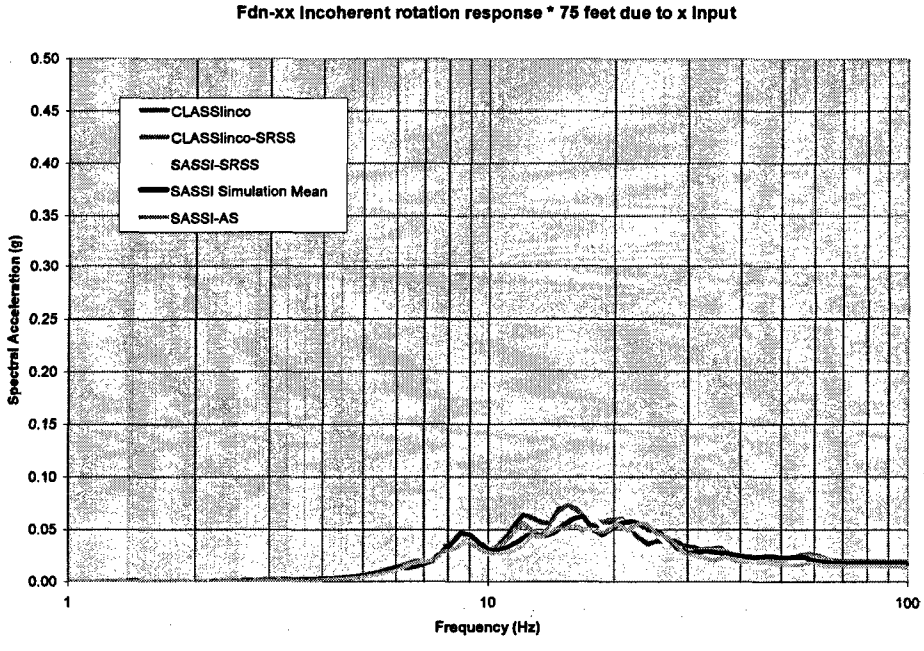

Figure A-5
Edge of Foundation Response Spectra –XX Rotation due to X Input –CLASSIinco, CLASSIinco-SRSS, SASSI-SRSS, SASSI Simulation Mean, SASSI-AS (Node 1)

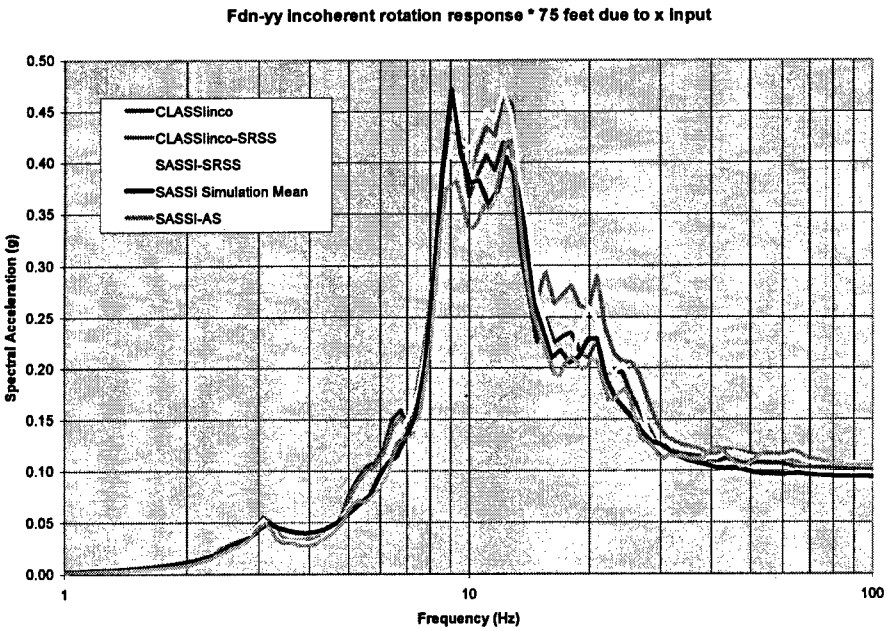

Figure A-6
Edge of Foundation Response Spectra –YY Rotation due to X input –CLASSIinco, CLASSIinco-SRSS, SASSI-SRSS, SASSI Simulation Mean, SASSI-AS (Node 1)

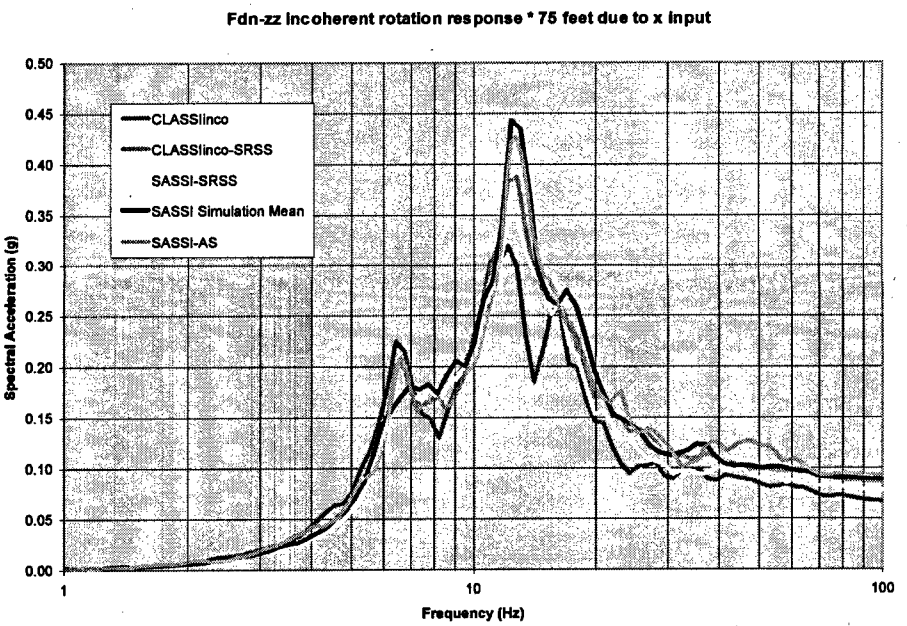

Figure A-7
Edge of Foundation Response Spectra –ZZ Rotation due to X input –CLASSIinco, CLASSIinco-SRSS, SASSI-SRSS, SASSI Simulation Mean, SASSI-AS (Node 1)

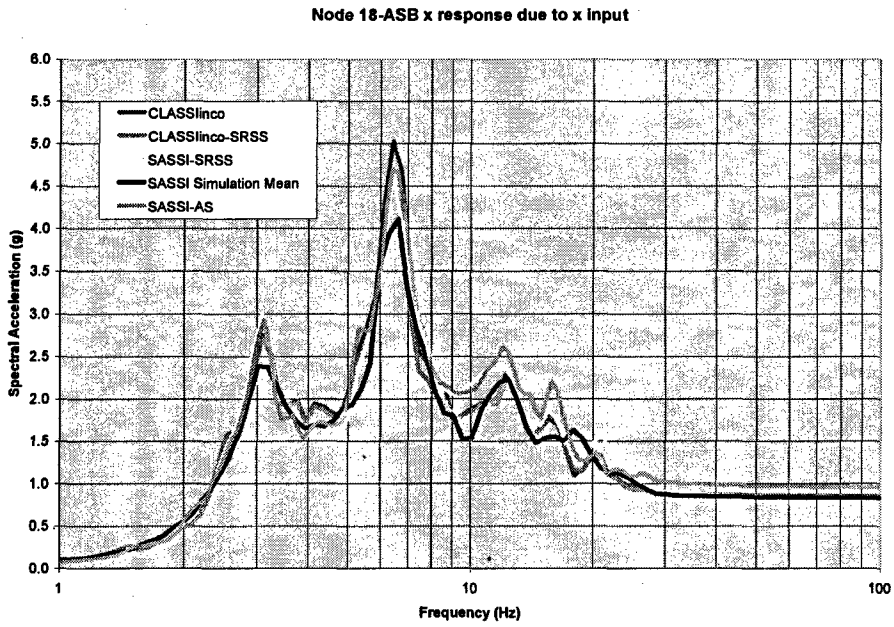

Figure A-8
Top of ASB Response Spectra – X Direction due to X Input –CLASSIinco, CLASSIinco-SRSS, SASSI-SRSS, SASSI Simulation Mean, SASSI-AS (Node 18)

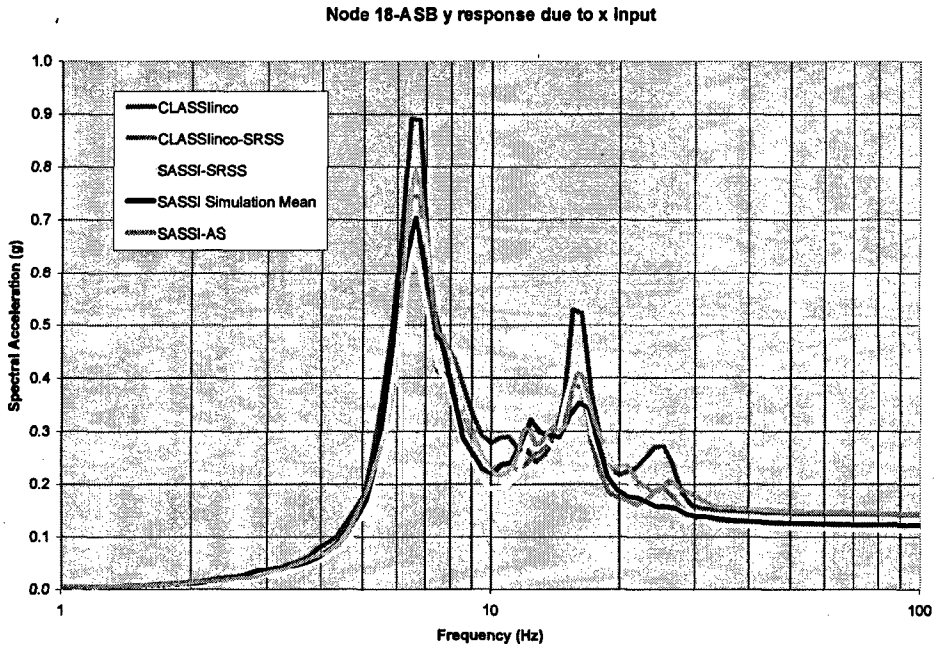

Figure A-9
Top of ASB Response Spectra – Y Direction due to X Input –CLASSIinco, CLASSIinco-SRSS, SASSI-SRSS, SASSI Simulation Mean, SASSI-AS (Node 18)

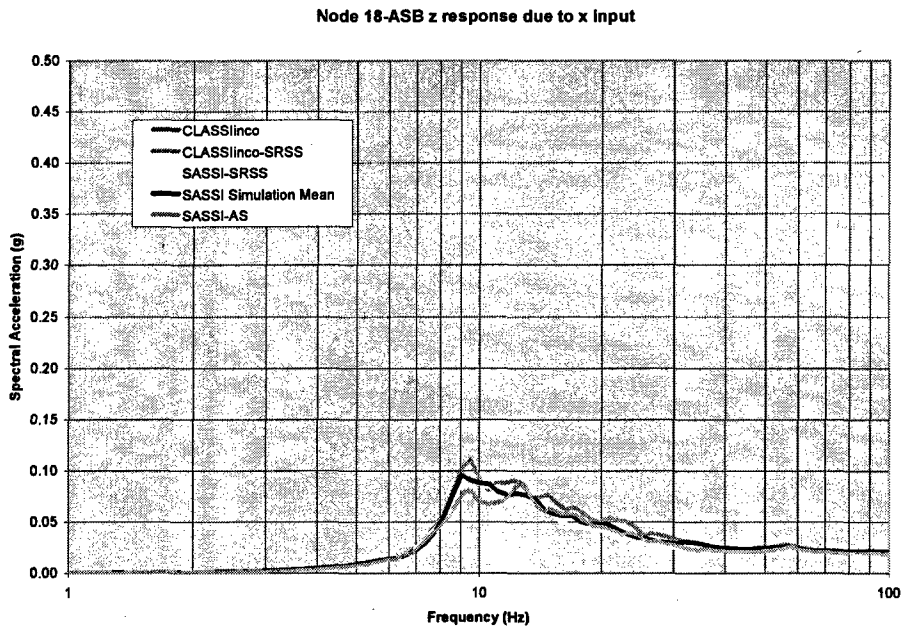

Figure A-10
Top of ASB Response Spectra – Z Direction due to X input –CLASSlinco, CLASSlinco-SRSS, SASSI-SRSS, SASSI Simulation Mean, SASSI-AS (Node 18)

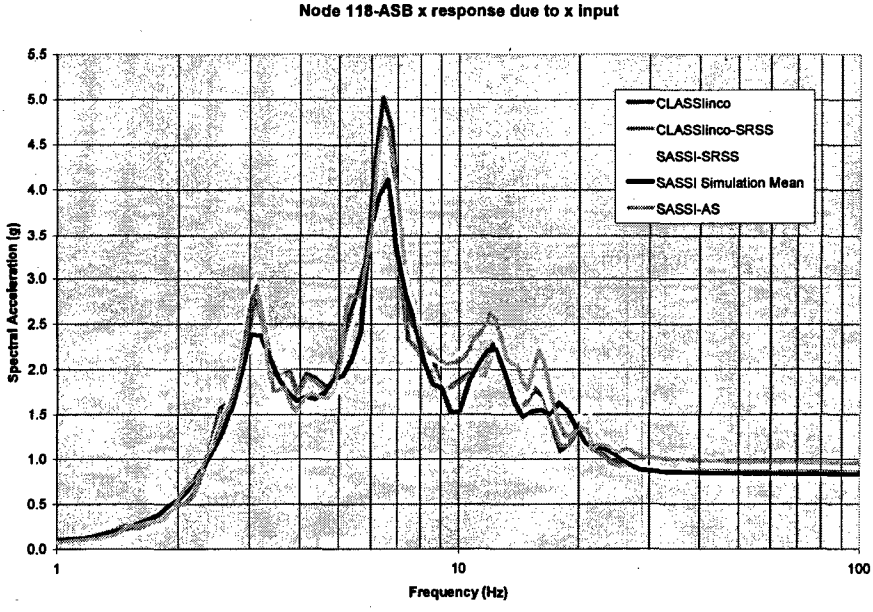

Figure A-11
ASB Outrigger Response Spectra – X Direction due to X input –CLASSlinco, CLASSlinco-SRSS, SASSI-SRSS, SASSI Simulation Mean, SASSI-AS (Node 118)

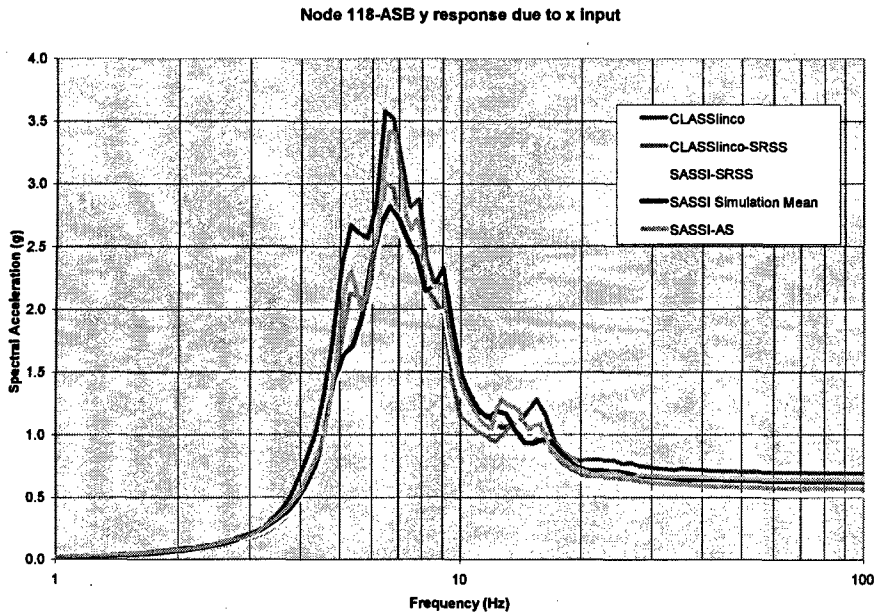

Figure A-12
ASB Outrigger Response Spectra – Y Direction due to X Input –CLASSlinco, CLASSlinco-SRSS, SASSI-SRSS, SASSI Simulation Mean, SASSI-AS (Node 118)

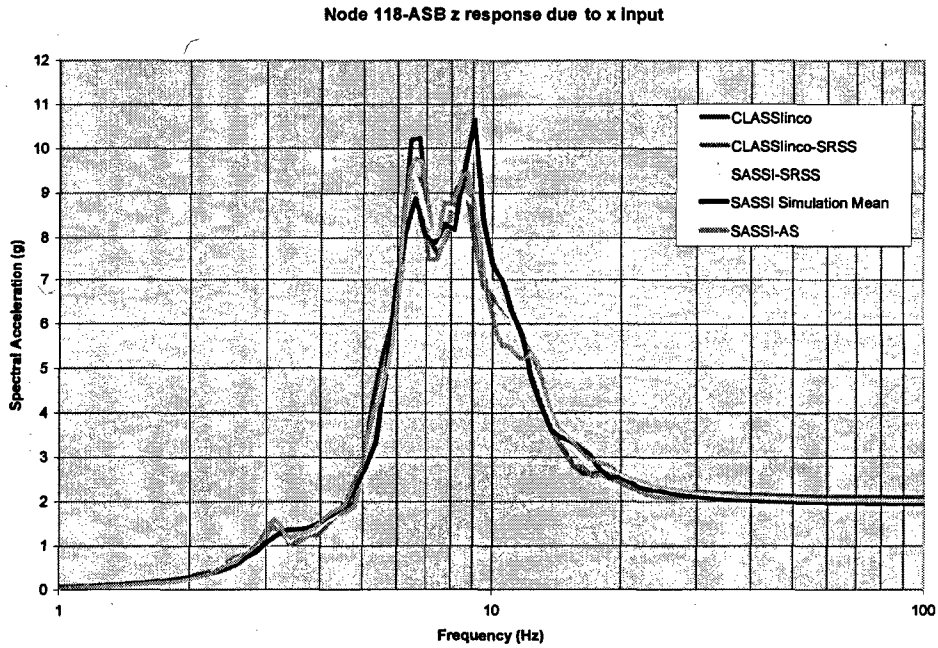

Figure A-13
ASB Outrigger Response Spectra – Z Direction due to X Input –CLASSlinco, CLASSlinco-SRSS, SASSI-SRSS, SASSI Simulation Mean, SASSI-AS (Node 118)

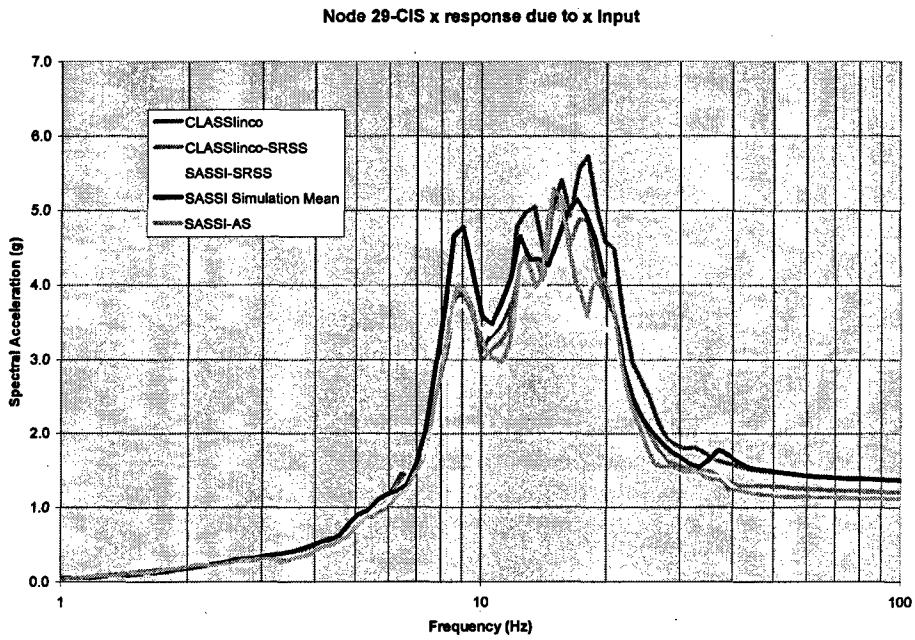

Figure A-14
Top of CIS Shear Center Response Spectra – X Direction due to X Input –CLASSlinco, CLASSlinco-SRSS, SASSI-SRSS, SASSI Simulation Mean, SASSI-AS (Node 29)

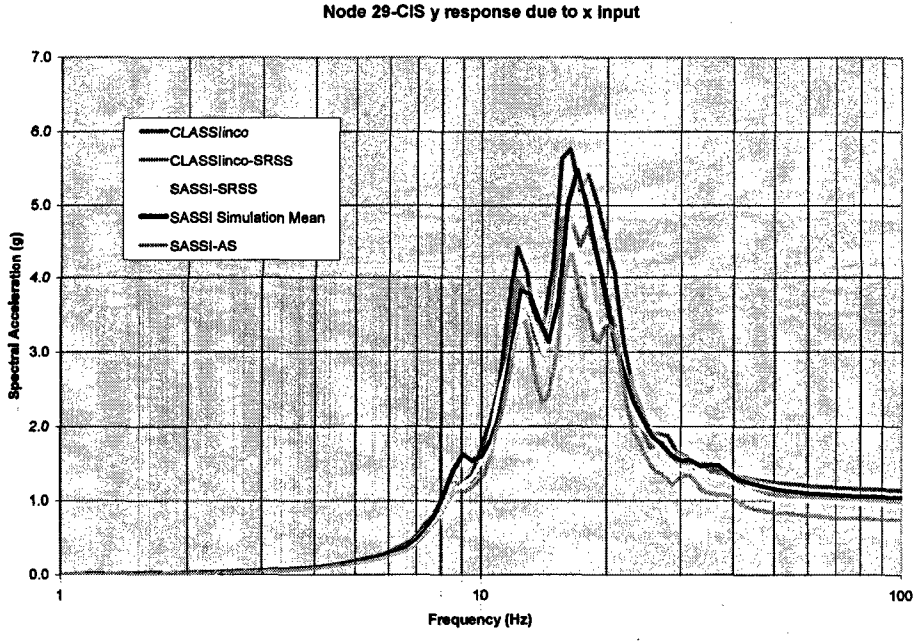

Figure A-15
Top of CIS Shear Center Response Spectra – Y Direction due to X Input –CLASSlinco, CLASSlinco-SRSS, SASSI-SRSS, SASSI Simulation Mean, SASSI-AS (Node 29)

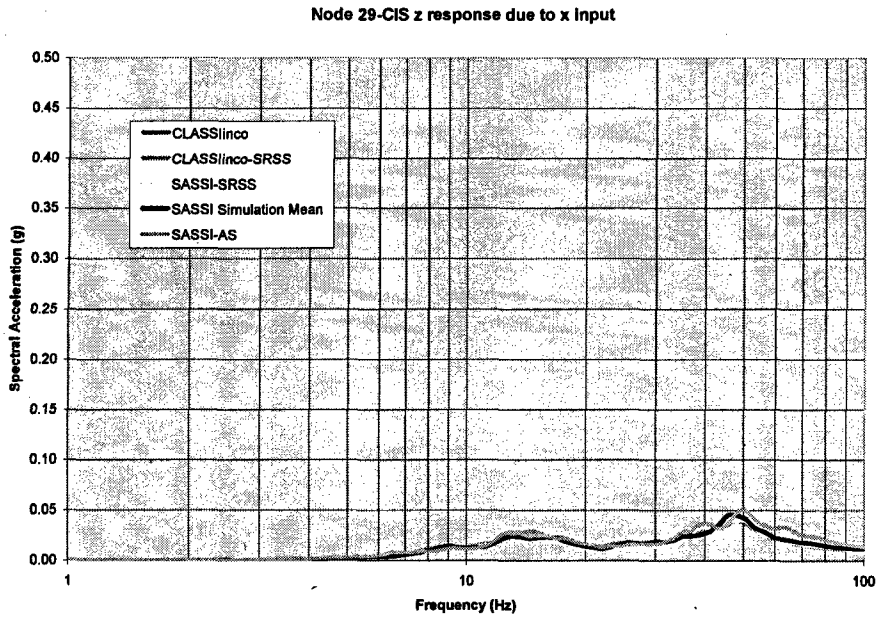

Figure A-16
Top of CIS Shear Center Response Spectra – Z Direction due to X Input –CLASSIinco, CLASSIinco-SRSS, SASSI-SRSS, SASSI Simulation Mean, SASSI-AS (Node 29)

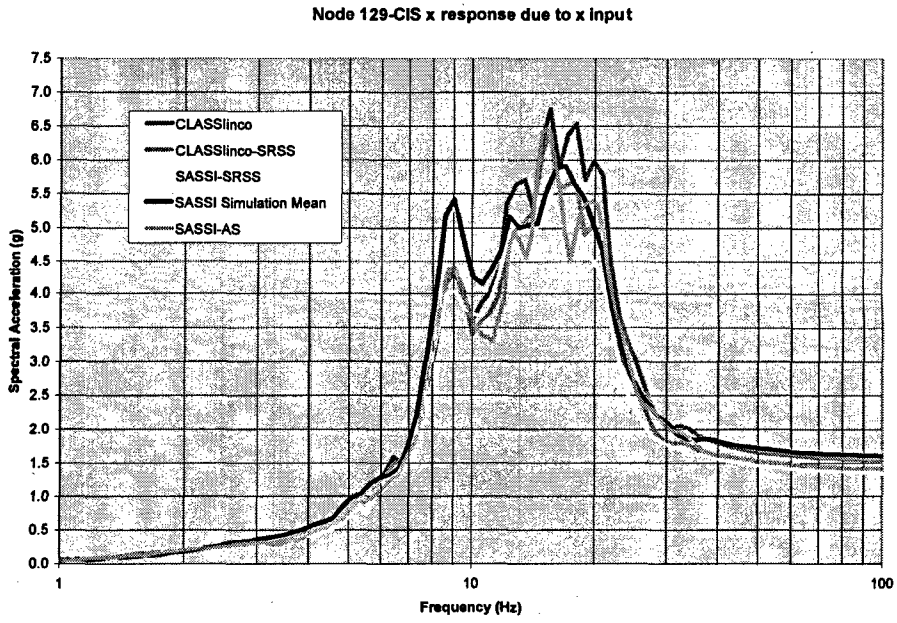

Figure A-17
Top of CIS Horizontal Mass Center Response Spectra – X Direction due to X Input – CLASSIinco, CLASSIinco-SRSS, SASSI-SRSS, SASSI Simulation Mean, SASSI-AS (Node 129)

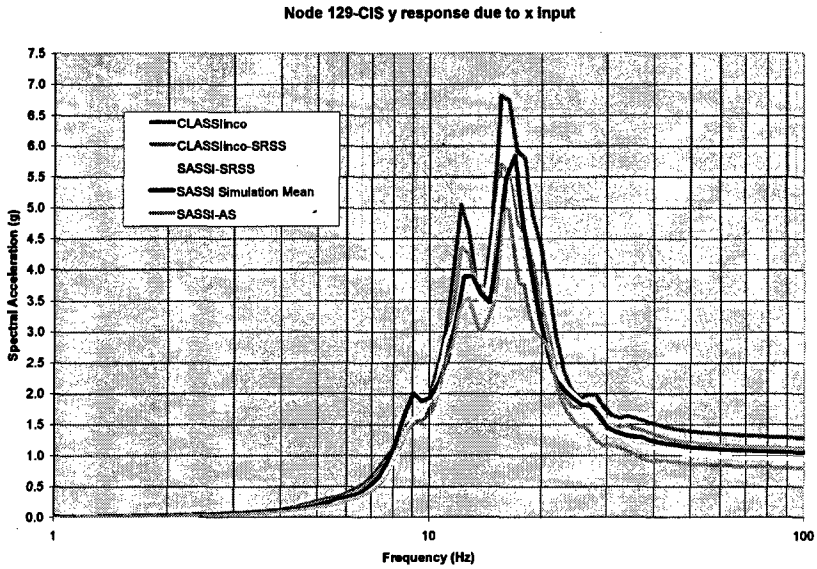

Figure A-18
Top of CIS Horizontal Mass Center Response Spectra – Y Direction due to X input – CLASSIinco, CLASSIinco-SRSS, SASSI-SRSS, SASSI Simulation Mean, SASSI-AS (Node 129)

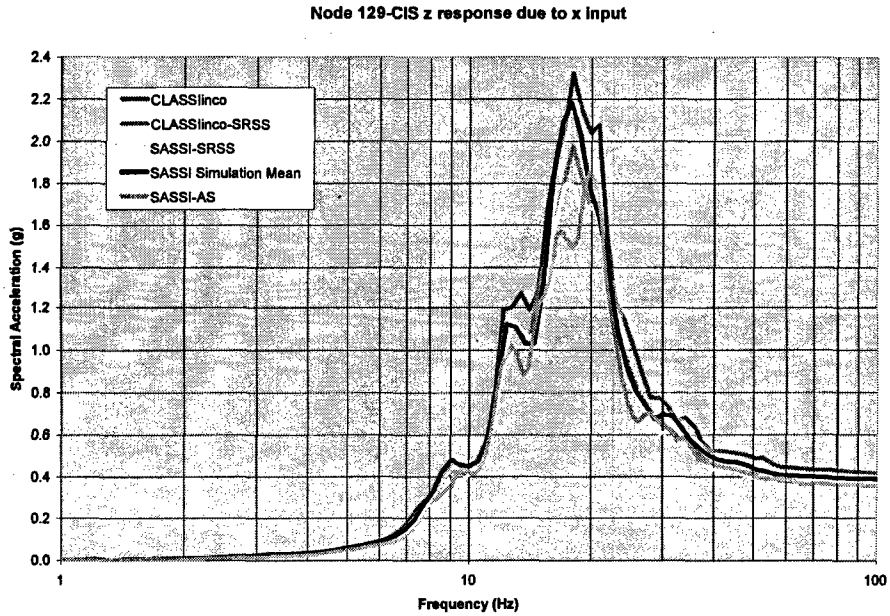

Figure A-19
Top of CIS Horizontal Mass Center Response Spectra – Z Direction due to X input – CLASSIinco, CLASSIinco-SRSS, SASSI-SRSS, SASSI Simulation Mean, SASSI-AS (Node 129)

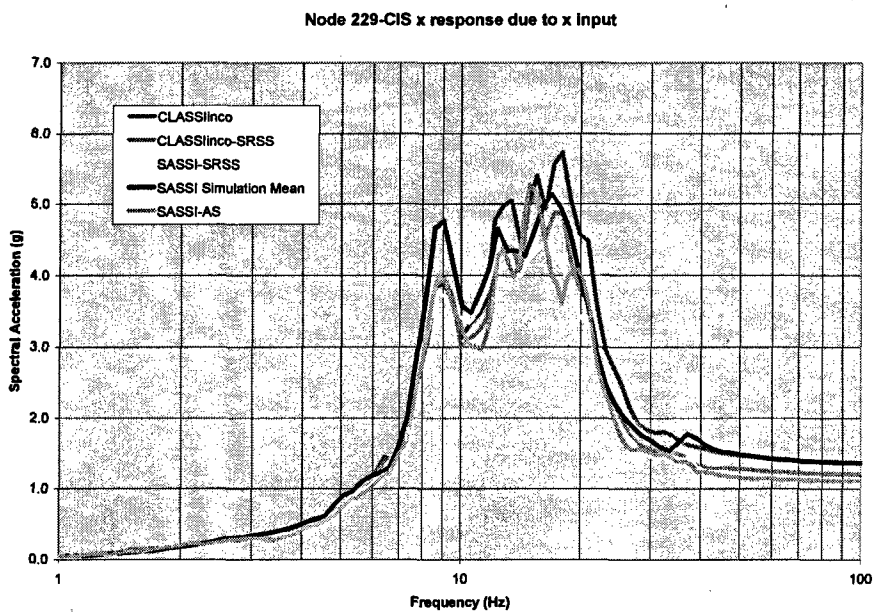

Figure A-20
CIS Outrigger Response Spectra – X Direction due to X input –CLASSIinco, CLASSIinco-SRSS, SASSI-SRSS, SASSI Simulation Mean, SASSI-AS (Node 229)

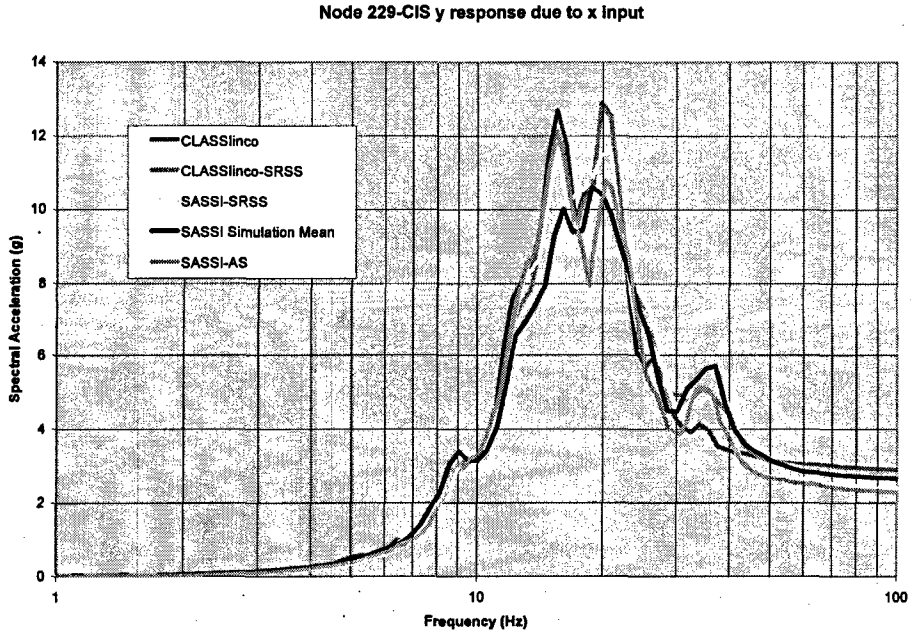

Figure A-21
CIS Outrigger Response Spectra – Y Direction due to X Input –CLASSIinco, CLASSIinco-SRSS, SASSI-SRSS, SASSI Simulation Mean, SASSI-AS (Node 229)

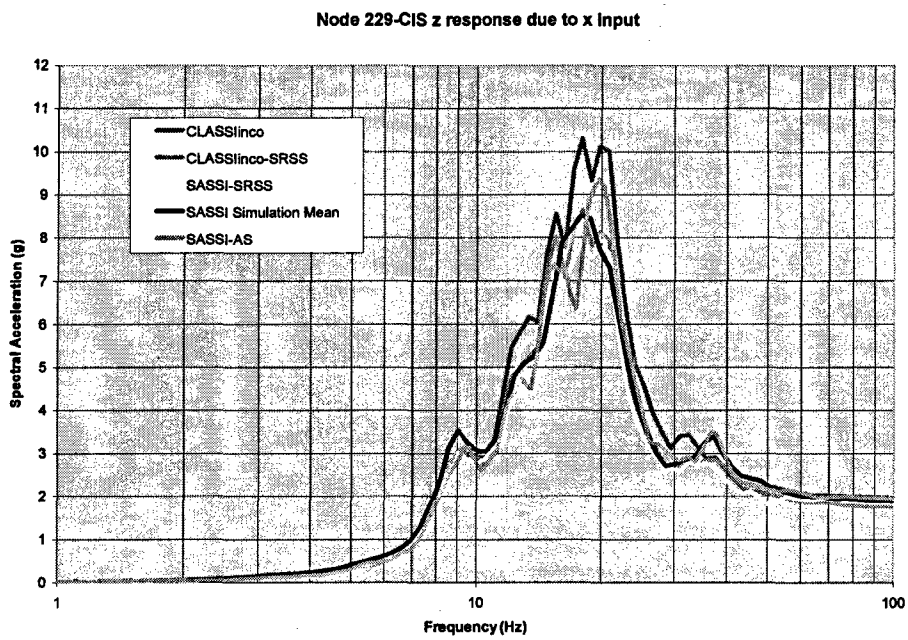

Figure A-22
CIS Outrigger Response Spectra – Z Direction due to X Input –CLASSIinco, CLASSIinco-SRSS, SASSI-SRSS, SASSI Simulation Mean, SASSI-AS (Node 229)

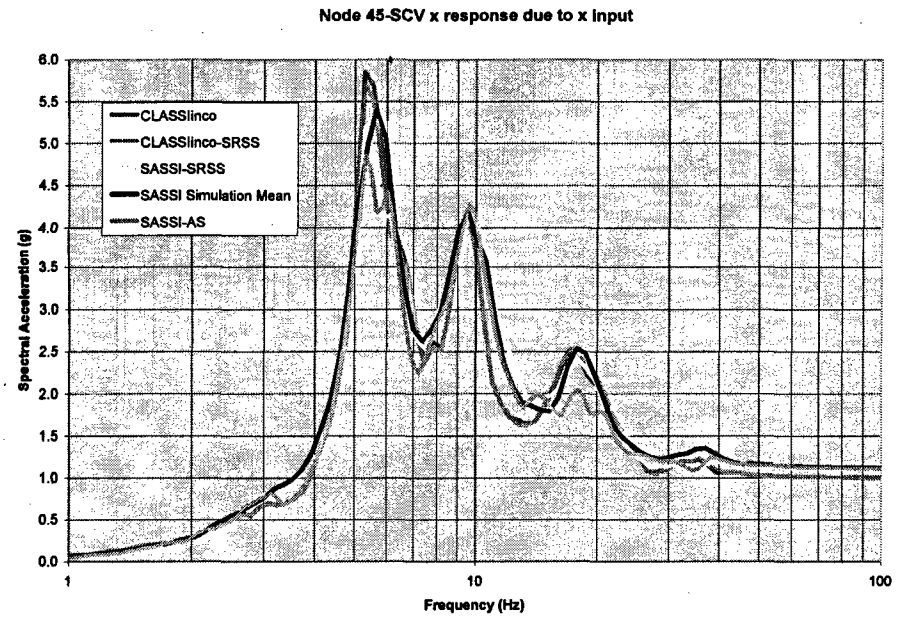

Figure A-23
Top of SCV Response Spectra – X Direction due to X Input –CLASSIinco, CLASSIinco-SRSS, SASSI-SRSS, SASSI Simulation Mean, SASSI-AS (Node 45)

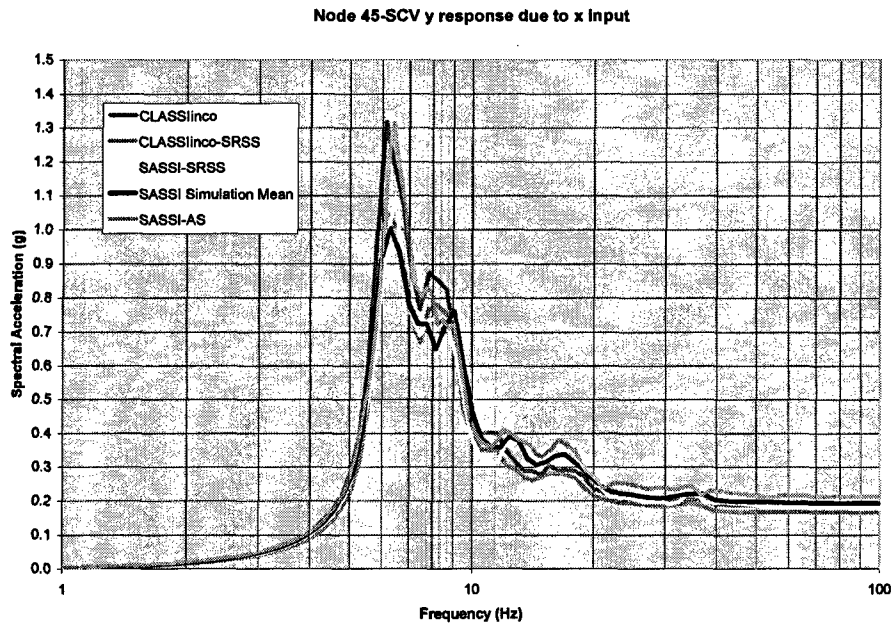

Figure A-24
Top of SCV Response Spectra – Y Direction due to X Input –CLASSIinco, CLASSIinco-SRSS, SASSI-SRSS, SASSI Simulation Mean, SASSI-AS (Node 45)

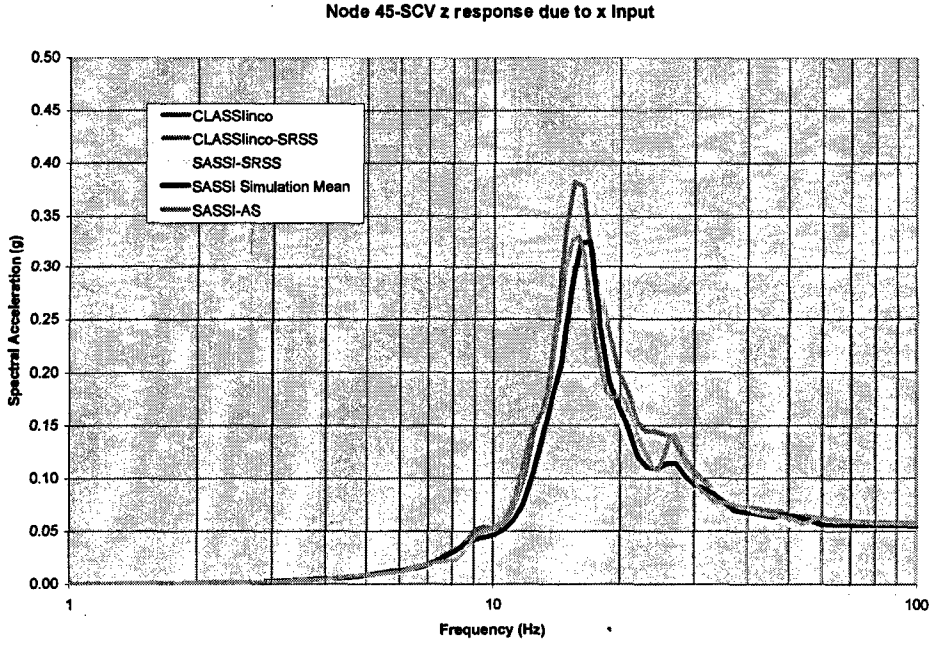

Figure A-25
Top of SCV Response Spectra – Z Direction due to X Input –CLASSIinco, CLASSIinco-SRSS, SASSI-SRSS, SASSI Simulation Mean, SASSI-AS (Node 45)

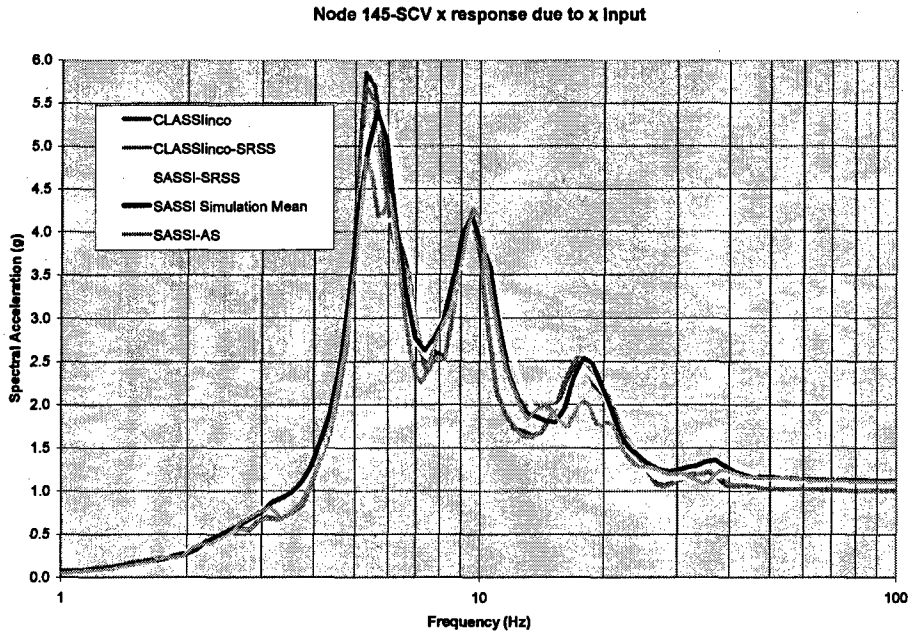

Figure A-26
SCV Outrigger Response Spectra – X Direction due to X input –CLASSlinco, CLASSlinco-SRSS, SASSI-SRSS, SASSI Simulation Mean, SASSI-AS (Node 145)

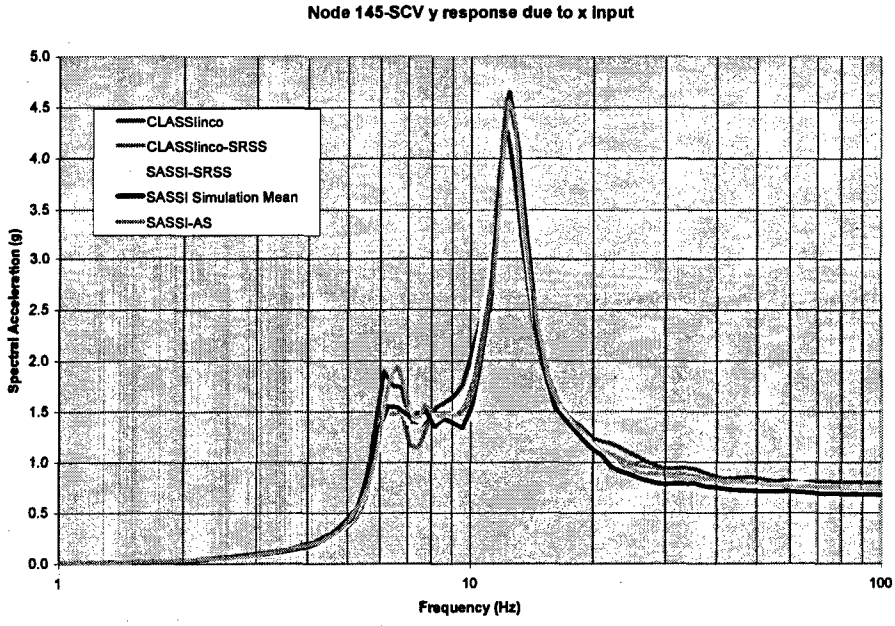

Figure A-27
SCV Outrigger Response Spectra – Y Direction due to X input –CLASSlinco, CLASSlinco-SRSS, SASSI-SRSS, SASSI Simulation Mean, SASSI-AS (Node 145)

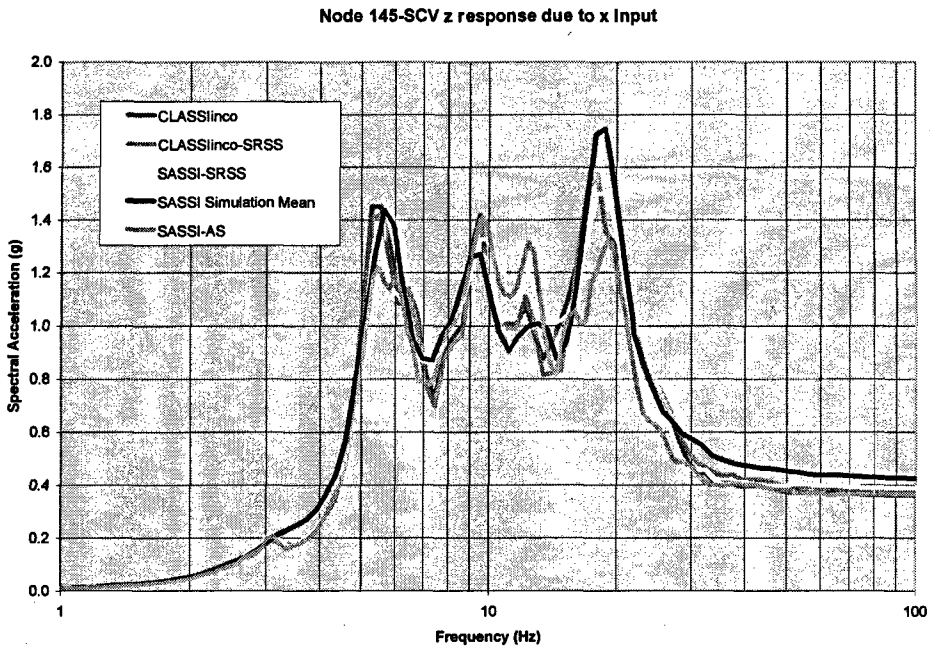

Figure A-28
SCV Outrigger Response Spectra – Z Direction due to X Input –CLASSIinco, CLASSIinco-SRSS, SASSI-SRSS, SASSI Simulation Mean, SASSI-AS (Node 145)

Y-Direction Input Ground Motion

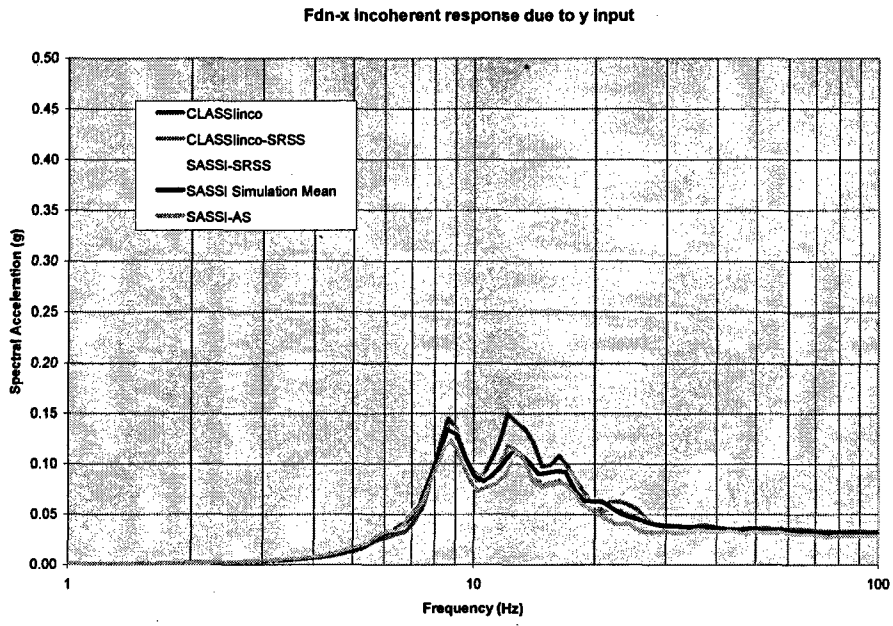

Figure A-29
Center of Foundation Response Spectra – X Direction due to Y Input –CLASSlinco, CLASSlinco-SRSS, SASSI-SRSS, SASSI Simulation Mean, SASSI-AS (Node 1)

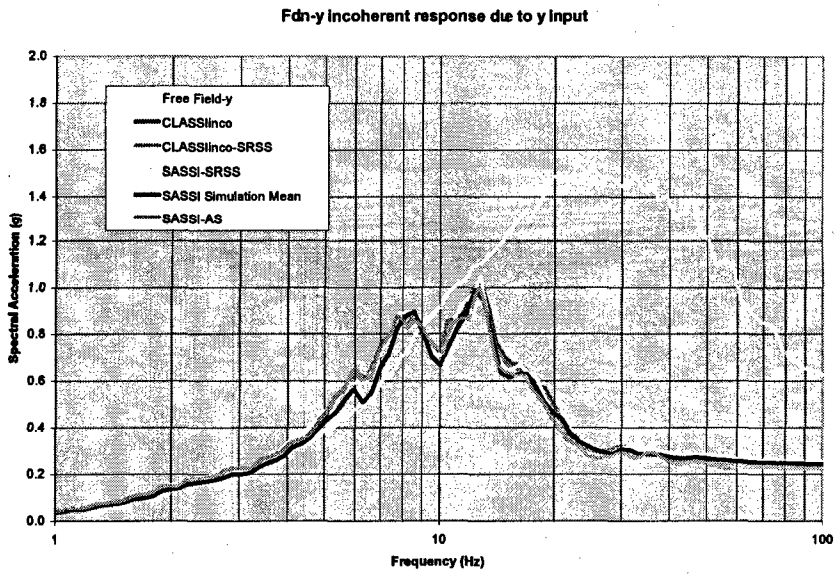

Figure A-30
Center of Foundation Response Spectra – Y Direction due to Y Input –CLASSlinco, CLASSlinco-SRSS, SASSI-SRSS, SASSI Simulation Mean, SASSI-AS (Node 1)

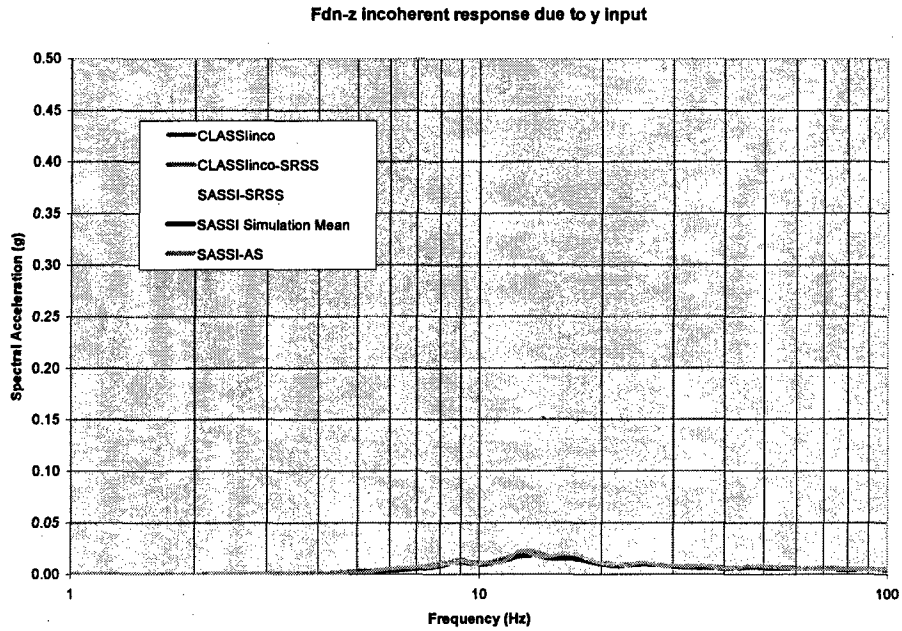

Figure A-31
Center of Foundation Response Spectra – Z Direction due to Y Input –CLASSIinco, CLASSIinco-SRSS, SASSI-SRSS, SASSI Simulation Mean, SASSI-AS (Node 1)

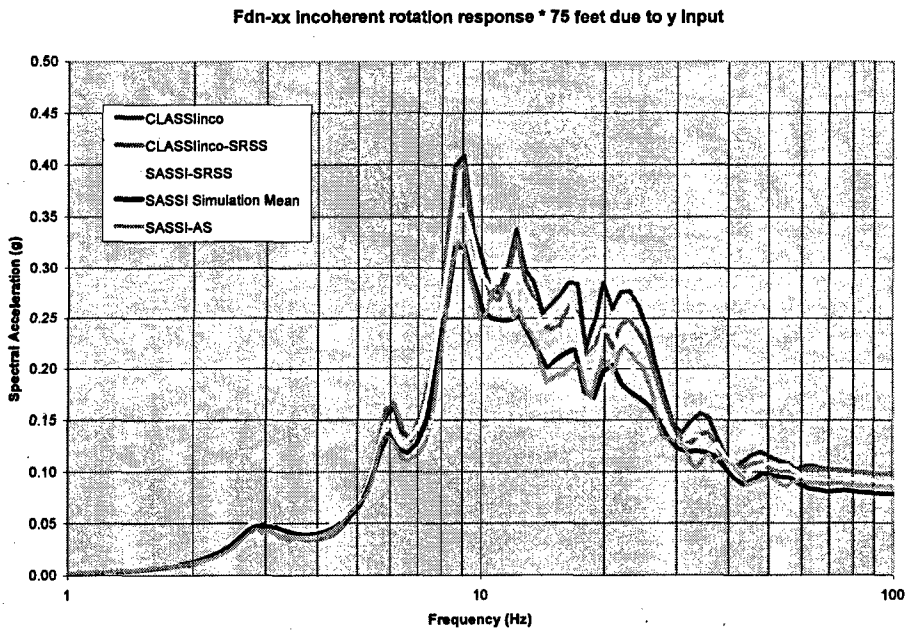

Figure A-32
Edge of Foundation Response Spectra –XX Rotation due to Y Input –CLASSIinco, CLASSIinco-SRSS, SASSI-SRSS, SASSI Simulation Mean, SASSI-AS (Node 1)

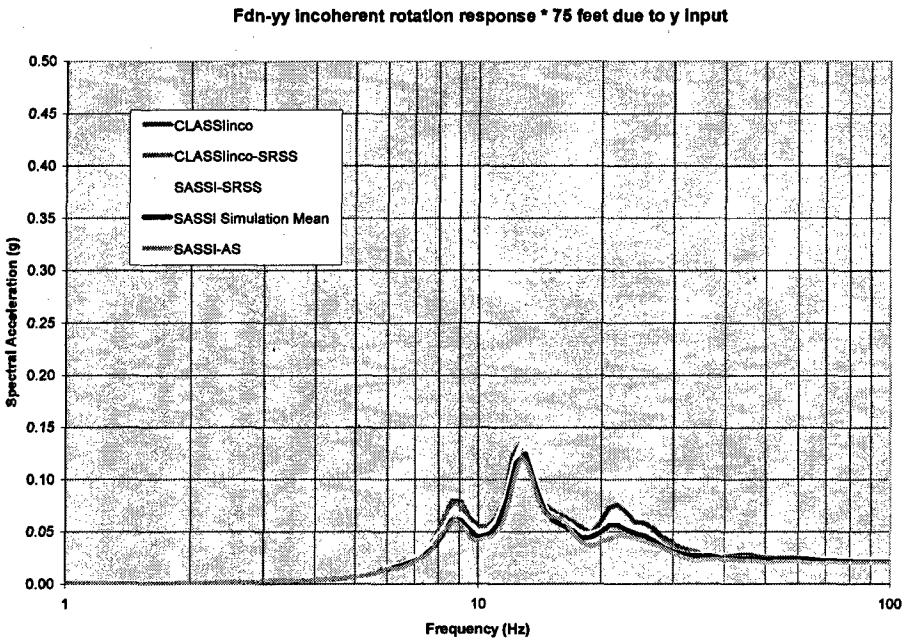

Figure A-33
Edge of Foundation Response Spectra –YY Rotation due to Y Input –CLASSIinco, CLASSIinco-SRSS, SASSI-SRSS, SASSI Simulation Mean, SASSI-AS (Node 1)

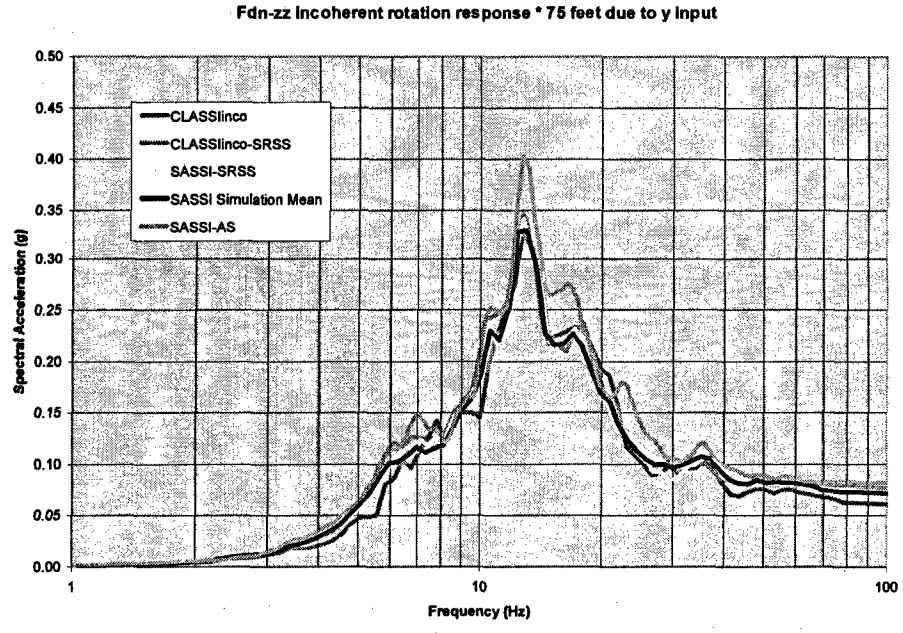

Figure A-34
Edge of Foundation Response Spectra –ZZ Rotation due to Y Input –CLASSIinco, CLASSIinco-SRSS, SASSI-SRSS, SASSI Simulation Mean, SASSI-AS (Node 1)

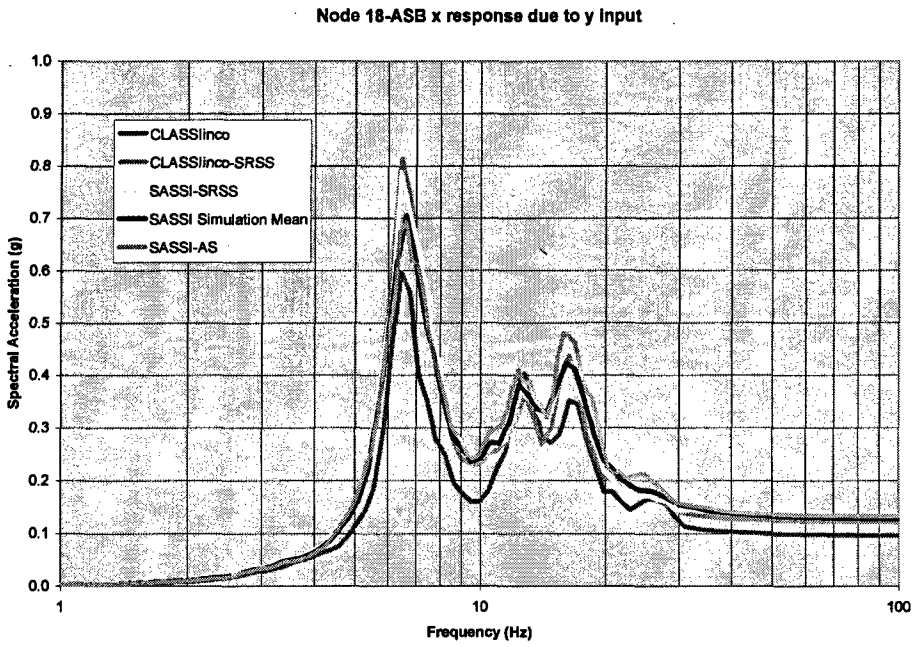

Figure A-35
Top of ASB Response Spectra – X Direction due to Y Input –CLASSlinco, CLASSlinco-SRSS, SASSI-SRSS, SASSI Simulation Mean, SASSI-AS (Node 18)

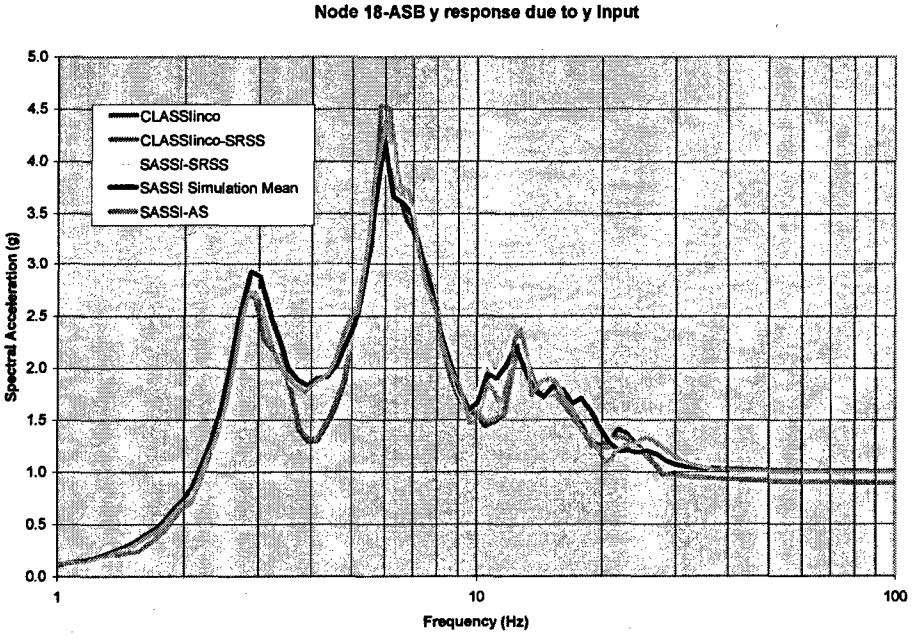

Figure A-36
Top of ASB Response Spectra – Y Direction due to Y Input –CLASSlinco, CLASSlinco-SRSS, SASSI-SRSS, SASSI Simulation Mean, SASSI-AS (Node 18)

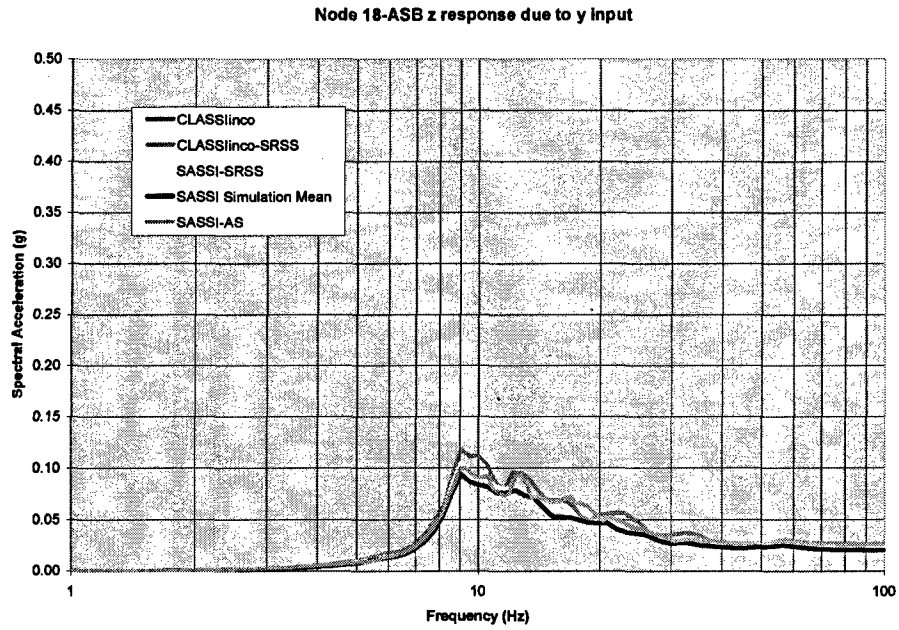

Figure A-37
Top of ASB Response Spectra – Z Direction due to Y Input –CLASSlinco, CLASSlinco-SRSS, SASSI-SRSS, SASSI Simulation Mean, SASSI-AS (Node 18)

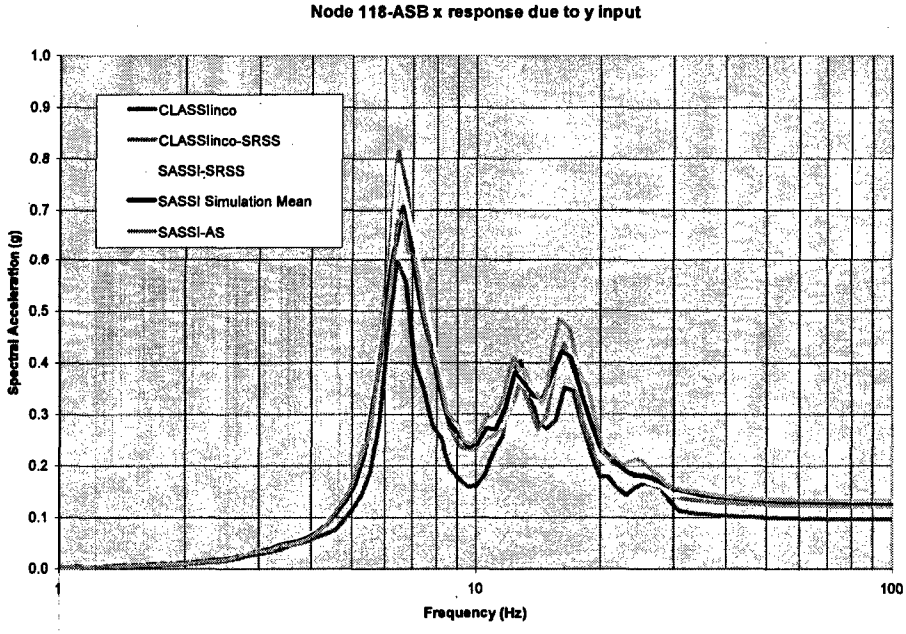

Figure A-38
ASB Outrigger Response Spectra – X Direction due to Y Input –CLASSlinco, CLASSlinco-SRSS, SASSI-SRSS, SASSI Simulation Mean, SASSI-AS (Node 118)

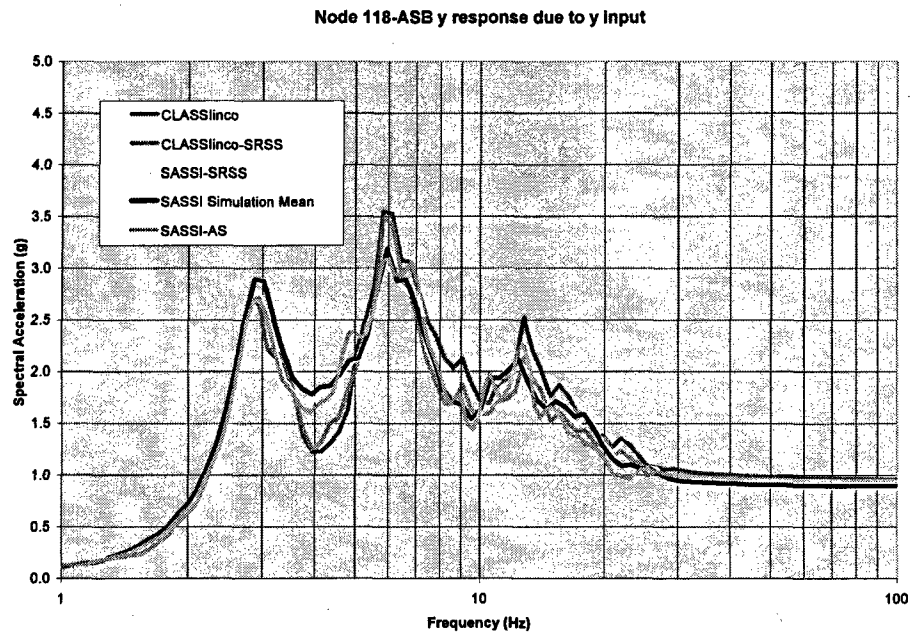

Figure A-39
ASB Outrigger Response Spectra – Y Direction due to Y Input –CLASSIinco, CLASSIinco-SRSS, SASSI-SRSS, SASSI Simulation Mean, SASSI-AS (Node 118)

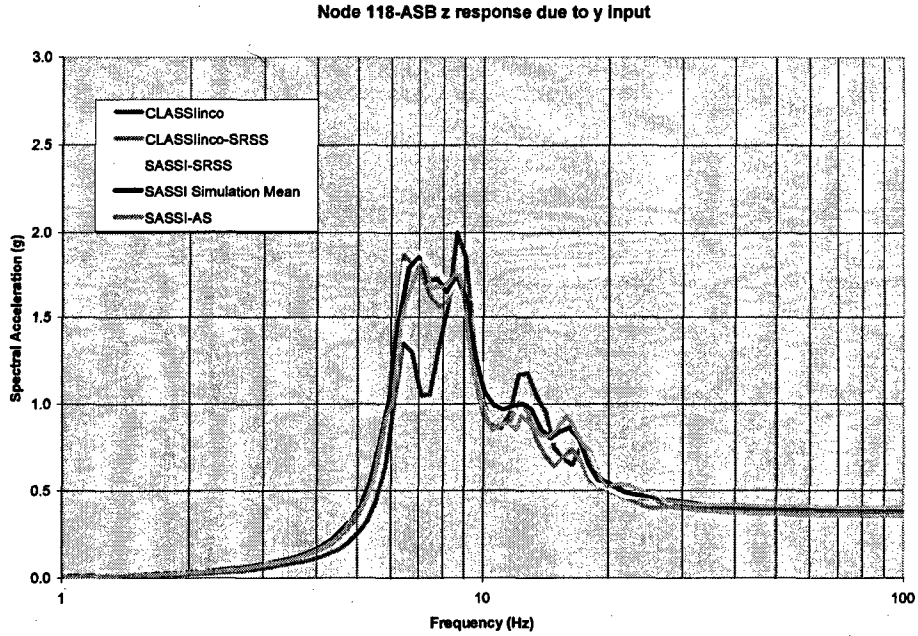

Figure A-40
ASB Outrigger Response Spectra – Z Direction due to Y Input –CLASSIinco, CLASSIinco-SRSS, SASSI-SRSS, SASSI Simulation Mean, SASSI-AS (Node 118)

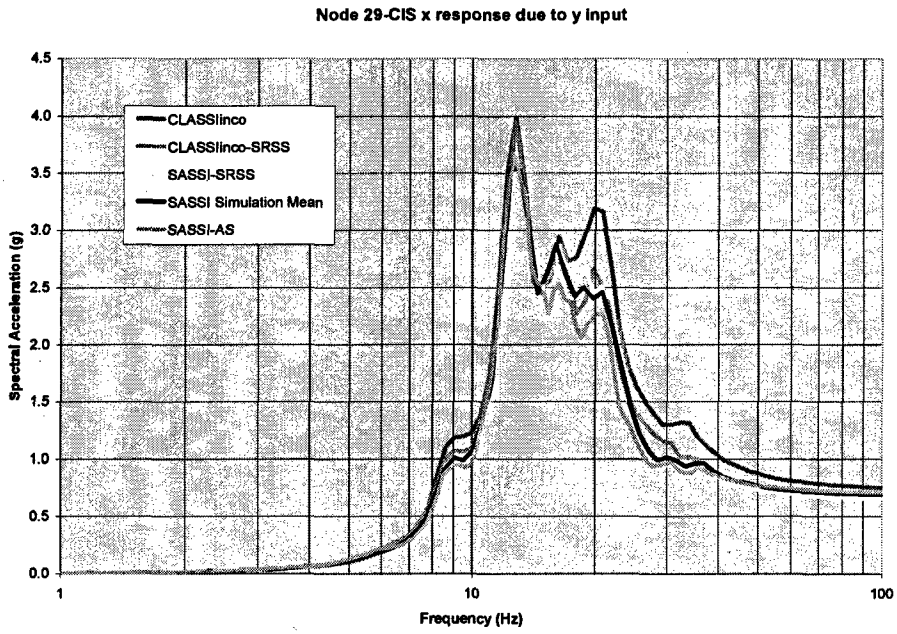

Figure A-41
Top of CIS Shear Center Response Spectra – X Direction due to Y Input –CLASSIinco, CLASSIinco-SRSS, SASSI-SRSS, SASSI Simulation Mean, SASSI-AS (Node 29)

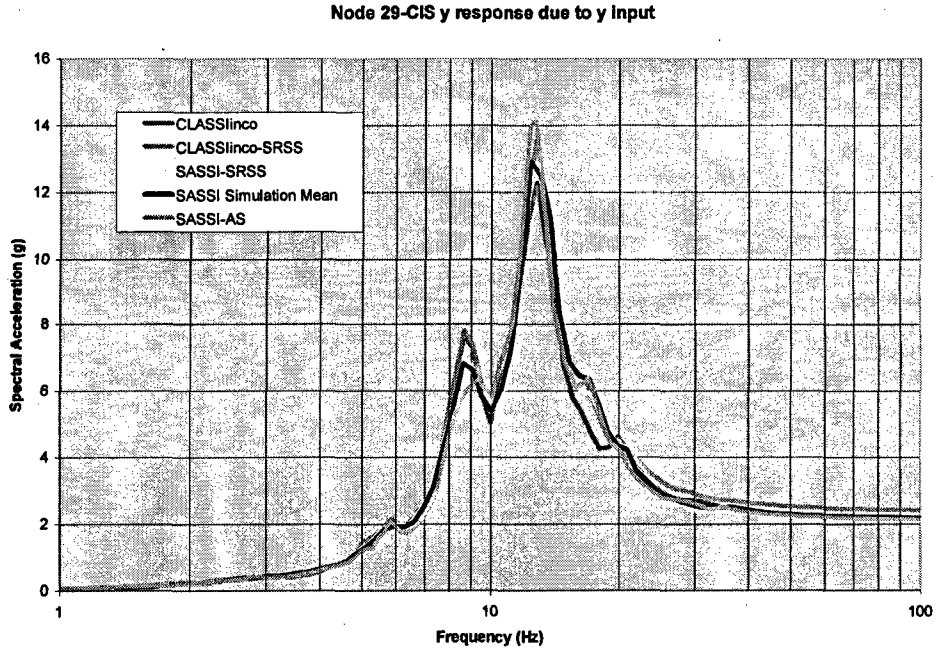

Figure A-42
Top of CIS Shear Center Response Spectra – Y Direction due to Y Input –CLASSIinco, CLASSIinco-SRSS, SASSI-SRSS, SASSI Simulation Mean, SASSI-AS (Node 29)

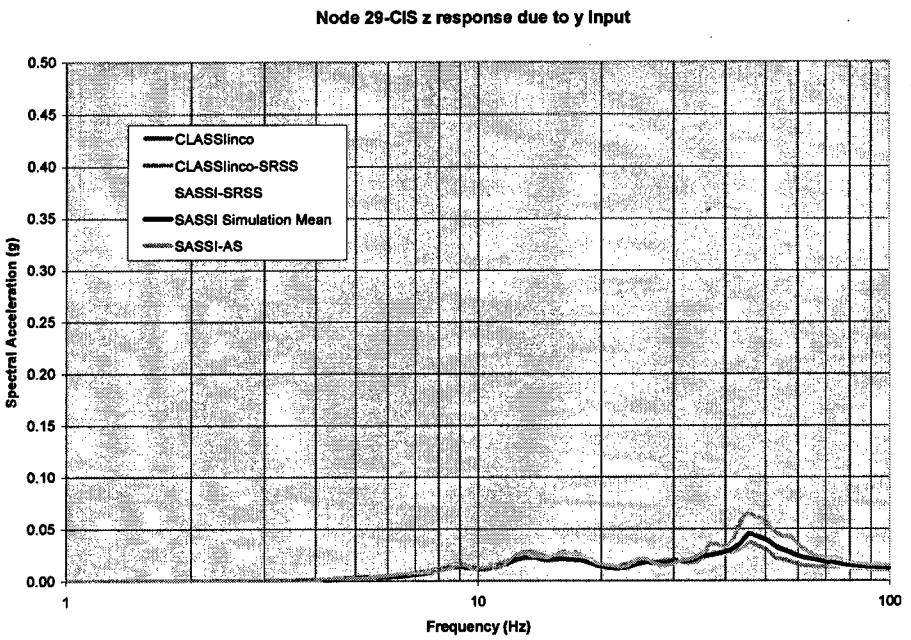

Figure A-43
Top of CIS Shear Center Response Spectra – Z Direction due to Y input –CLASSlinco, CLASSlinco-SRSS, SASSI-SRSS, SASSI Simulation Mean, SASSI-AS (Node 29)

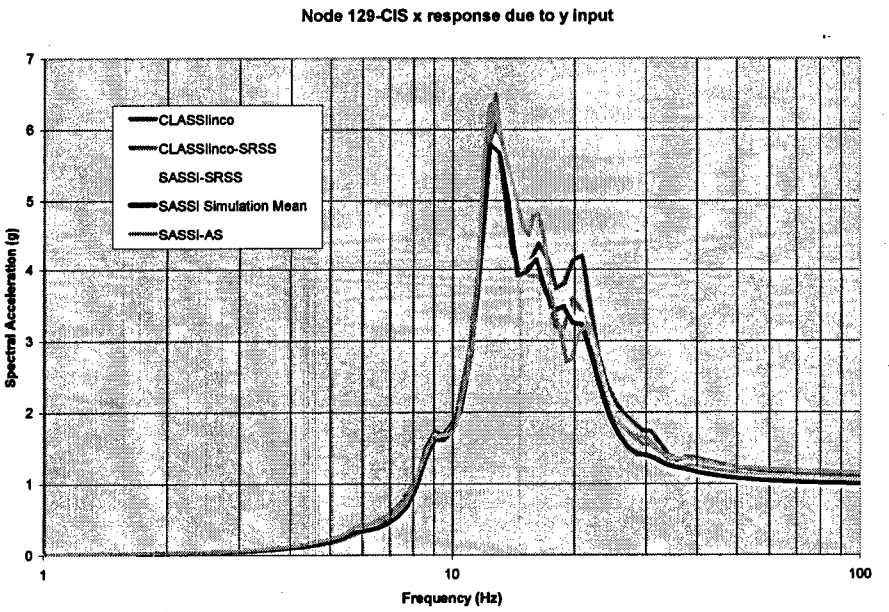

Figure A-44
Top of CIS Horizontal Mass Center Response Spectra – X Direction due to Y input – CLASSlinco, CLASSlinco-SRSS, SASSI-SRSS, SASSI Simulation Mean, SASSI-AS (Node 129)

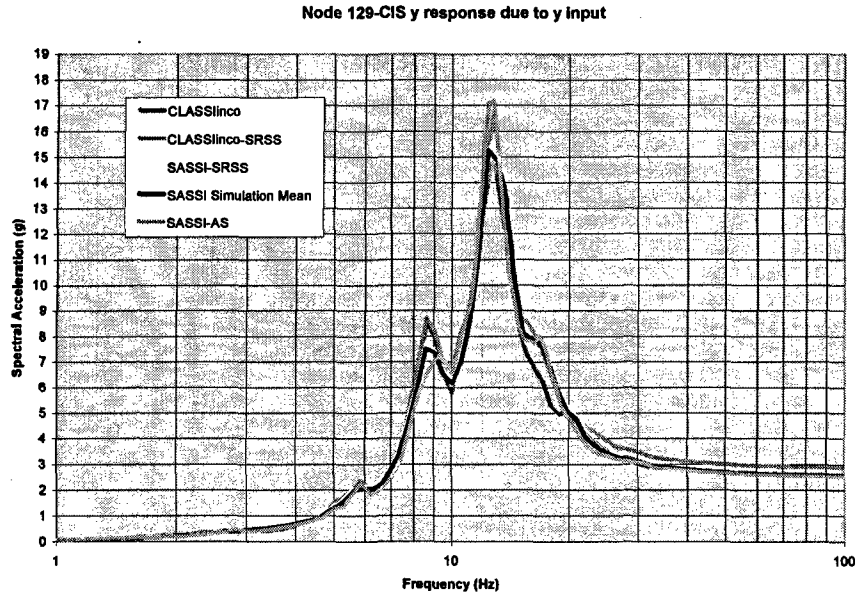

Figure A-45
Top of CIS Horizontal Mass Center Response Spectra – Y Direction due to Y Input – CLASSlinco, CLASSlinco-SRSS, SASSI-SRSS, SASSI Simulation Mean, SASSI-AS (Node 129)

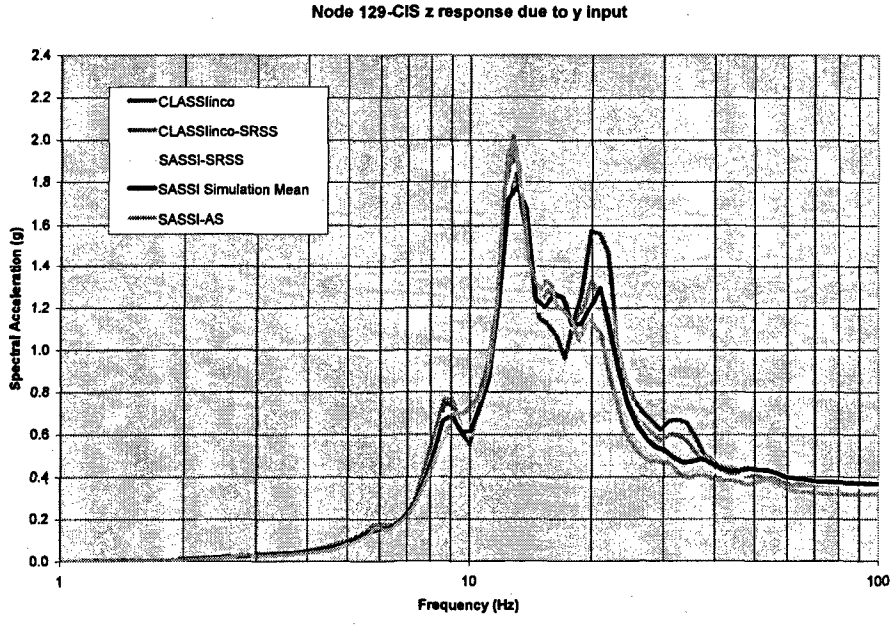

Figure A-46
Top of CIS Horizontal Mass Center Response Spectra – Z Direction due to Y Input – CLASSlinco, CLASSlinco-SRSS, SASSI-SRSS, SASSI Simulation Mean, SASSI-AS (Node 129)

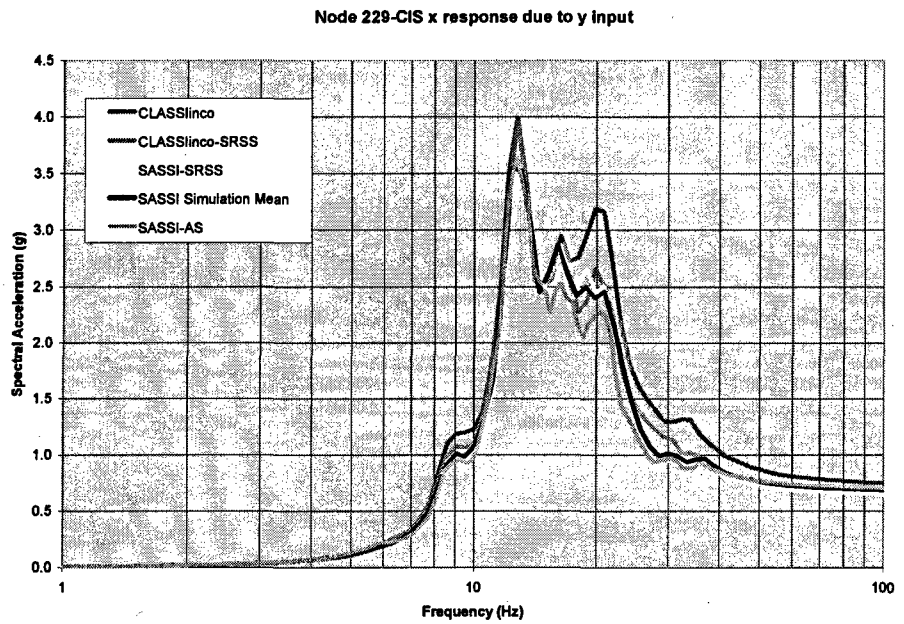

Figure A-47
CIS Outrigger Response Spectra – X Direction due to Y input –CLASSlinco, CLASSlinco-SRSS, SASSI-SRSS, SASSI Simulation Mean, SASSI-AS (Node 229)

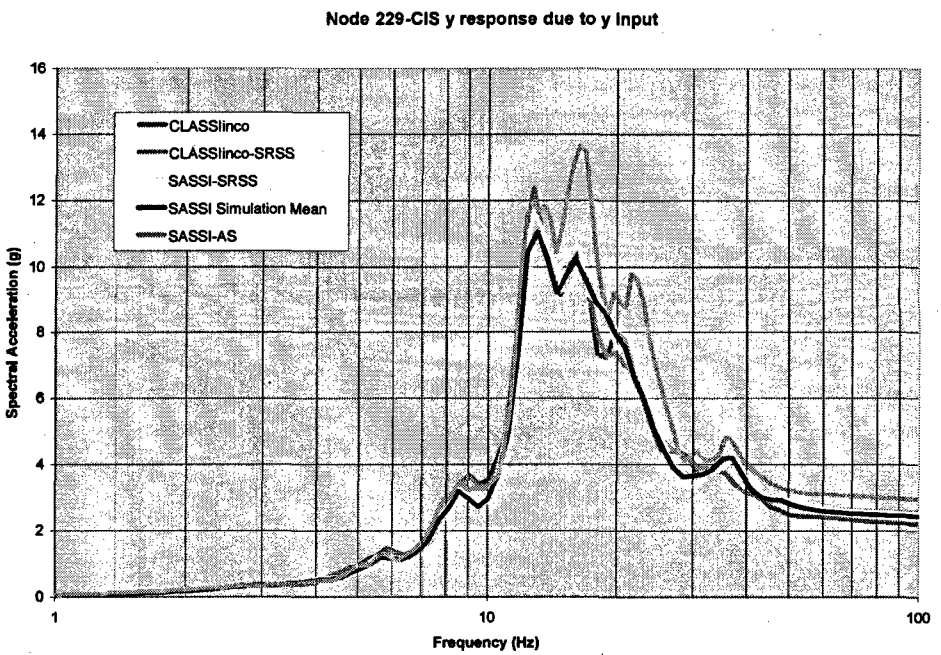

Figure A-48
CIS Outrigger Response Spectra – Y Direction due to Y input –CLASSlinco, CLASSlinco-SRSS, SASSI-SRSS, SASSI Simulation Mean, SASSI-AS (Node 229)

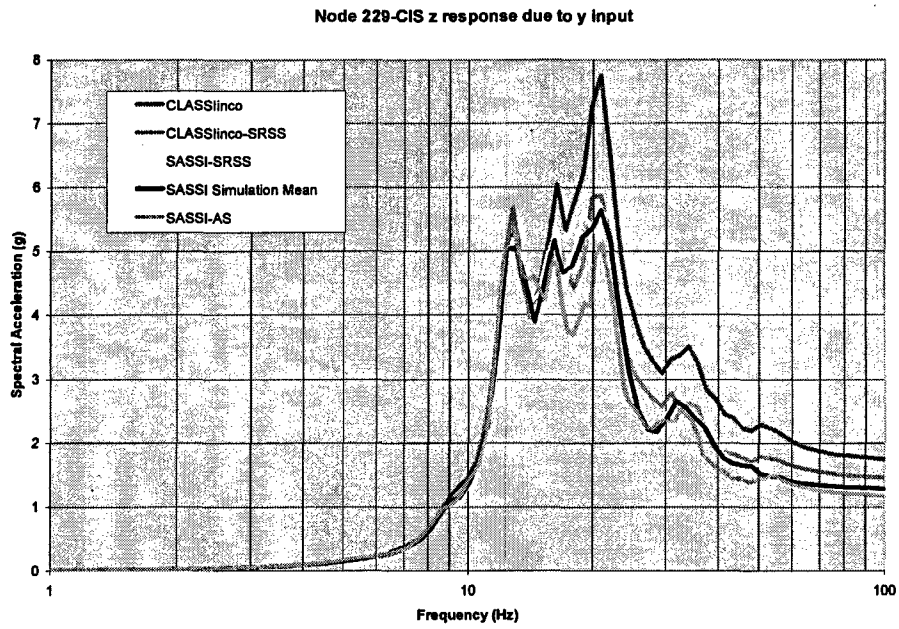

Figure A-49
CIS Outrigger Response Spectra – Z Direction due to Y Input –CLASSlinco, CLASSlinco-SRSS, SASSI-SRSS, SASSI Simulation Mean, SASSI-AS (Node 229)

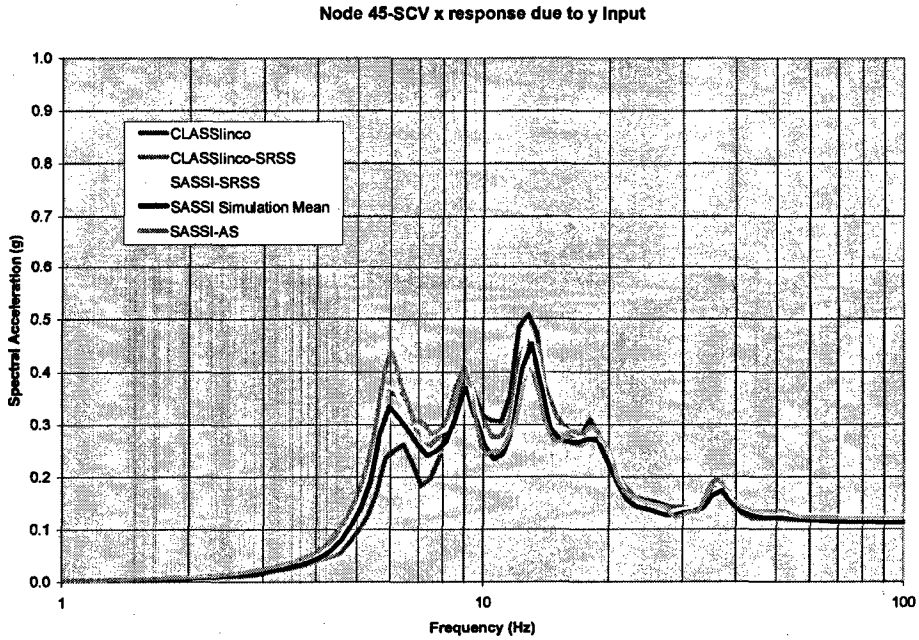

Figure A-50
Top of SCV Response Spectra – X Direction due to Y Input –CLASSlinco, CLASSlinco-SRSS, SASSI-SRSS, SASSI Simulation Mean, SASSI-AS (Node 45)

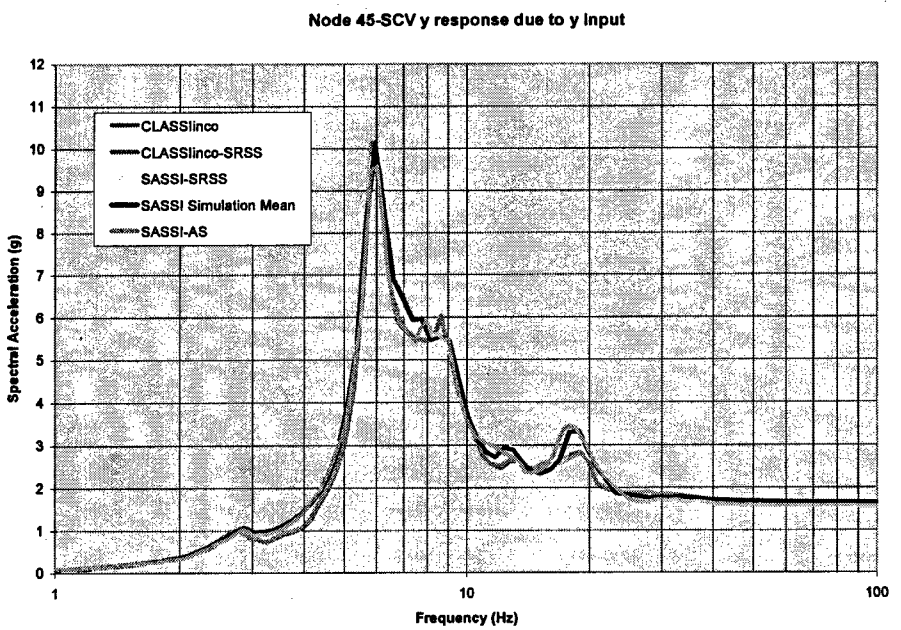

Figure A-51
Top of SCV Response Spectra – Y Direction due to Y input –CLASSlinco, CLASSlinco-SRSS, SASSI-SRSS, SASSI Simulation Mean, SASSI-AS (Node 45)

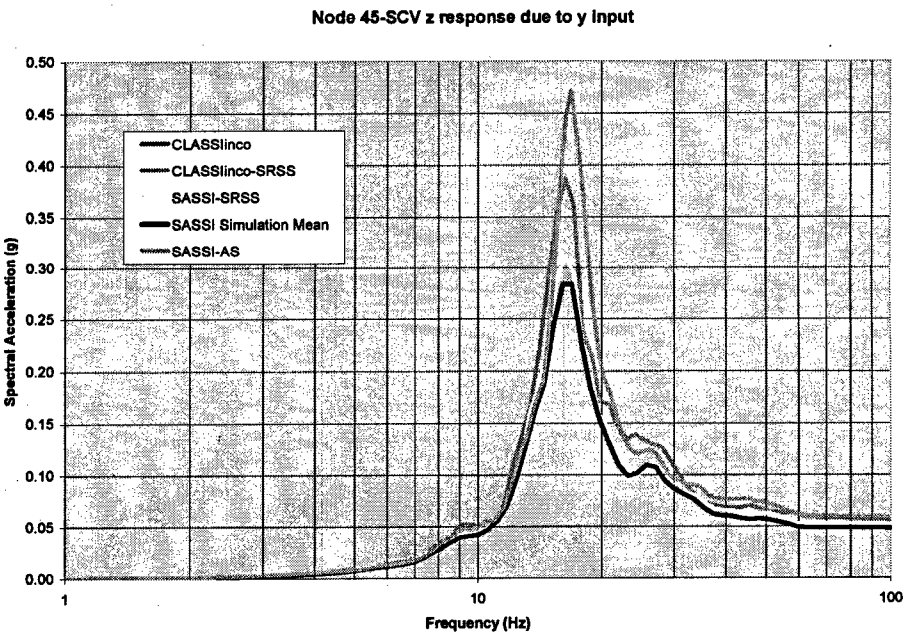

Figure A-52
Top of SCV Response Spectra – Z Direction due to Y input –CLASSlinco, CLASSlinco-SRSS, SASSI-SRSS, SASSI Simulation Mean, SASSI-AS (Node 45)

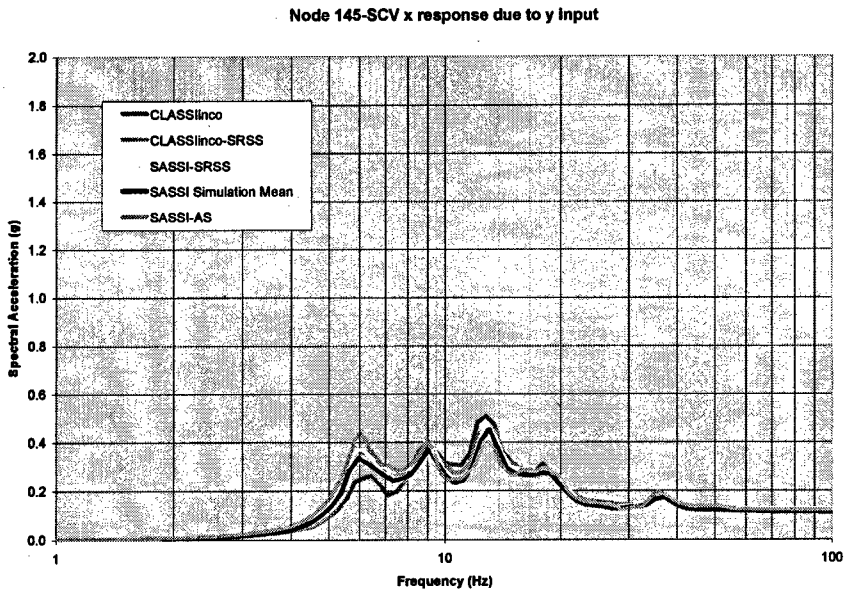

Figure A-53
SCV Outrigger Response Spectra – X Direction due to Y input –CLASSIinco, CLASSIinco-SRSS, SASSI-SRSS, SASSI Simulation Mean, SASSI-AS (Node 145)

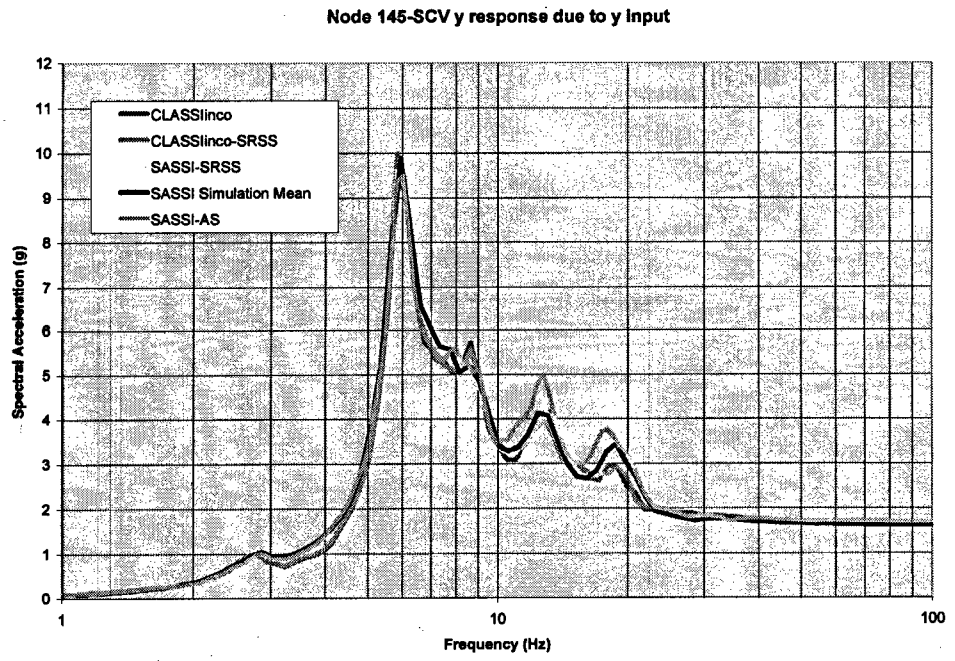

Figure A-54
SCV Outrigger Response Spectra – Y Direction due to Y input –CLASSIinco, CLASSIinco-SRSS, SASSI-SRSS, SASSI Simulation Mean, SASSI-AS (Node 145)

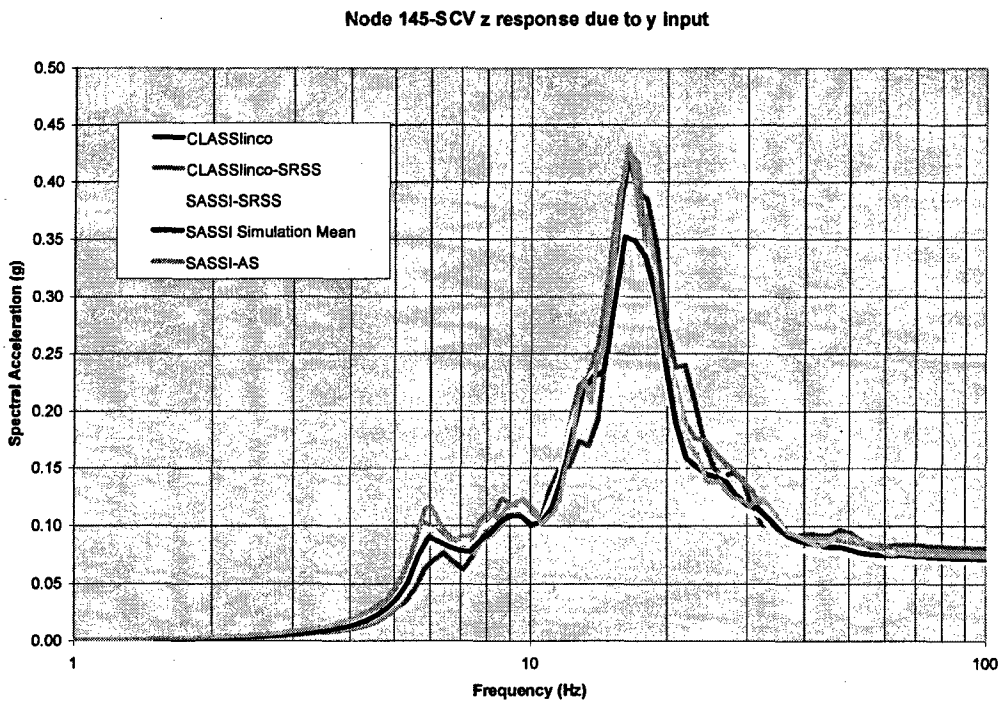

Figure A-55
SCV Outrigger Response Spectra – Z Direction due to Y input –CLASSIinco, CLASSIinco-SRSS, SASSI-SRSS, SASSI Simulation Mean, SASSI-AS (Node 145)

Z-Direction Input Ground Motion

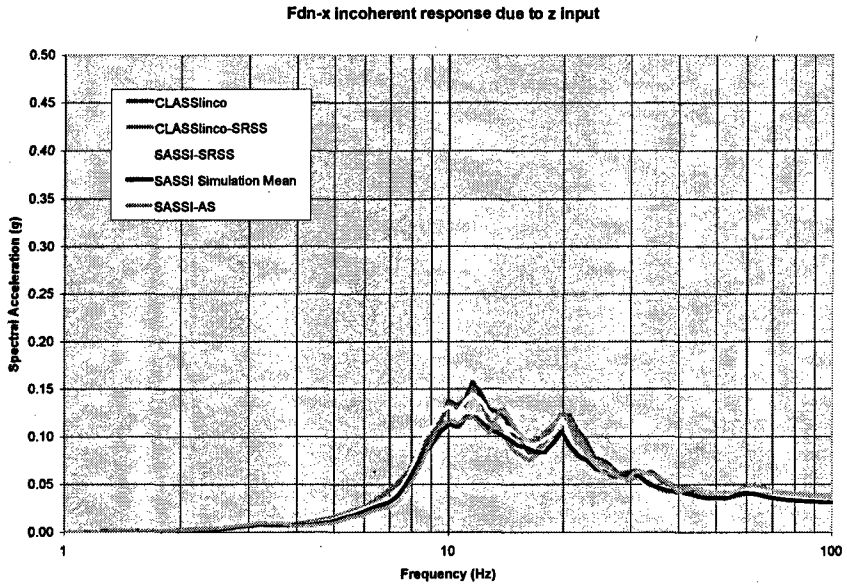

Figure A-56
Center of Foundation Response Spectra – X Direction due to Z Input –CLASSlinco, CLASSlinco-SRSS, SASSI-SRSS, SASSI Simulation Mean, SASSI-AS (Node 1)

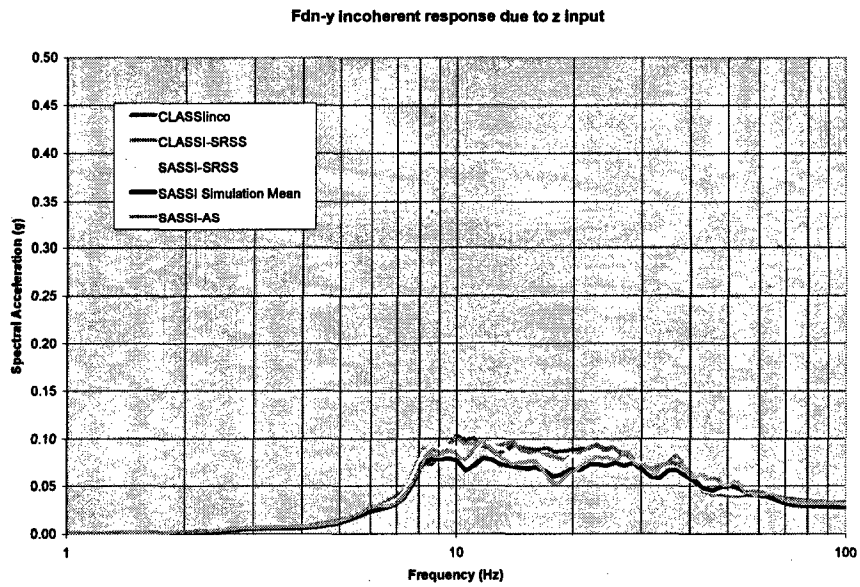

Figure A-57
Center of Foundation Response Spectra – Y Direction due to Z Input –CLASSlinco, CLASSlinco-SRSS, SASSI-SRSS, SASSI Simulation Mean, SASSI-AS (Node 1)

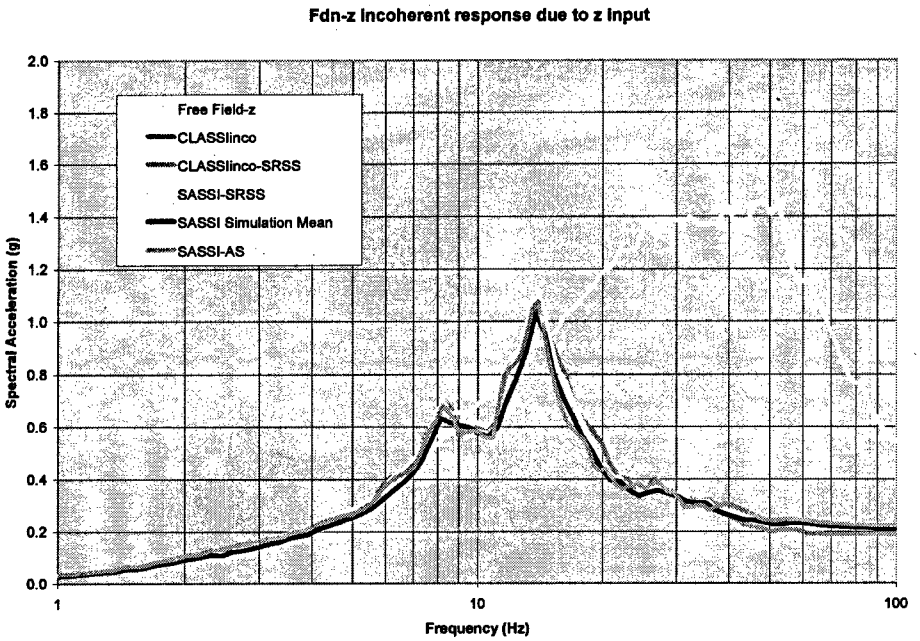

Figure A-58
Center of Foundation Response Spectra – Z Direction due to Z input –CLASSIinco, CLASSIinco-SRSS, SASSI-SRSS, SASSI Simulation Mean, SASSI-AS (Node 1)

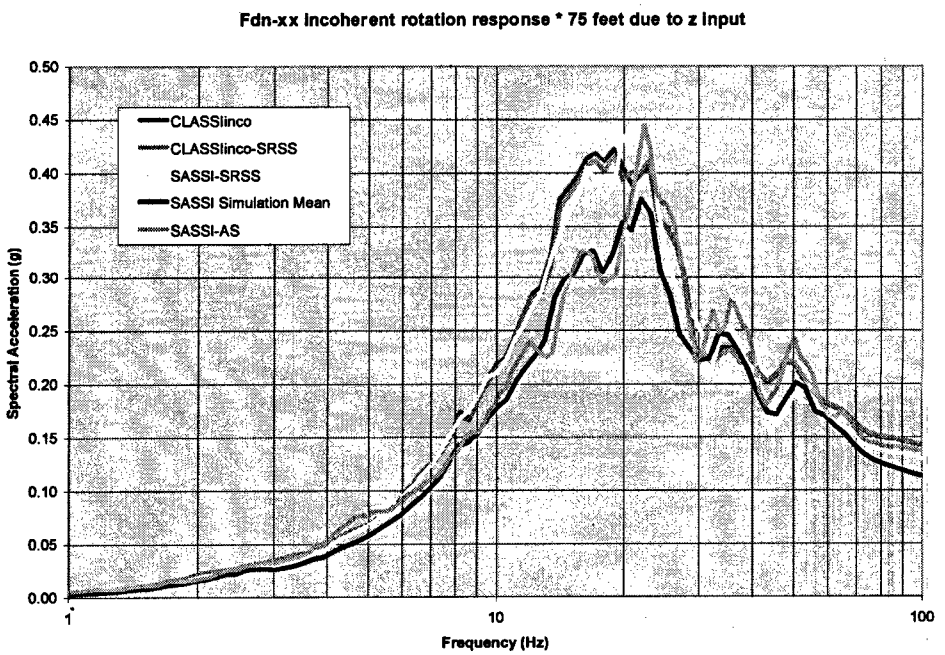

Figure A-59
Edge of Foundation Response Spectra –XX Rotation due to Z input –CLASSIinco, CLASSIinco-SRSS, SASSI-SRSS, SASSI Simulation Mean, SASSI-AS (Node 1)

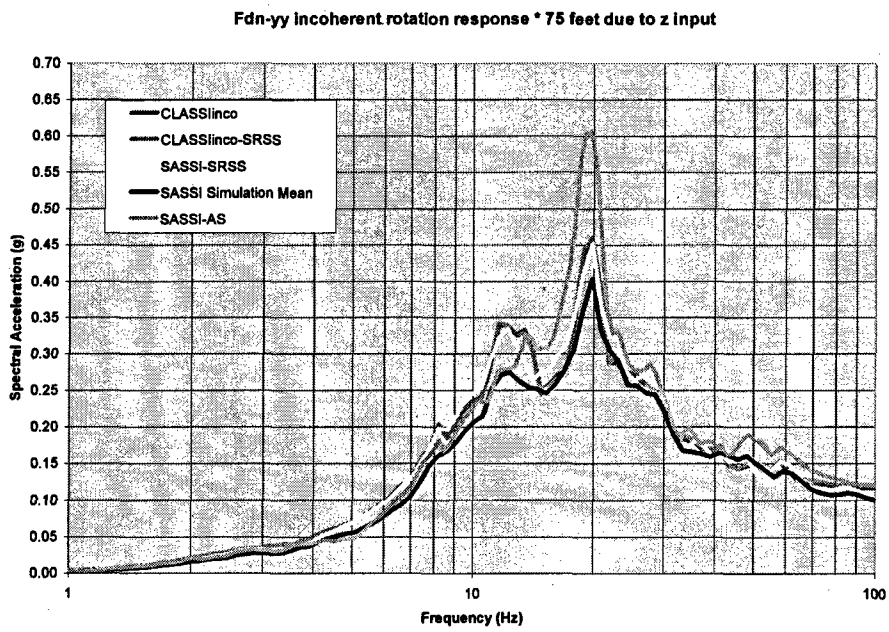

Figure A-60
Edge of Foundation Response Spectra –YY Rotation due to Z Input –CLASSlinco, CLASSlinco-SRSS, SASSI-SRSS, SASSI Simulation Mean, SASSI-AS (Node 1)

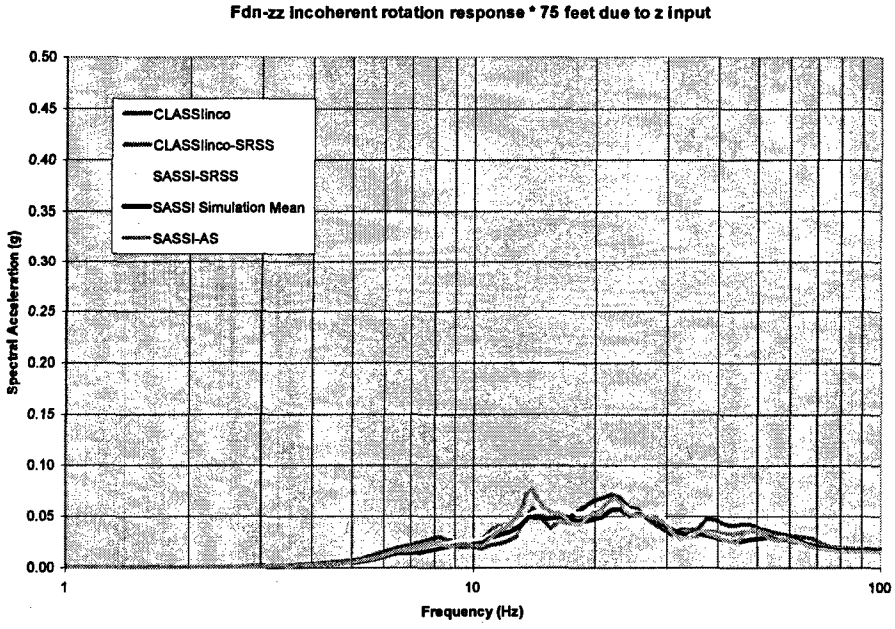

Figure A-61
Edge of Foundation Response Spectra –ZZ Rotation due to Z Input –CLASSlinco, CLASSlinco-SRSS, SASSI-SRSS, SASSI Simulation Mean, SASSI-AS (Node 1)

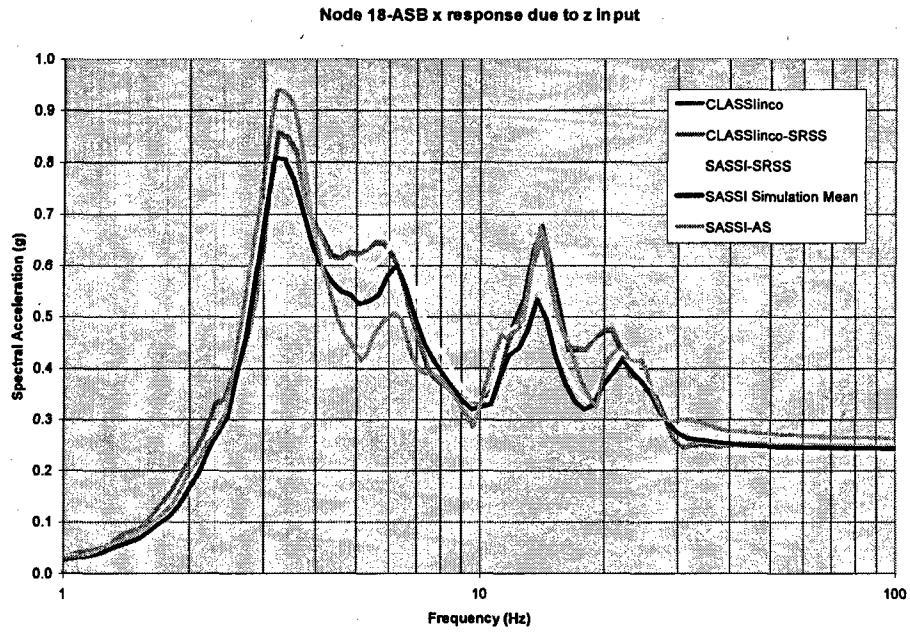

Figure A-62
Top of ASB Response Spectra – X Direction due to Z Input –CLASSlinco, CLASSlinco-SRSS, SASSI-SRSS, SASSI Simulation Mean, SASSI-AS (Node 18)

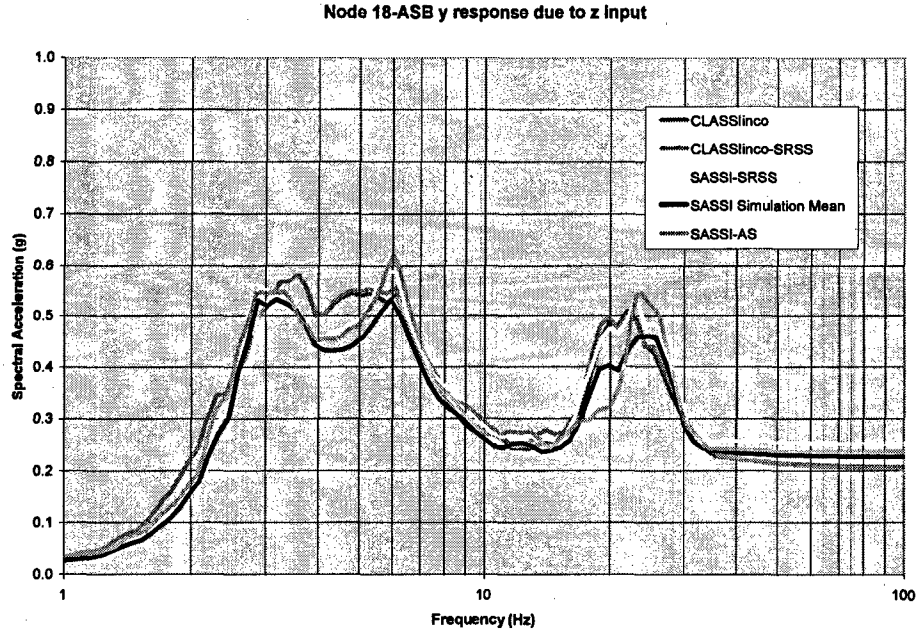

Figure A-63
Top of ASB Response Spectra – Y Direction due to Z Input –CLASSlinco, CLASSlinco-SRSS, SASSI-SRSS, SASSI Simulation Mean, SASSI-AS (Node 18)

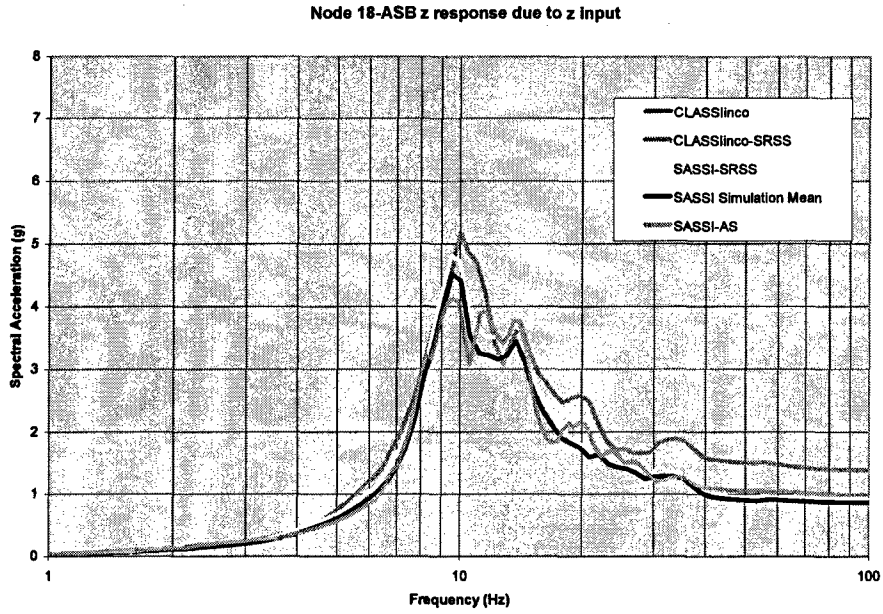

Figure A-64
Top of ASB Response Spectra – Z Direction due to Z Input –CLASSIinco, CLASSIinco-SRSS, SASSI-SRSS, SASSI Simulation Mean, SASSI-AS (Node 18)

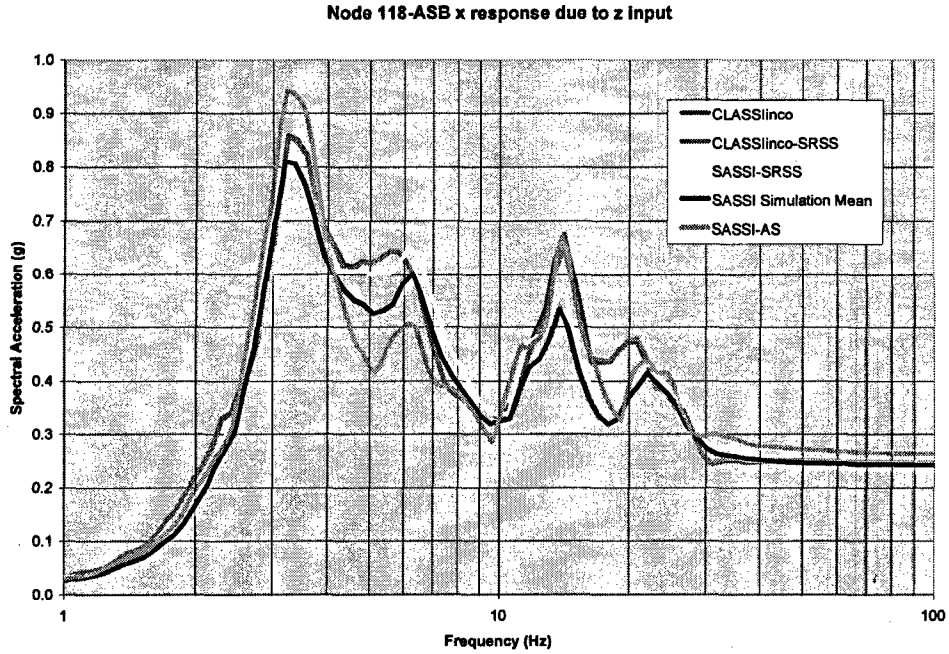

Figure A-65
ASB Outrigger Response Spectra – X Direction due to Z input –CLASSIinco, CLASSIinco-SRSS, SASSI-SRSS, SASSI Simulation Mean, SASSI-AS (Node 118)

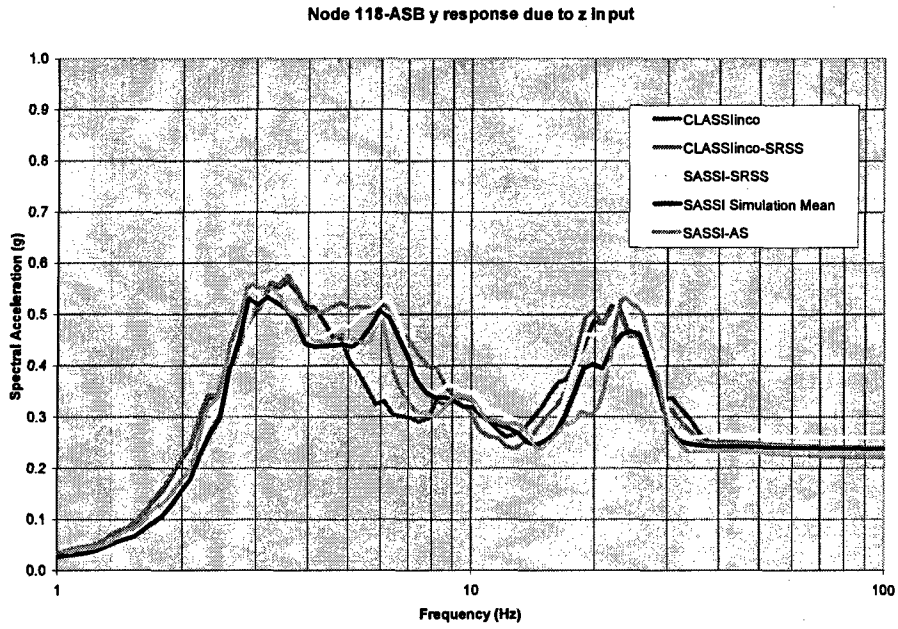

Figure A-66
ASB Outrigger Response Spectra – Y Direction due to Z Input –CLASSIinco, CLASSIinco-SRSS, SASSI-SRSS, SASSI Simulation Mean, SASSI-AS (Node 118)

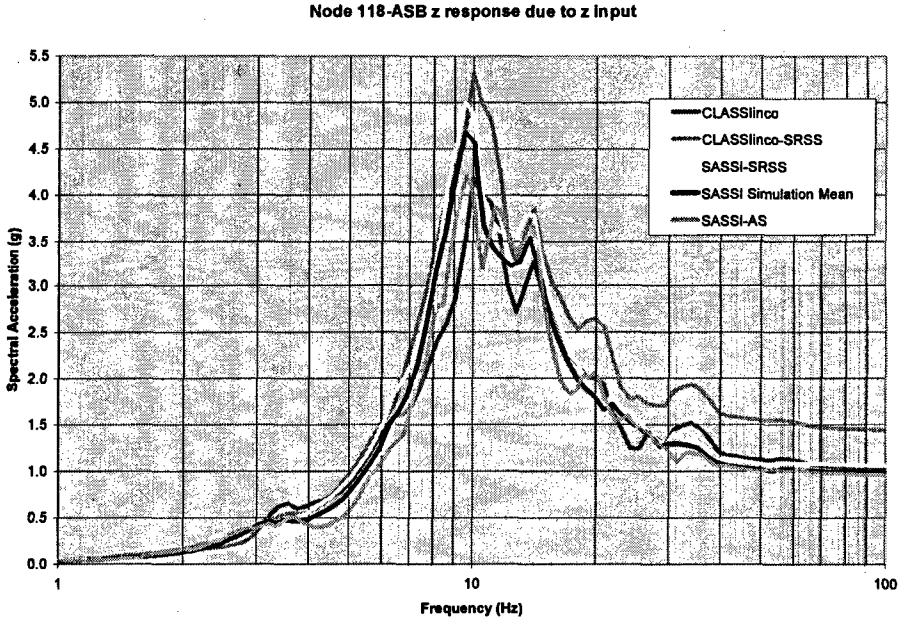

Figure A-67
ASB Outrigger Response Spectra – Z Direction due to Z Input –CLASSIinco, CLASSIinco-SRSS, SASSI-SRSS, SASSI Simulation Mean, SASSI-AS (Node 118)

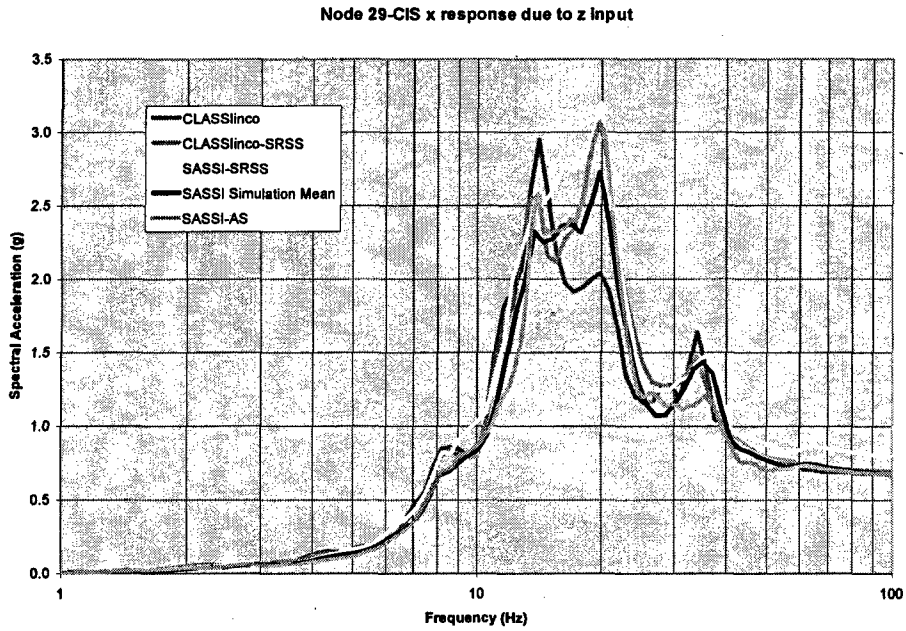

Figure A-68
Top of CIS Shear Center Response Spectra – X Direction due to Z Input –CLASSIinco, CLASSIinco-SRSS, SASSI-SRSS, SASSI Simulation Mean, SASSI-AS (Node 29)

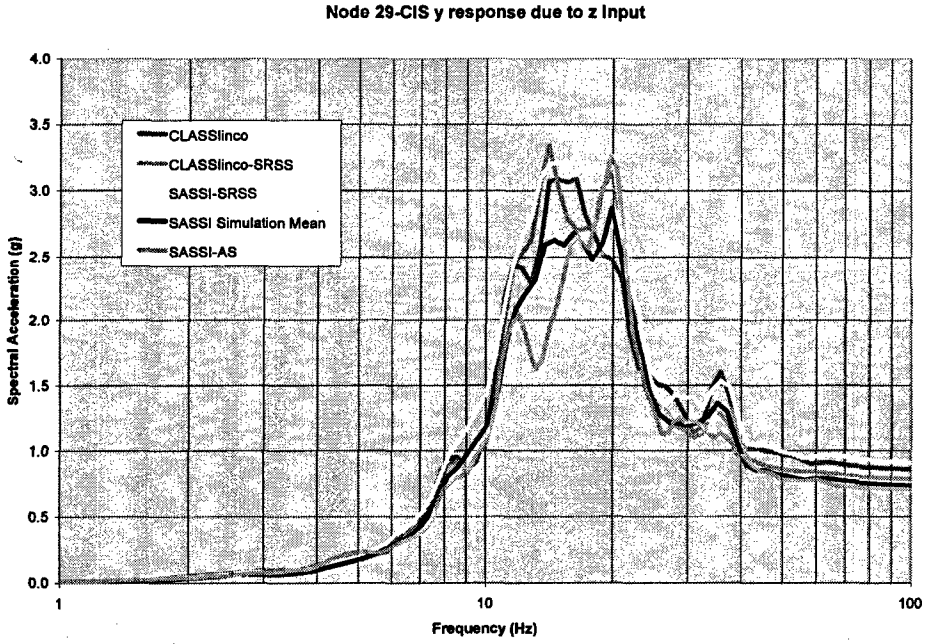

Figure A-69
Top of CIS Shear Center Response Spectra – Y Direction due to Z Input –CLASSIinco, CLASSIinco-SRSS, SASSI-SRSS, SASSI Simulation Mean, SASSI-AS (Node 29)

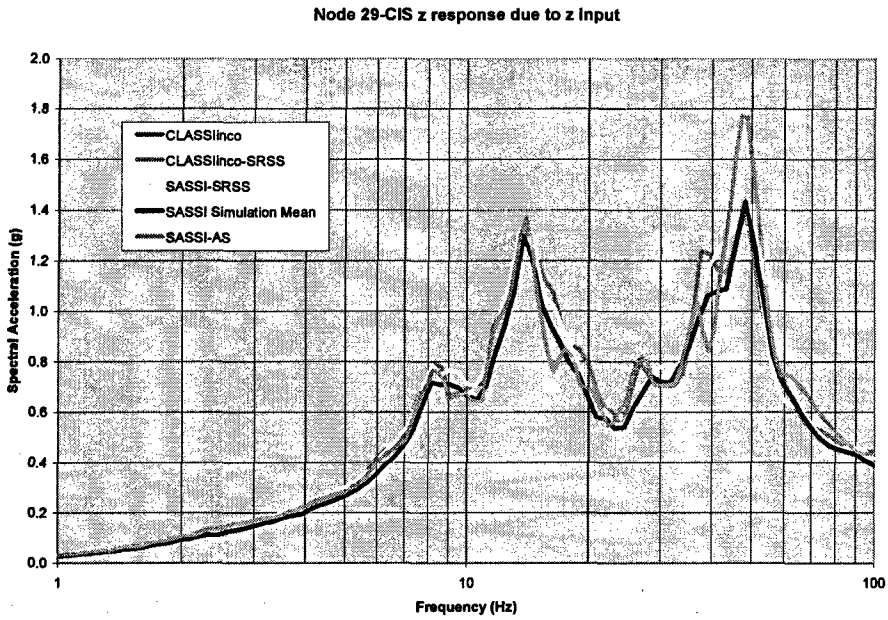

Figure A-70
Top of CIS Shear Center Response Spectra – Z Direction due to Z Input –CLASSIinco, CLASSIinco-SRSS, SASSI-SRSS, SASSI Simulation Mean, SASSI-AS (Node 29)

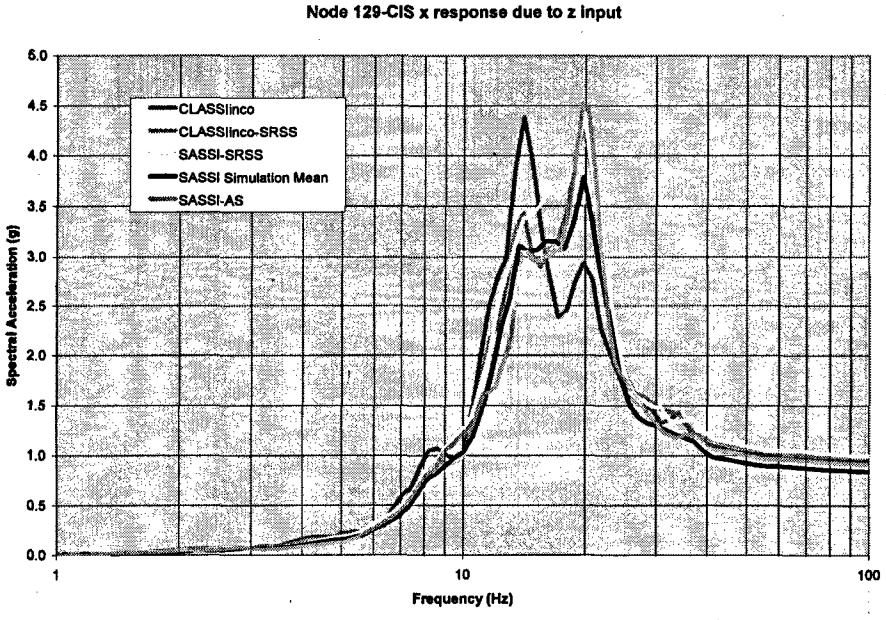

Figure A-71
Top of CIS Horizontal Mass Center Response Spectra – Z Direction due to X Input – CLASSIinco, CLASSIinco-SRSS, SASSI-SRSS, SASSI Simulation Mean, SASSI-AS (Node 129)

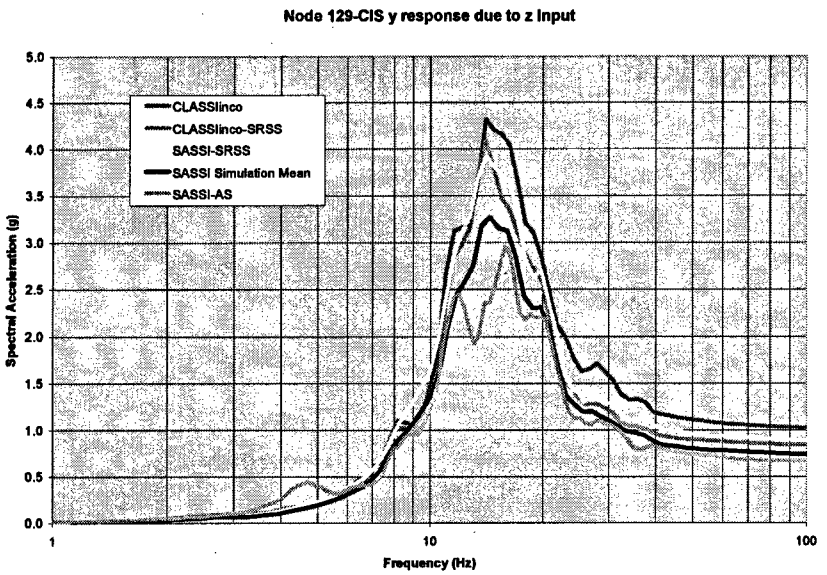

Figure A-72
Top of CIS Horizontal Mass Center Response Spectra – Y Direction due to Z Input – CLASSIinco, CLASSIinco-SRSS, SASSI-SRSS, SASSI Simulation Mean, SASSI-AS (Node 129)

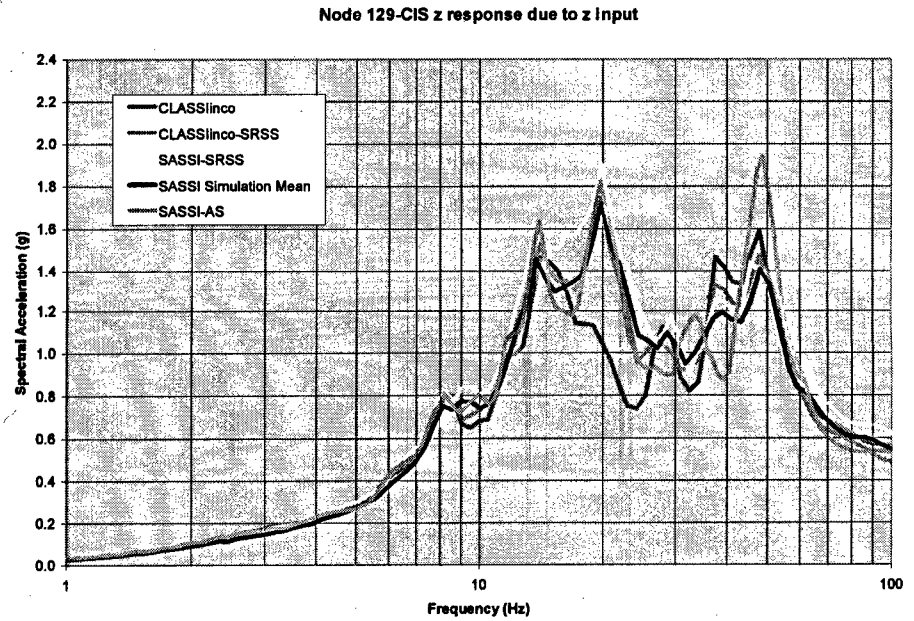

Figure A-73
Top of CIS Horizontal Mass Center Response Spectra – Z Direction due to Z Input – CLASSIinco, CLASSIinco-SRSS, SASSI-SRSS, SASSI Simulation Mean, SASSI-AS (Node 129)

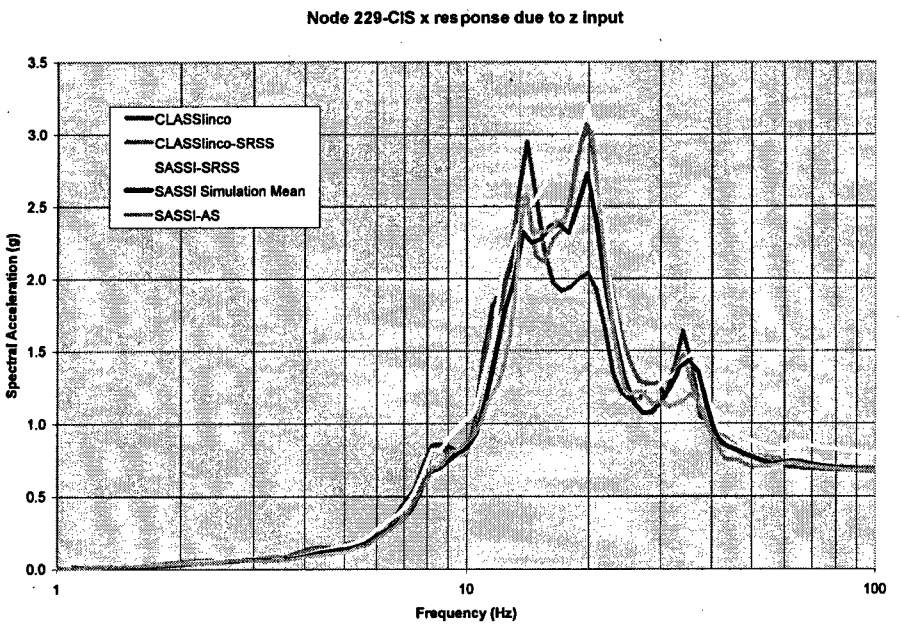

Figure A-74
CIS Outrigger Response Spectra – X Direction due to Z Input –CLASSIinco, CLASSIinco-SRSS, SASSI-SRSS, SASSI Simulation Mean, SASSI-AS (Node 229)

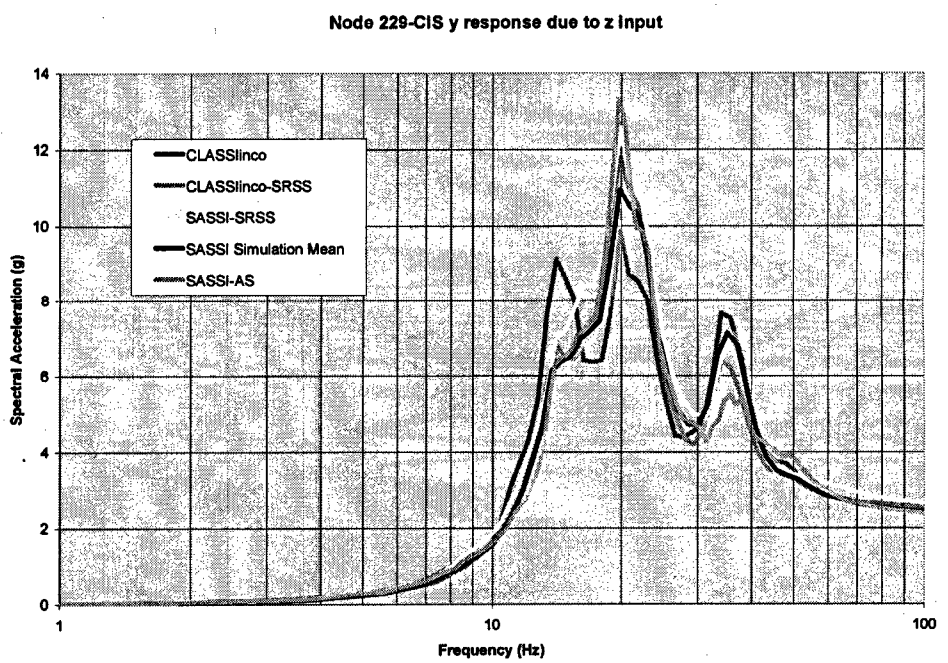

Figure A-75
CIS Outrigger Response Spectra – Y Direction due to Z Input –CLASSIinco, CLASSIinco-SRSS, SASSI-SRSS, SASSI Simulation Mean, SASSI-AS (Node 229)

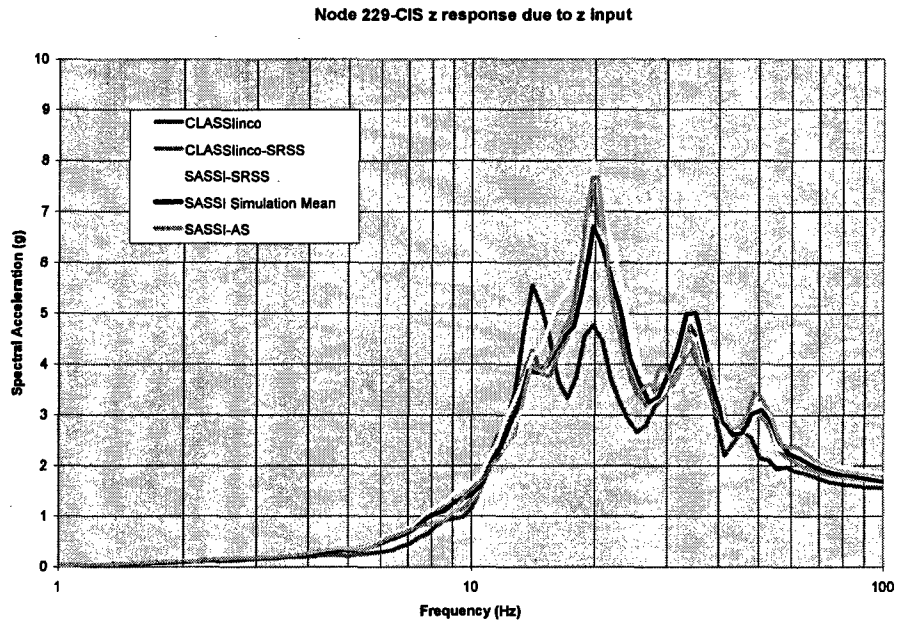

Figure A-76
CIS Outrigger Response Spectra – Z Direction due to Z Input –CLASSlinco, CLASSlinco-SRSS, SASSI-SRSS, SASSI Simulation Mean, SASSI-AS (Node 229)

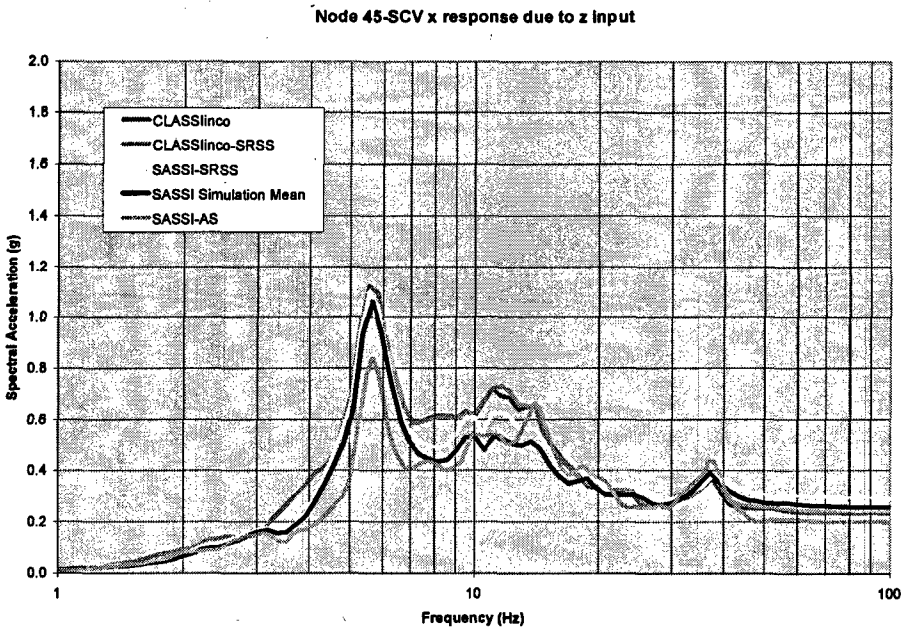

Figure A-77
Top of SCV Response Spectra – X Direction due to Z Input –CLASSlinco, CLASSlinco-SRSS, SASSI-SRSS, SASSI Simulation Mean, SASSI-AS (Node 45)

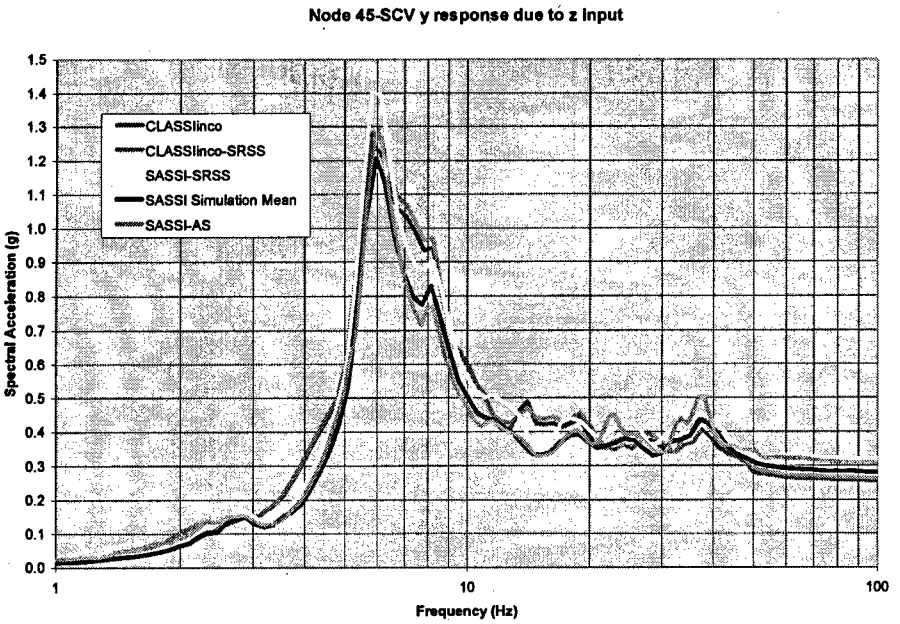

Figure A-78
Top of SCV Response Spectra – Y Direction due to Z input –CLASSIinco, CLASSIinco-SRSS, SASSI-SRSS, SASSI Simulation Mean, SASSI-AS (Node 45)

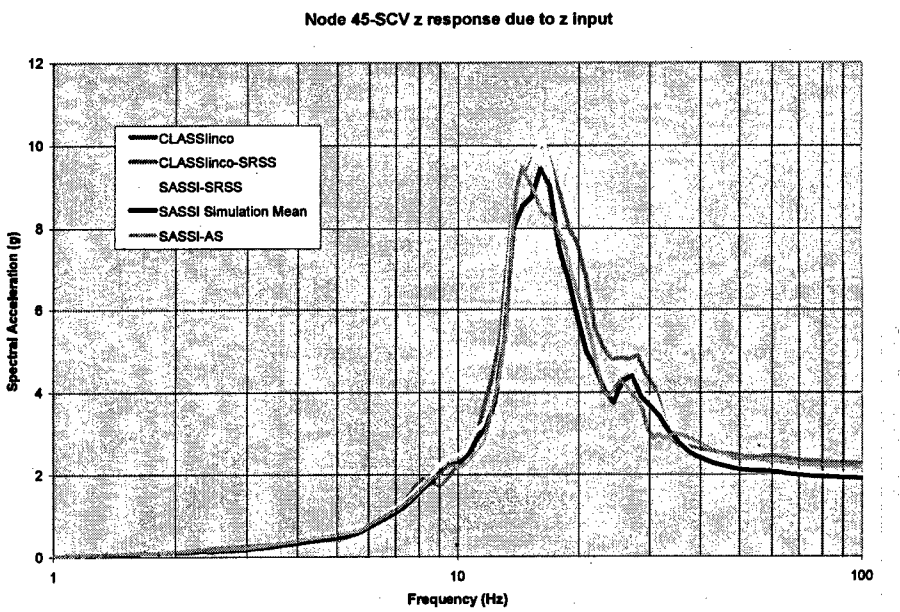

Figure A-79
Top of SCV Response Spectra – Z Direction due to Z input –CLASSIinco, CLASSIinco-SRSS, SASSI-SRSS, SASSI Simulation Mean, SASSI-AS (Node 45)

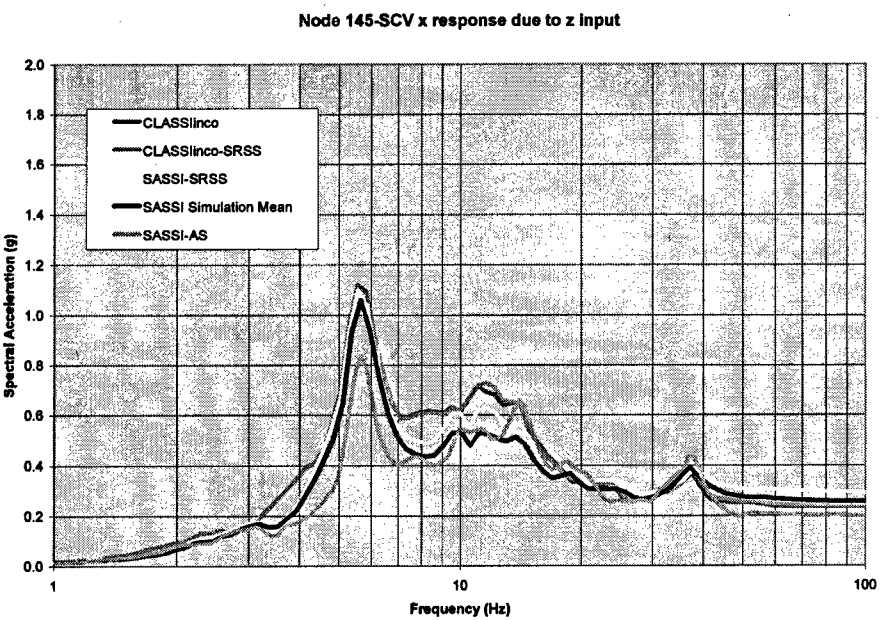

Figure A-80
SCV Outrigger Response Spectra – X Direction due to Z Input –CLASSIinco, CLASSIinco-SRSS, SASSI-SRSS, SASSI Simulation Mean, SASSI-AS (Node 145)

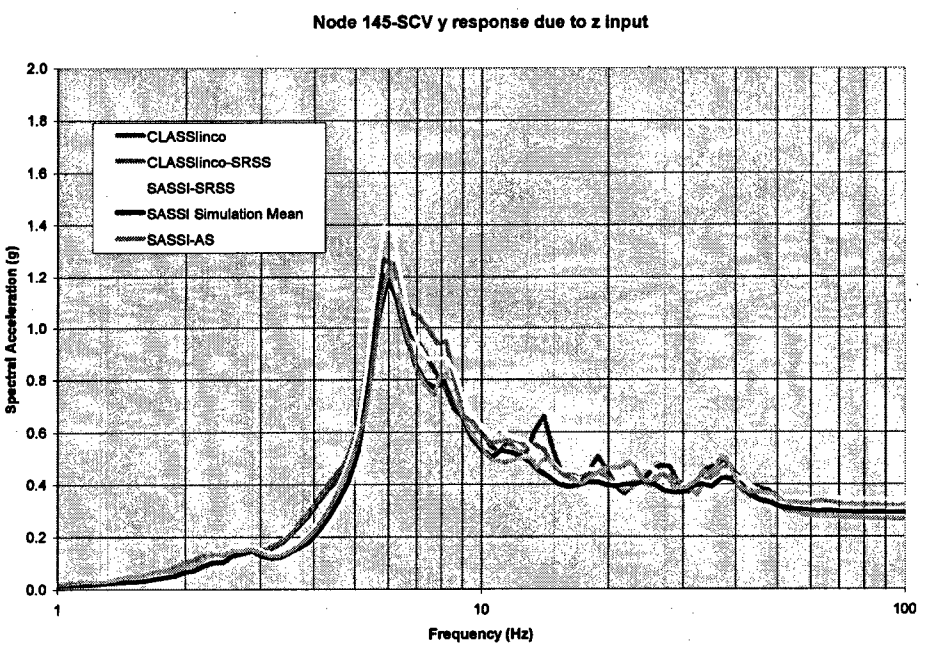

Figure A-81
SCV Outrigger Response Spectra – Y Direction due to Z Input –CLASSIinco, CLASSIinco-SRSS, SASSI-SRSS, SASSI Simulation Mean, SASSI-AS (Node 145)

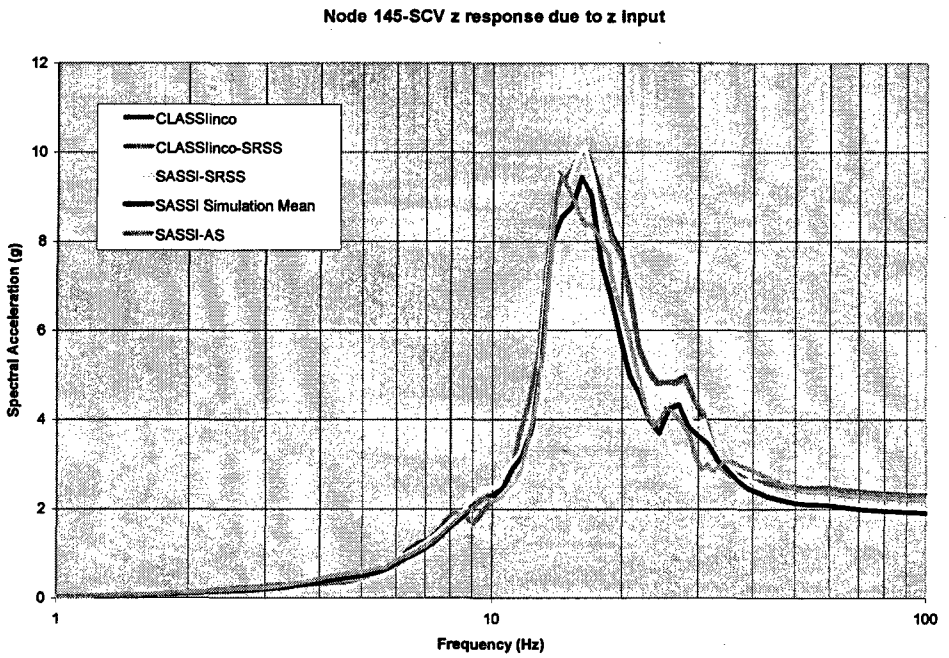

Figure A-82
SCV Outrigger Response Spectra – Z Direction due to Z Input –CLASSIinco, CLASSIinco-SRSS, SASSI-SRSS, SASSI Simulation Mean, SASSI-AS (Node 145)